

UC Berkeley

UC Berkeley Electronic Theses and Dissertations

Title

Dual mechanism for APC/C activation by integrated ubiquitylation and dephosphorylation

Permalink

<https://escholarship.org/uc/item/9rm2b4h1>

Author

Craney, Allison Christine

Publication Date

2015

Peer reviewed|Thesis/dissertation

**Dual mechanism for APC/C activation by
integrated ubiquitylation and dephosphorylation**

by

Allison Craney

A dissertation submitted in partial satisfaction of the
requirements for the degree of
Doctor of Philosophy
in
Molecular and Cell Biology
in the Graduate Division
of the University of California at Berkeley

Committee in charge:

Professor Michael Rape (chair)

Professor Douglas Koshland

Professor Rebecca Heald

Professor David Wemmer

Spring 2015

University of California, Berkeley

Dual mechanism for APC/C activation by integrated
ubiquitylation and dephosphorylation

©2015

by Allison Craney

Abstract

Dual mechanism for APC/C activation by integrated ubiquitylation and dephosphorylation

by

Allison Craney

Doctor of Philosophy in Molecular and Cell Biology

University of California, Berkeley

Professor Michael Rape, Chair

The Anaphase Promoting Complex (APC/C) is a multi-subunit ubiquitin ligase that is essential for cell cycle progression. Ube2S and Ube2C are dedicated APC/C E2-conjugating enzymes that build ubiquitin chains upon mitotic substrates. Two critical outcomes exist for this activity. First, proteins which have fulfilled their mitotic roles are removed by proteasomal degradation. Second, ubiquitylation is required to disrupt inhibitory binding of the mitotic checkpoint complex (MCC) to APC/C through the promotion of CDC20 degradation, thereby silencing the spindle assembly checkpoint (SAC). Surprisingly, however, depletion of Ube2S and Ube2C does not prevent mitotic exit. We decided to perform a Ube2S genetic interaction screen in order to better understand the functional importance of the E2 enzymes in mitosis. We discovered that Ube2S activity is essential for cell survival when one of several regulators of kinetochore-microtubule dynamics is depleted, such as the mitotic kinesin Kif18A. Co-depletion of Ube2S with one or more of these regulators results in a prolonged or permanent prometaphase arrest dependent upon the SAC. These data suggest a role for Ube2S and the APC/C in prometaphase, a time in which APC/C activity has been thought to be low. Further analysis of Ube2S in prometaphase has revealed that Ube2S contributes heavily to proper oscillatory movement of kinetochores. We also examined changes in APC/C composition when its ubiquitylation activity had been compromised, to mimic Ube2S depletion. We found that when APC/C activity is limited in prometaphase, phosphatases interact with APC/C in a Cdc20-dependent manner. Furthermore, removal or depletion of phosphatase activity results in decreased ubiquitylation of APC/C substrates and subsequent stabilization of proteins such as geminin. Reduced APC/C activity when dephosphorylation is blocked is likely due to reduced activity of Ube2S and to loss of co-activator function by CDC20. Taken together, these data have identified a necessary, integrated function for ubiquitylation and phosphatase activity in the regulation of cell division.

Table of Contents

Table of Figures and Tables	ii
Acknowledgments	v
List of Abbreviations	vii
Introduction	1
An introduction to the ubiquitin system.....	1
Why ubiquitin-dependent regulation?.....	2
Ubiquitin and the eukaryotic cell cycle.....	3
The APC/C regulates mitotic progression.....	3
Early mitotic events require a ‘wait anaphase’ signal.....	6
Ubiquitin and human disease.....	7
Chapter 1: Identification of a critical function for APC/C-specific E2 enzymes in monitoring kinetochore-microtubule attachments	9
Abstract.....	9
Introduction.....	9
Materials and Methods.....	12
Results.....	19
Discussion.....	37
Chapter 2: Regulated degradation of spindle assembly factors by the APC/C	46
Abstract.....	46
Introduction.....	47
Materials and Methods.....	48
Results.....	51
Discussion.....	64
References	76
Appendix A: Co-depletion of Ube2S and Kif18A results in a synergistic mitotic arrest that is dependent upon Aurora A kinase signaling	90
Appendix B: The mitotic motor KIFC1 is protected from APC/C-dependent degradation by importin-α	103
Appendix C: Kif18A is a novel substrate of the APC/C and is protected from degradation by microtubules	113
Appendix D	130

Table of Figures and Tables

Table of Figures and Tables.....	ii
Acknowledgments.....	v
List of Abbreviations.....	vii
Introduction.....	1
Figure 1. An enzymatic cascade occurs in order to ubiquitylate a substrate protein.....	1
Figure 2. Ube2S synthesizes branched ubiquitin chains upon substrates..	4
Figure 3. The APC/C is dynamically regulated by the MCC in early mitosis.....	5
Figure 4. Cancer cells experience proteotoxic stress.....	7
Chapter 1.....	9
Figure 1. The APC/C genetically interacts with regulators of kinetochore-microtubule dynamics.....	20
Figure 2. The APC/C genetically interacts with regulators of kinetochore-microtubule dynamics in order to promote progression through metaphase.....	23
Figure 3. Spindle Assembly Checkpoint (SAC) signaling is required for maintaining the mitotic arrest caused by co-depletion of Ube2S and Kif18A.	25
Figure 4. Ube2S is important for proper microtubule spindle dynamics....	27
Figure 5. Determination of the early mitotic APC/C interactome.....	30
Figure 6. APC/C ^{CDC20} interacts with PP2A ^{B⁵⁶} in prometaphase.	32
Figure 7. PP2A phosphatase activity co-precipitates with APC/C ^{CDC20}	34
Figure 8. Figure 8. Cdc20, but not Ube2S, is required for PP2A association with APC/C in prometaphase.	36
Figure 9. Phosphatase activity is required for efficient APC/C activation.....	38
Table 1. Genes targeted by the mitotic siRNA library utilized to determine putative Ube2S genetic interactors.....	44
Chapter 2.....	46
Figure 1. Microtubules stabilize spindle assembly factors.....	52
Figure 2. Microtubules prevent ubiquitylation of spindle assembly factors by the APC/C.....	53
Figure 3. HURP contains two microtubule-binding motifs.	55
Figure 4. The MBD1 is required and sufficient for the regulation of HURP-stability by microtubules.....	57
Figure 5. Microtubule-binding stabilizes HURP during mitosis.....	60
Figure 6. Stabilization of HURP interferes with spindle structure and function.....	62
Figure 7. The APC/C and importin-β regulate spindle function.....	63

Figure S1. Soluble spindle assembly factors can be targeted by APC/C ^{Cdc20}	68
Figure S2. Importin-β recognizes the MBD2 of HURP.....	70
Figure S3. Characterization of the effects of mutants and fusions of the MBD1 on APC/C-substrate ubiquitylation and degradation.....	72
Figure S4. Microtubules protect HURP from degradation.....	73
Figure S5. Stabilization of HURP causes spindle pole fragmentation.....	74
Figure S6. APC/C and importin-β together regulate spindle structure and function.....	75
Appendix A.....	90
Figure 1. Aurora A is required for the synergistic mitotic arrest caused by co-depletion of Kif18A and Ube2S/Kif18A.....	91
Figure 2. Verification that Aurora A is required for the synergistic mitotic arrest caused by co-depletion of Ube2S and Kif18A.....	91
Figure 3. Aurora B, despite its role in promoting SAC signaling, is not essential for maintaining the mitotic arrested caused by co-depletion of Kif18A.....	92
Figure 4. Aurora A kinase signaling is required for the synergistic mitotic arrest caused by co-depletion of Ube2S and Kif18A.....	93
Figure 5. Aurora A is required for the synergistic mitotic arrest caused by co-depletion of Ube2S and Kif18A.....	93
Figure 6. Ube2S and Kif18A are required for proper CENP-E localization.....	95
Figure 7. Ube2S is important for maintaining CENP-E at the spindle poles when Aurora A activity has been lost.....	96
Appendix B.....	103
Figure 1. KIFC1 is a substrate of the APC/C <i>in vitro</i>	105
Figure 2. Endogenous KIFC1 is degraded within 2hr of release from nocodazole-induced mitotic arrest in HeLa cells.....	106
Figure 3. Endogenous KIFC1 is degraded in mitotic extract in which APC/C is activated by addition of p31 ^{comet} and Ube2C.....	106
Figure 4. KIFC1 has a bipartite NLS in its N-terminus.....	107
Figure 5. A direct interaction between KIFC1 and importinα is strengthened by the addition of importinβ but competed off by the addition of RanQ69L.....	108
Figure 6. Importinα binding to a bipartite NLS in KIFC1 blocks ubiquitylation and degradation by the APC/C.....	109
Figure 7. Microtubules delay KIFC1 degradation.....	110
Appendix C.....	113
Table 1. Human kinesin genes (identified by 'kinesin' in FASTA sequence identifier).....	115

Table 2. Mitotic kinesin proteins that possess APC/C recognition sites. Proteins were chosen using gene ontology (GO) terms of “M Phase”, “Cell Division”, and/or “Mitotic Cell Cycle Process.”	117
Figure 1. Kif18A is degraded by the mitotic ubiquitin-proteasome system (UPS).....	118
Figure 2. Kif18A is degraded by APC/C in mitosis.....	118
Figure 3. The presence of microtubules retards Kif18A degradation in HeLa cell mitotic extract, but not the degradation of soluble APC/C substrates securin and geminin.....	119
Figure 4. HA-Kif18A cargo domain is a minimal APC/C substrate.....	120
Figure 5. Degradation of Kif18A requires a leucine followed by an arginine at its C-terminus.....	121
Figure 6. Kif18A associates with the APC/C in HeLa cell extract arrested in prometaphase.....	122
Figure 7. Kif18A possesses a microtubule binding domain (MTD) in its cargo domain that allows for protection from degradation when bound to microtubules.....	123
Figure 8. Identification of Kif18A’s microtubule binding domain (MTB) in its cargo domain.....	124
Appendix D.....	130

Acknowledgments

I primarily draw inspiration from those around me. This section serves as a small token of thanks and acknowledgement. First, I want to thank my students from Northwestern High School. Teaching high school in Baltimore City quite simply gave me a new perspective on what it means to be a scientist, a community member, and an advocate for scientific literacy. Thank you for your perseverance and grit, and for illustrating the inequities that should not exist in our country, particularly not in science.

Tremendous thanks must be given to my Teach For America-Baltimore and alumni communities for their endless support, unity, and commitment to our core values. Thank you to my content learning team (Razaan, Elisabeth, Kate, Gayatri, and Jerry). You continue to illustrate that the best scientists are also teacher leaders; you inspire me, and our CLT sessions were powerful.

The Berkeley community has been outstanding. Thank you to my boss, Michael Rape, for all of the opportunities and support you provided. Thank you also to my thesis committee: Michael Rape, Doug Koshland, Rebecca Heald, Dave Wemmer, and Karsten Weis for all of the feedback, support, encouragement, and ideas you have provided throughout my tenure at Berkeley. Also, Mike Eisen, Jasper Rine, Barbara Meyer, and Tom Alber provided some of my earliest desires to go to Berkeley and some of my first lessons. Thank you.

Te-Wen Lo and Aileen Kelly have been two of the most important people in my Berkeley life, and I am so thankful to call both of you lifelong friends. Te-Wen- you combine the hardest work ethic of anyone I've ever met with the most generosity. I would be much less successful without your advice, motivation, and all of the little intangibles that go into friendship (double hot yoga sessions, bouldering, etc. that end almost every evening and Saturday in lab), and also, for demonstrating how to be the kind of person who never sees a problem she can't solve. Aileen, you have been a great lab-mate, but you surpass that in your friendship. The extent to which you care for others while maintaining a high level of rigor in lab, volunteer work, and athletics inspires me. I'm grateful for you.

Special thanks also goes to my labmates, in particular Adam Williamson, Ling Song, Hermann-Josef Meyer, Aileen Kelly, and Indro Fedrigo. Working with Ling has been a wonderful part of graduate school. Ling, you are a talented and patient teacher, and your constant encouragement has meant so much. Adam, lab-work was always better when you were there for coffee, Red Sox games, and chatting across the bench. Thank you for your friendship, most importantly, but also for your mentorship. You made my projects stronger and you made me more creative and forward thinking in all aspects of my life. Indro and Aileen, besides being wonderful supports, also provided laboratory assistance that made my project possible. Hermann- you were my first mentor in the lab and I was struck by the intellectual rigor and care you brought to every discussion, journal club, or lab meeting. You made me a stronger scientist and a more critical thinker, but you also demonstrated how the smartest scientists listen as critically as they think. That's a lesson that has and will help me immensely in my career.

Thank you also to my Berkeley friends, including Kate, Debbie, Aisha, Christine, Lauren, Elaine, Falina, Caitlin, Claire, and Wendy. Aisha, thank you for

being by my side for our first marathon. Kate, I wish I had totaled how many miles we have put in. Your spirit is beautiful and such a gift. Debbie, without our weekly Friday coffee dates, graduate school would have been much harder. Christine, as my first mentor at Berkeley and now a friend, all I can say is that you've taught me so much, and that I'm sure my rotation placement was not an accident. Wendy- thank you for inspiring peace, meditation, travel, and laughter.

Each year at Berkeley, I had three-to-five science related personal goals. Several of these goals related to coding, and I am proud to have developed skills and a foundation for continuous improvement. Thank you first to Roy Kishony, for being the kind of mentor who would teach me MatLab code, and pair me with computational scientists like Remy, Pam, JB, Alex, Elaine, Matt, Kalin, and Noam. The Kishony Lab at Harvard was a family to me, and thanks to all of you for your inspiration, teaching, coffee, and more. Thank you also to the Genome Projects class and the summer Python course and their organizers, Rachel Brem, Mike Eisen, Terry Lang, and Matt Davis, as well as Eugene Oh. You taught me what a code-able problem is, and gave me the skills to tackle it.

I have been lucky to have mentors from other institutions. Gary Gills and Stan Rachootin provided the first encouragement to go to graduate school. Roy Kishony has given me numerous opportunities for success, and I will always appreciate how you adapted your mentoring for your lab- you knew when to provide structure, when to give freedom, and when to bring tea. Julie Welburn, our collaborator, has been a great partner, and brought so much to the table. Dan Hebert, thank you for your support and mentorship. Iain Cheeseman, your support has meant so much. Thank you for believing in me and for challenging me simultaneously. I'm lucky to learn from you.

Thank you to the Girls On The Run-Bay Area organization for the opportunities you bring to the girls and to all of the volunteers of the greater Bay Area. The GOTR community has been amazing. Thank you to Yoga To The People and the running organizations in Berkeley for providing a home.

The ultimate thanks goes to my family, and especially to my dad. Dad, you've seen me through big successes and large failures and you've taught me that both are learning opportunities. I can't imagine having a better father or cheerleader, and if I were to say 'thank you' a thousand times, it wouldn't encompass my gratitude. Thank you to the rest of my family for everything you've provided- the list is long and I'm blessed to have you all.

Finally, thank you to my brother, Adam, for always pushing me the hardest. It would have meant the world to me to share this with you. I miss you and think about you everyday, and when times are hard, it's your voice I hear in my head.

Thank you to the Berkeley community, MCB and beyond. I'm so excited about the future and will take with me many gifts from the past six years.

List of Abbreviations

APC/C: Anaphase Promoting Complex

ATP: Adenosine tri-phosphate

CP: Checkpoint

DMEM: Dulbecco's Modified Eagle Medium

DUB: Deubiquitylating enzyme

E1, E2, E3: Activating, conjugating, and ligating enzymes of the ubiquitylation cascade, respectively ('E' stands for 'eluate')

FBS: Fetal Bovine Serum

G.I. score: Genetic Index score

GTP: Guanosine-5'-triphosphate

HA: human influenza hemagglutinin

IF: Immunofluorescence

JSON: JavaScript Object Notation

MBP: maltose-binding protein

MTB: Microtubule-binding domain

MCC: Mitotic Checkpoint Complex

NA: Numerical Aperture

NCBI: National Center for Biotechnology Information

SAC: Spindle Assembly Checkpoint

SAF(s): Spindle Assembly Factor(s)

STLC: S-Trityl-L-Cysteine

UPS: Ubiquitin-proteasome system

Introduction

The ubiquitin system

Ubiquitin is one of the most highly conserved proteins in the eukaryotic lineage. Only three of its 76 amino acids differ between *S. cerevisiae* and *H. sapiens*, with conservation of its compact, globular tertiary structure (Schlesinger, 1990). The covalent attachment of ubiquitin to a substrate protein is a post-translational modification that can lead to one of many potential downstream consequences such as proteolytic degradation or changes in localization. Ubiquitin has been discovered in high cellular concentration in virtually all eukaryotes, and over twenty years of research on the ubiquitin system have demonstrated its prevalence and importance in maintaining cellular homeostasis and preserving cell integrity through regulation of essential cellular pathways.

An adenosine tri-phosphate (ATP)-dependent enzymatic cascade consisting of ubiquitin-activating (E1), ubiquitin-conjugating (E2), and ubiquitin-ligating (E3) enzymes is required for ubiquitylation of a substrate (Figure 1, adapted from Schulman and Harper, 2009). In a two-step process requiring ATP, the E1 activates a ubiquitin molecule. The E1-ubiquitin complex can then charge an E2 enzyme through ubiquitin transfer. Finally, the E3, which determines substrate specificity, interacts with the charged E2 and catalyzes formation of an isopeptide bond between the C-terminus of ubiquitin and a substrate residue, often a lysine (Dikic, et al., 2009; Hershko, et al., 1980; Komander and Rape, 2012; Pickart, 2004; Schulman and Harper, 2009; Ye and Rape, 2009). One complete round of this cascade results in monoubiquitylation. Monoubiquitylation can occur at one substrate residue, or along multiple residues in a domain (Hoegge, et al., 2002; Carter, et al., 2007). Alternatively, ubiquitin transfer to the substrate can happen multiple times, resulting in a polyubiquitin chain (Wickliffe, et al., 2011, Williamson, et al., 2009; Ye and Rape, 2009).

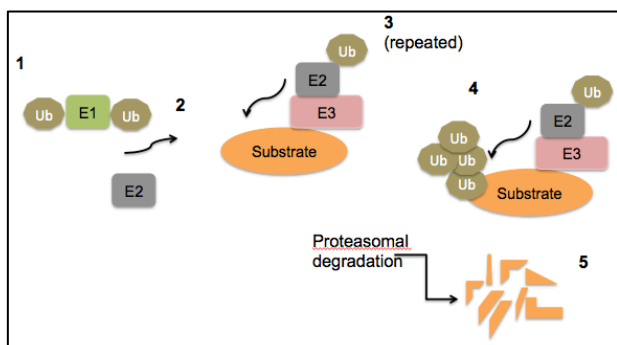


Figure 1. An enzymatic cascade occurs in order to ubiquitylate a substrate protein. (figure adapted from Schulman and Harper, 2009). In the first step, an E1 enzyme (green) activates a ubiquitin molecule (gold) through the formation of an adenylated ubiquitin intermediate (not shown). The E1 can then attack the adenylated-ubiquitin to form an E1-ubiquitin complex via a thiol ester, and completes a second adenylation round in order to bind an additional ubiquitin adenylate (Haas, et al., 1982). The doubly ubiquitin bound E1 can bind and charge an E2 molecule (green) through ubiquitin transfer (step 2). In a third step dependent upon the E3 (pink),

the E2-E3 pair can transfer one or multiple ubiquitin molecules to a substrate (orange) residue, often a lysine (step 4). The 26S proteasome (not pictured) can recognize a chain of at least four ubiquitin molecules of particular linkages (Thrower, et al., 2000). The ubiquitin chain is cleaved by DUBs, and the substrate is subsequently degraded. (Schulman and Harper, 2009) (step 5).

One canonical outcome of a polyubiquitin chain consisting of at least four ubiquitin molecules is substrate proteolysis by the 26S proteasome (Ciechanover, et al., 1984; Finley, et al., 1984; Thrower, et al., 2000). The ubiquitin chain itself is cleaved by the action of deubiquitylases (DUBs) prior to substrate degradation (Hershko, et al., 1980). Thus, a canonical outcome results in loss of substrate protein function while allowing for recycling of the ubiquitin molecules that triggered this demise. Figure 1 depicts this downstream function of substrate ubiquitylation by the ubiquitin-proteasome system (UPS).

Why regulate cellular processes by ubiquitin?

The ubiquitin system regulates a variety of critical cellular functions, including DNA damage repair, immune system pathways, endocytosis, and cell-cycle progression (Pickart, 2004). In fact, nearly all of the processes in a eukaryotic cell are likely subject to ubiquitin-dependent regulation. The prevalence of this regulation begs the question, why is the ubiquitin system such a powerful master regulator?

First, ubiquitin chains are diverse in structure and function. For a given substrate, the E1, E2, E3 enzymatic cascade could occur once per substrate residue, usually a lysine, resulting in one or more mono-ubiquitin marks on the protein (Komander and Rape, 2012; Schulman and Harper, 2009; Deshaies, 2014). Monoubiquitylation can drive changes in substrate localization activity, or binding partners, as observed in chromatin remodeling and endocytosis pathways (Dikic, et al., 2009).

Alternatively, the E2 conjugating enzyme(s) may link additional moieties to the initial ubiquitin, via the N-terminus of ubiquitin or one of its seven lysine residues (K6, K11, K27, K19, K33, K48, or K63). Chains can be homotypic or heterotypic in nature, depending on whether the same ubiquitin residue is modified during elongation (homotypic), or different residues are modified (heterotypic). A heterotypic polyubiquitin chain can be further categorized into mixed chains, where different residues of ubiquitin are modified as elongation occurs, or branched chains, in which chains are extended from different residues of the same ubiquitin (Komander, et al., 2009; Komander and Rape, 2012; Meyer and Rape, 2014; Ye and Rape, 2009).

These diverse polyubiquitin structures may code for a variety of consequences, such as proteasomal degradation (K11, K48, branched), immune system functions (Met-linked, linear), and use in signaling pathways (K63) to regulate processes such as DNA damage repair (Dikic, et al., 2009, Jin, et al., 2008; Komander and Rape, 2012; Meyer and Rape, 2014; Kelly, et al., 2014, Tokunaga, et al., 2009). To add more complexity, DUBs may antagonize any of these processes, possibly in a linkage-dependent manner (Komander, et al.,

2009). Together, the diversity of structure of ubiquitin marks upon a substrate leads to an amazing array of downstream functions.

Second, the UPS can modify substrates rapidly and lead to irreversible loss of substrate function. The cell cycle, apoptosis, anaphase initiation, and DNA replication are all examples of pathways that must be unidirectional and irreversible in order to preserve cell or tissue viability. Ubiquitylation can occur on a millisecond scale (Pierce, et al., 2009), and degradation by the 26S proteasome of substrates allows for rapid, permanent loss of protein functions that must be eliminated in order for a given pathway to continue in its forward direction. The nature of ubiquitin-dependent regulation is perfectly poised to fit the criteria and constraints of these processes.

The eukaryotic cell cycle is controlled by ubiquitin-regulated processes

One critical example that exemplifies the necessity of a unidirectional, irreversible direction is the eukaryotic cell cycle. The ubiquitin network integrally regulates the processes that comprise the cell cycle. Ubiquitin-dependent pathways drive separation of sister chromatids at anaphase, guard against genomic instability, and direct responses to environmental stimuli.

One of the largest groups of E3 ubiquitin ligases is the Cullin Ring Ligase (CRL) family, which includes the Skp/Cullin/F-box ligases (SCFs) and the Anaphase Promoting Complex (APC/C). Active throughout the cell cycle, SCF activity is important in many processes, such as ensuring the unidirectional nature of cell cycle progression by targeting both cyclins and cyclin-dependent inhibitors for proteolytic degradation. For example, SCF ubiquitylates the CDK2 inhibitor p27 in order to drive the G1/S transition, and cyclin E to regulate S phase timing (Ang and Harper, 2005; Craney and Rape, 2013; King, et al., 1996). The APC/C is most active from the metaphase-anaphase transition in mitosis through G1, and is responsible for degrading cell cycle regulators such as Cyclin B, securin, and geminin (Teixeira and Reed, 2013). Together, these ligases maintain much of the responsibility for the progression of the cell cycle; correspondingly, UPS mutations are often found in diseases such as cancer that exhibit unregulated division (Chou, et al., 2014; Diehl and Ponugoti, 2010; Jiang, et al., 2010; Teixeira and Reed, 2013).

The APC/C drives mitotic progression

Over 600 E3 ubiquitin ligases exist in the human proteome. One ligase, however, is essential for directing mitotic events: the APC/C (Peters, 2006; Rape, et al., 2004). Structurally, the APC/C possesses more than a dozen protein subunits and has a molecular mass of over 1 MDa (Schreiber, et al., 2011). The APC/C cooperates with two dedicated E2 enzymes, Ube2C and Ube2S, to robustly modify over one hundred distinct substrates (Meyer and Rape, 2011) throughout mitosis and G1.

In recent years, our laboratory has focused upon elucidating the biochemical mechanisms of the APC/C E2 enzymes, Ube2C and Ube2S (Jin, et

al., 2008; Kelly, et al., 2014; Meyer and Rape, 2014; Wickliffe, et al., 2009; Williamson, et al., 2011). Ube2C (Figure 3; orange) adds the initial ubiquitin residues to a mitotic substrate (Figure 3; blue) with K11-, K48, and K-63 linkages (Kirkpatrick, et al., 2006; Meyer and Rape, 2014). Ube2S (Figure 3; orange) also interacts with the APC/C and can extend and add branches to the growing ubiquitin chain by adding ubiquitin molecules to free K11 residues in the existing chain (Meyer and Rape, 2014).

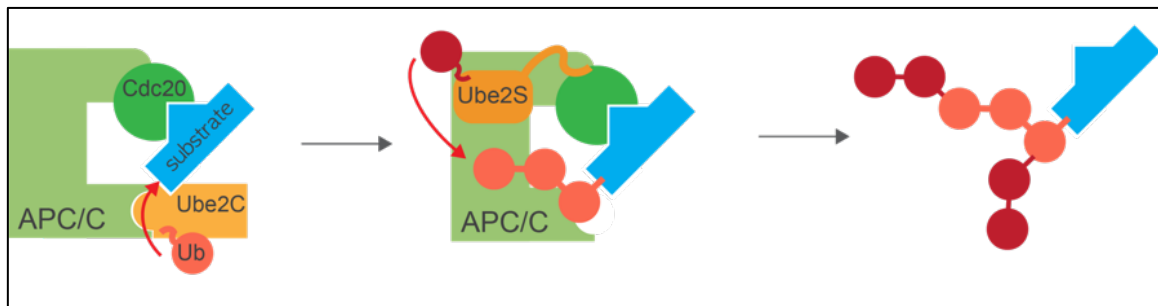


Figure 2. Ube2S synthesizes branched ubiquitin chains upon substrates. Initial ubiquitin molecules are added to a substrate by Ube2C. Ube2S can extend and branch a ubiquitin chain by adding additional ubiquitin molecules through free K11 residues in the existing chain (Meyer and Rape, 2014).

Why add branches to a growing ubiquitin chain? Work in our laboratory has recently shown that branched ubiquitin chains generated by Ube2S and the APC/C result in an enhanced degradation of substrates (Meyer and Rape, 2014). As longer ubiquitin chains do not necessarily speed the proteolysis of the substrate protein by the proteasome (Meyer and Rape, 2014; Thrower, et al., 2000), branched chains may be necessary for robust and rapid turnover over many substrates by one ligase in mitosis. There is also sequence evidence suggesting that branched chains may not be unique to the APC/C and Ube2S (Meyer and Rape, 2014). It would be interesting to see if other ligases that have heavy substrate and timing burdens also rely upon branched ubiquitin chains for their efficient functions, such as during responses to environmental stress and other cell cycle junctions like G1/S.

The APC/C is most active at the metaphase-to-anaphase transition through G1, when it helps direct important processes that commit the cell to sister chromatid separation and division.

How is the APC/C regulated in mitosis?

For a cell to maintain homeostasis despite a changing environment, ubiquitin dependent substrate regulation must occur in a robust and regulated fashion. Dynamic regulation of the ubiquitin machinery has emerged as a common principle to explain how cellular responses to the environment can be rapidly produced and coordinated. One key example illustrates how APC/C activity is restricted in prometaphase, but is sharply activated once the cell is ready to proceed to anaphase.

APC/C drives anaphase entry and mitotic exit by promoting ordered degradation of its substrates (Rape, et al., 2006; Williamson, et al., 2011).

Therefore, APC/C activity must be restrained until proper sister chromatid biorientation, which is monitored by the spindle assembly checkpoint (SAC). APC/C activity is low if even one improper kinetochore-microtubule attachment persists, but sharply increases once the SAC is inactivated. Inappropriate tuning of APC/C activity can have devastating consequences. Premature anaphase can lead to genomic instability, while an extended mitotic delay often results in cohesion fatigue, aneuploidy and/or cell death (Daum, et al., 2011; Stevens, et al., 2011).

Prometaphase inhibition of APC/C is performed by a soluble entity known as the Mitotic Checkpoint Complex (MCC) composed of BUBR1, MAD2, and BUB3. MAD2 and BUBR1 bind both each other and the APC/C activator CDC20. A recent crystal structure of the fission yeast MCC revealed that the position of CDC20 within APC/C^{MCC} is distinct from APC/C^{CDC20} (Chao, et al., 2012). Additionally, BUBR1 and MAD2 binding disrupt CDC20's ability to recognize and promote ubiquitylation of certain substrates; for example, BUBR1 blocks the KEN-box-binding site of CDC20 (Chao, et al., 2012; Tian, et al., 2012). Thus, APC/C activity is restrained by conformational change and substrate shielding induced by MCC binding.

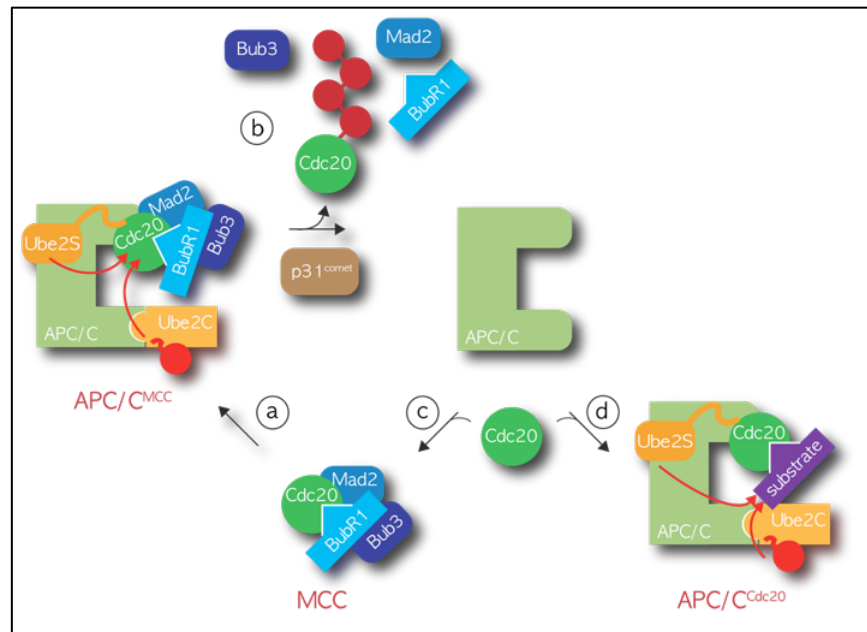


Figure 3. The APC/C is dynamically regulated by the MCC in early mitosis. Before all chromosomes are aligned at the metaphase plate, APC/C activity must be restricted in order to halt the initiation of anaphase. (a) MCC binding to the APC/C co-activator CDC20 blocks recognition and processive ubiquitylation of most substrates. (b) While MCC is bound, the APC/C can autoubiquitylate CDC20; together with p31 activity, this results in disassembly of the MCC. (c) The APC/C holoenzyme rebinds CDC20, and can either be inhibited of re-binding of MCC, or (d) initiate anaphase by ubiquitylation of key substrates (Craney and Rape, 2013).

Interestingly, APC/C^{MCC} is disassembled by APC/C-dependent ubiquitylation of CDC20, generating a positive auto-feedback loop essential for SAC inactivation (Reddy, et al., 2007; Williamson, et al., 2009). However, it is

unclear how CDC20 autoubiquitylation is robustly achieved in the presence of a soluble inhibitor. One model suggests that a dynamic homeostasis is regulated between APC/C and APC/C^{MCC} states. In this model, CDC20 autoubiquitylation and subsequent degradation would generate additional apo-APC/C that could bind newly synthesized CDC20 to increase the pool of APC/C^{CDC20} necessary for rapid ubiquitylation of substrates once the genome is properly arranged at the metaphase plate (Varetti, et al., 2011; Mocciaro and Rape, 2012).

The dynamic homeostatic model suggests that disassembly must be an intrinsic property of APC/C^{MCC}, which would enable cells the ability to both sensitively monitor kinetochore-microtubule attachment status and to robustly inactivate the SAC when appropriate. In support, the conformational change in CDC20's interaction with APC/C^{MCC} may promote its ubiquitylation (Chao, et al., 2012).

Additional regulators are needed for robust CDC20 autoubiquitylation including the dedicated APC/C E2 enzymes UBE2C and UBE2S (Reddy, et al., 2007; Williamson, et al., 2009), a novel APC/C subunit APC15 (Uzunova, et al., 2012; Foster, et al., 2012), and the MAD2 binding protein p31^{comet} (Reddy, et al., 2007; Varetti, et al., 2011). While the mechanisms of MCC disassembly from the APC/C are still not well understood, evidence suggests a multi-faceted mode of regulation. More work is needed to determine the mechanistic role of each protein important for CDC20 autoubiquitylation and to characterize the interplay between APC/C activation and other non-ubiquitin-dependent mechanisms that help remove MCC from kinetochores.

Early mitotic events require a 'wait anaphase' signal

Cells may divide for a variety of purposes, including to promote growth, perform tissue repair, and heal wounds. Genetic mutations or cellular hijacks may also promote cell division based upon inappropriate internal or external signals. Why is it critical that the anaphase-promoting machinery (APC/C and related enzymes) and the anaphase-pausing machinery (SAC and MCC proteins) are tightly regulated throughout early mitosis? If early mitotic events are not tightly regulated, separation of sister chromatids may occur before all chromosomes are properly attached and aligned to the mitotic spindle. As anaphase is an irreversible and unidirectional process, a mistake in the decision to initiate anaphase could lead to disastrous consequences for the newly formed daughter cells.

Thus far, the regulation between MCC and APC/C has been discussed, but work in my dissertation also focuses upon what processes are taking place while MCC and APC/C are interacting. Early mitotic events include spindle assembly, attachment of chromosomes to microtubules via the kinetochore, correction of inappropriate attachments that often occur during initial attachments, and alignment of sister chromatids at the equator, or metaphase plate. These events will be discussed in more detail in the introduction to Chapter 1 in this work.

Ubiquitin and human disease

Reinforcing its importance in cell cycle control, cancer genomics studies have revealed that ubiquitin pathway perturbations are common in disease. The number of therapeutics targeting the ubiquitin network has risen sharply over the past decade, and an increasingly urgent need to characterize network dynamics has followed.

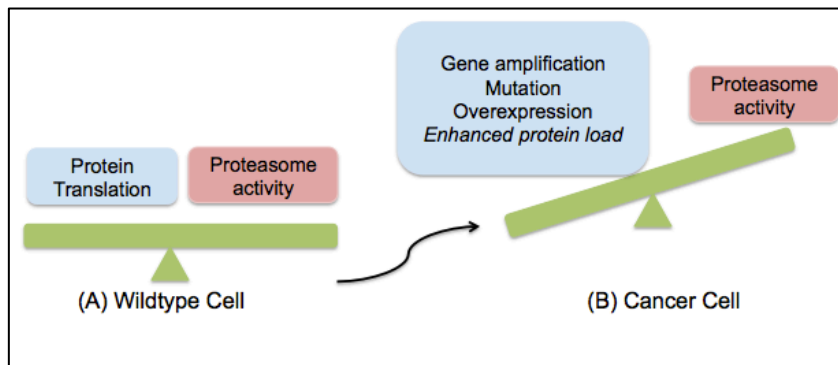


Figure 4. Cancer cells experience proteotoxic stress. In a healthy cell, the normal protein load is balanced in part by proteolysis by the 26S proteasome. However, in cancer cells, aneuploidy, which could include additional chromosomes greater than the normal diploid complement, could produce a corresponding increase in total protein due to gene amplification, mutation, and overexpression. However, if the total proteasome activity stays the same, it is possible that it will fail to process the additional load, and proteotoxic stress could occur (figure adapted from Deshaies, 2014).

Proteotoxic stress is a common problem in cancer cells, as exhibited by Figure 5. Because cancer cells possess mutations that cause them to divide uncontrollably, aneuploidy, often in the form of supernumerary chromosomes or pieces of chromosomes, result in increased protein translation. In turn, protein proteolysis becomes increasingly important in order to maintain a sense of homeostasis that allows cancer cells to outcompete wildtype cells. Cancer cells, therefore, are dependent upon the UPS, and protein translation pathways, to survive (Deshaies, 2014; Torres, et al., 2008; Torres, et al., 2010). It has been shown that increasing the rate of protein proteolysis via the 26S proteasome confers a survival advantage upon aneuploid cells (Torres, et al., 2010).

These studies, as well as numerous others, reflect the importance of the UPS to cancer cell survival. Therefore, targeting the UPS by small molecule inhibitors and generating loss-of-function effects in cancer cells remains of vital importance to the pharmaceutical industry, and to the potential for improving overall human health. More regulatory, genetic, and proteomic analyses shedding light on the UPS will augment these efforts.

What is the functional consequence of Ube2S activity?

The ubiquitin system plays an essential role in maintaining the health and homeostasis of eukaryotic cells. Our lab has been interested in APC/C

regulation, substrate identification, and biochemical mechanisms for many years. One puzzling question involves the APC/C E2 enzyme Ube2S. The importance of the APC/C in regulating mitosis is undisputed, as is the critical nature of Ube2S activity upon the APC/C's activity (Kelly, et al., 2014; Meyer and Rape, 2014; Wickliffe, et al., 2011; Williamson, et al., 2009). However, depletion of the E2 Ube2S to 90% does not result in overt phenotypes, only a slight delay at the metaphase-to-anaphase transition (personal observation/quantification, Meyer and Rape, 2014). It does, however, result in almost complete loss of detection of the 'K11' ubiquitin chain signal as measured by immunofluorescence and western blot (Matsumoto, et al., 2010; Williamson, et al., 2009), and stabilization of Nek2A and Cdc20 binding to the APC/C in prometaphase (Meyer and Rape, 2014). These seemingly paradoxical observations have led us to ask what the functional consequences of Ube2S are *in vivo*. The main bulk of my thesis work, as illustrated in Chapter 1, addresses this question.

Chapter 1:

Identification of a critical function for APC/C-specific E2 enzymes in monitoring kinetochore-microtubule attachments

Craney, A., Kelly, A., Young, S., Song, L., Fedrigo, I., Welburn, J.P.I., and Rape, M.
Manuscript in preparation for eLife submission in 2015

Abstract

Progression of the eukaryotic cell cycle requires the Anaphase Promoting Complex (APC/C), an essential E3 ubiquitin ligase that targets key regulators for proteasomal degradation. Ube2S is a dedicated APC/C E2 enzyme that enhances degradation of substrates. Despite the importance of Ube2S to overall APC/C activity, the biological processes that require Ube2S function have remained elusive. Here, we describe an siRNA-based screening approach for Ube2S genetic interactors in mitosis. We determine that Ube2S is required for initiation of anaphase when the cell has sustained challenges to proper kinetochore-microtubule dynamics. Additionally, Ube2S is required for proper kinetochore oscillatory behavior in prometaphase. These findings point to new roles for APC/C activity in prometaphase. Importantly, a proteomics approach indicates that APC/C^{Cdc20} interacts with kinetochore and PP2A complexes in an enhanced manner when the prometaphase ubiquitin-proteasome system (UPS) activity is limited. We elucidate the nature of the binding interaction between PP2A and APC/C and demonstrate that both Ube2S and PP2A are required for proper APC/C activation at metaphase. Thus, we have characterized an important link between the direct monitoring of kinetochore microtubule attachment status and APC/C activation. These data may help explain how the coordination between proper kinetochore attachment and enhancement of APC/C activity inactivate SAC signaling with efficient and appropriate timing at the metaphase-to-anaphase transition.

Introduction

Cells must properly align and segregate sister chromatids during mitosis to ensure that each daughter cell receives one full complement of genomic material. This faithful transmission of sister chromatids in mitosis requires proper formation of the mitotic spindle, amphitelic attachment of kinetochores to spindle microtubules, and the coordinated action of many proteins such as spindle assembly factors (SAFs), spindle assembly checkpoint (SAC) proteins including the mitotic checkpoint complex (MCC), and the ubiquitin-proteasome system (UPS). Additionally, these tasks must be completed within a rapid time window, as prolonged prometaphase and metaphase, even in the absence of spindle defects or attachments errors, result in cell death or inappropriate division following cohesion fatigue (Daum, et al., 2011; Stevens, et al., 2011).

One consequence of mitotic errors is aneuploidy, a chromosome gain or loss that is not equal to a haploid complement of the genome. Aneuploidy is the leading cause of miscarriages in humans (Hassold, et al., 2007), and can also lead to cell death. Viable aneuploid conditions are also extremely detrimental to the organism, as well as to society at large. For example, in humans and other animals, aneuploidy causes Down Syndrome, mental retardation, and is a hallmark of nearly all human cancers (Gordon, et al., 2012). Therefore, aneuploidy, almost regardless of phenotype, places enormous burdens on the individual, and has significant social and economic consequences. All of these reasons have led researchers to identify aneuploidy, and the causes of this condition, as key targets for pharmaceuticals, disease therapy, and molecular diagnostics.

Chromosome replication prior to mitotic entry results in attached sister chromatids each bound to a kinetochore. Each sister kinetochore must properly attach to a kinetochore fiber bundle and must bind microtubules that are oriented toward opposite spindle poles as chromosomes congress to the metaphase plate. As a bipolar spindle forms in early mitosis, kinetochores are captured by microtubules in an initially error-prone process. Kinetochore-microtubule capture that is non-amphitelic could be considered both an intermediate form of attachment and also an error; regardless of the classification, they must be converted prior to sister chromatid segregation at anaphase to avoid the potentially devastating consequences described above (Godek, et al., 2015; Kapoor, et al., 2006; Stumpff, et al., 2012).

The correction of kinetochore-microtubule attachment errors depends on spindle microtubule forces, which can be generated from the intrinsic dynamics of the microtubules themselves and by kinetochores. These forces are directed in part by kinesins, molecular motor proteins with functions in polar ejection force, kinetochore movements, microtubule depolymerization, microtubule stabilization, and more (Cai, et al., 2009; Civelekoglu-Scholey, et al., 2013; Ganem, et al., 2005; Kapoor, et al., 2006; Khodjakov and Kapoor, 2005; Song and Rape, 2010; Stumpff, et al., 2008; Stumpff, et al., 2012; Waters, et al., 1996). End-on microtubule attachment to kinetochores also requires activity by multiple kinetochore proteins, such as the NDC80 complex and KNL1 (Cheeseman and Desai, 2008; Cheeseman, et al., 2006; DeLuca, et al., 2005; DeLuca, et al., 2006; Mattiuzzo, et al., 2011; Rago, et al., 2015).

Besides mechanical mechanisms required to physically correct kinetochore-microtubule attachment errors, error-sensing mechanisms are also needed. In eukaryotic cells, the Aurora kinases and phosphatases play essential roles. Aurora B, for example, localizes to the centromere and phosphorylates targets necessary for de-stabilizing kinetochore-microtubule attachments, allowing for new attachments to form. Phosphatases such as PP2A antagonize Aurora B function by removing phosphorylation marks (Foley, et al., 2011). When the activity of phosphatases exceeds the placement of phosphorylation marks, kinetochore-microtubule attachments are stabilized. The localization of Aurora B at the centromere supports a spatial model in which lack of tension due to incorrect kinetochore-microtubule attachments allows for access of Aurora B to

essential targets, such as the outer kinetochore-microtubule network (Welburn, et al., 2010). Tension, while restricting access of Aurora B to targets, has been shown to redistribute PP2A^{B⁵⁶}, potentially giving it access for removal of previously placed phospho-marks in order to stabilize attachments (Foley, et al., 2011).

Establishing and correcting kinetochore-microtubule attachments are essential, and many protein complexes are involved in sensing and performing these necessary functions. Much research has also been done to explore other aspects of mitotic spindle assembly, inspired, in part, by over fifty years of biophysical study and observations of the properties of microtubules *in vitro* and *in vivo*. For example, during prometaphase, it has been observed that microtubules flux toward the minus ends, or spindle poles, in a consistent manner (Mitchison, 1989). While microtubule flux is conserved throughout metazoans, it is not strictly required for proper completion of mitosis. It does, however, likely contribute to faithful chromosome segregation. For example, it has been shown that abolishing flux leads to more rapid chromosome segregations (Ganem, et al., 2005; Khodajakov and Kapoor, 2005).

Once chromosomes are properly attached to spindle microtubules and have congressed to the metaphase plate, the correct attachments also must be maintained. The chromosomes are not statically aligned at the metaphase plate, but instead, undergo oscillations about the plate (Jaqaman, et al., 2010; Skibbens, et al., 1993; Stumpff, et al., 2012). These oscillations must be regulated with regard to space and speed, and critically, must not cause amphitelic attachments to be lost. Therefore, the regulation of kinetochore oscillations about the metaphase plate is also important. Depletion of factors that can affect kinetochore oscillation speeds, for example, also causes chromosome congression errors to accumulate (Jaqaman, et al., 2010; Stumpff, et al., 2008; Stumpff, et al., 2012).

Significant evidence suggests that APC/C also plays an integral role in spindle assembly and maintenance through functions that are not yet completely understood. First, core subunits of the APC/C are known to localize to the spindle (Kraft, et al., 2003; Peters, 2006), and disruption of APC/C machinery such as co-depletion of Ube2C and Ube2S results in spindle defects (Goshima, et al., 2007; Williamson, et al., 2009). Second, our lab has recently identified a class of SAFs that are jointly regulated by APC/C and the GTPase Ran (Song and Rape, 2010), as well as spindle microtubules (Song, et al., 2014). Disruption of this regulation also results in spindle defects, while dual disruption through inhibition of the Ran pathway and APC/C, for example, can lead to cell death (Song, et al., 2014).

To elucidate the importance of Ube2S and the APC/C in mitosis, we completed a synthetic mitotic arrest screen in which we depleted Ube2S in combination with one of many siRNA oligos targeting a mitotic regulator. To our surprise, synthetic mitotic arrest occurred in several double depletion conditions, but always in combination with an important prometaphase regulator that acted primarily at the kinetochore, or near the interface of kinetochore-microtubules and chromosomes. These double depletion conditions led to a permanent pre-

metaphase arrest dependent upon the spindle checkpoint, and suggested that a critical, yet undiscovered role for Ube2S activity exists in prometaphase. Further analysis yielded a direct connection between Ube2S activity and proper spindle dynamics prior to anaphase.

Ube2S and the APC/C genetically interact with proteins that regulate spindle microtubule dynamics and the microtubule-kinetochore interface in early mitosis. When Ube2S was co-depleted with a genetic interactor, cells experienced a prolonged prometaphase arrest dependent upon SAC activation and signaling. These findings suggested an important role for the APC/C in early mitotic regulation. Research of the prometaphase APC/C structure and function have resulted in the identification of three APC/C substrates (Nek2A, Cyclin A, and Cdc20) and have focused upon the dynamic regulation of the APC/C and MCC. Taken together, however, we believe that these findings point to novel functions of the APC/C.

In this chapter, we identify important roles for Ube2S in regulating microtubule and kinetochore dynamics in early mitosis. We also define a prometaphase APC/C interactome that consists of MCC, kinetochore, and phosphatase interactors, as well as known binding proteins. Further, we show that PP2A and Ube2S both contribute to efficient APC/C activation, and potentially represent a critical integration point between the monitoring of microtubule-kinetochore attachments and rapid APC/C activation at kinetochores.

Materials and Methods

Antibodies and siRNA oligos

Antibodies

The antibodies used in this chapter are as follows: α -tubulin (mouse monoclonal, Calbiochem, DM1A), cleaved caspase-3 (Asp175) (rabbit polyclonal, Cell Signaling Technology, 9661S), BubR1, Hec1, CENP-E (mouse monoclonal, Abcam, 54894, 3613, 5093), HURP, Kif18A, PPP1CC (rabbit polyclonal; Bethyl Laboratories; A300-853A, A301-080A, A300-906A), Kif2C (mouse monoclonal, Santa Cruz, 81305), Mad2, PP2A catalytic α subunit (mouse monoclonal, BD Transduction Laboratories, 610679, 610555), Ube2S, Ppp25A (rabbit polyclonal, Novus Biologicals, 22570002, 100-41412), β -actin (mouse monoclonal, MP Biomedicals LLC, 08691001), Mad1 (gift from A. Musacchio), APC4, APC7, APC5, CDC27, cyclin B1, Cdc20, geminin, PP2A-B55(h300) (rabbit polyclonal, Santa Cruz, 20985, 20987, 20986, 5618, 594, H-175/8358, FL209, 33191). For immunoprecipitation, the following antibodies were used: Cdc27 and Cdc20 (mouse monoclonal; Santa Cruz; 9972, 13162), α -FLAG (rabbit polyclonal, Sigma-Aldrich, F7425), normal rabbit IgG (Santa Cruz, 2027), and normal mouse IgG (Santa Cruz, 2025).

siRNA

ON-TARGETplus siRNA-SMARTpools were ordered through Dharmacon and contain four distinct oligos for each target. The following sequences were used:

Ube2S (3'UTR: GGCACUGGGACCUGGAUUUUU, Dharmacon; ORF: CCCGATGGCATCAAGGTCTTT, Qiagen flexitube #5), Kif18A (ORF: Qiagen flexitubes #1,3,5; ON-TARGETplus siRNA-SMARTpool; 3'UTR: two distinct oligos designed using Dharmacon tools), Mad2 (ORF: CUAUUGAAUCAGUUUCCAA, Dharmacon), Mps1 (ORF: Qiagen flexitube #6), BubR1 (ORF: Qiagen flexitubes 5 and 6), All Stars negative control (CAGGGTATCGACGATTACAAA, Qiagen), Cdc20 (ORF: ON-TARGETplus siRNA-SMARTpool), p31^{comet} (ON-TARGETplus siRNA-SMARTpool).

Cell culture and synchronizations

Cells were maintained at 37°C and 5% CO₂ in DMEM media containing 10% FBS. HeLa cells that stably express mCherry-histone H2B and GFP-tubulin (gift from R. Heald) were maintained in DMEM media with 10% FBS, 1µg/ml puromycin (Sigma), and 350µg/ml hygromycin B (Invitrogen). The HeLa cell line expressing siRNA-resistant Ube2S was prepared as described (Meyer and Rape, 2014; Wickliffe, et al., 2011). Cells were passaged every two to three days after reaching 80-90% confluence. For mitotic synchronization, cells at 75-90% confluency were treated with 2mM thymidine (Sigma Aldrich) for 20-24 hours, incubated in fresh media with no drug for 3 hours, and arrested in early mitosis with 100ng/ml nocodazole (Sigma) or 5µg/ml STLC (Sigma Aldrich) for 12 hours. MG132 (UBPBio) and reversine (Cayman Chemical Co) were used at 20µM and 0.5-1µM, respectively, for the time periods indicated. Paclitaxel (Sigma-Aldrich) was added to cells at the concentrations indicated ranging from 0-75nM.

Genetic interaction screens

Cell cycle flexiplate library screens

Cell cycle flexiplate siRNA libraries were designed and subsequently ordered through Qiagen. Each well of a 96well plate of the library contained two distinct siRNA oligos for a given gene. Flexiplate libraries were obtained in lyophilized form, re-suspended in 1x siRNA buffer (Invitrogen) to 20µM final concentration, aliquotted into sterile 96well plates, and frozen at -80°C until use. Flexiplate library aliquots were thawed no more than three times prior to discarding. Screening was performed in sterile, black-bottomed 96well plates (Corning). HeLa cells were reverse-transfected with siRNA as follows. Query oligo was spotted in combination with the flexiplate library oligo at equimolar concentrations (100nM-200nM) using Oligofectamine (Life Technologies) with standard procedures. HeLa cells were plated in DMEM (no FBS) at ~60% density. After four hours, FBS was added to 10%, and cells were incubated at 37°C with 5% CO₂ for 45-48hr. Cells were stained with Hoescht (VWR International) and fixed with 5% formaldehyde. Imaging occurred within one week of fixation.

Ubiquitin Family siRNA library screen

The ubiquitin flexiplate library was designed by members of the Rape Lab and ordered through Dharmacon (with special thanks to Adam Williamson for his leadership). Each well of the library plate contained four unique siRNA oligos targeting the same gene. The flexiplate library was obtained in lyophilized form,

and was re-suspended in 1x siRNA buffer (Invitrogen) using a Bravo Automated Liquid Handler robot (Agilent). 20 μ M aliquots were prepared in sterile 384well plates and frozen at -80°C until use. Resuspension and protocol writing (robotics and sterile—handling techniques) were co-written and performed by Adam Williamson and myself with help from Trish Birk of the UC Berkeley Screening Center. Flexiplate library aliquots were thawed no more than three times prior to discarding. HeLa cells were reverse-transfected with siRNA as follows. Query oligo was spotted in combination with the flexiplate library oligo at equimolar concentrations (20nM final) using Lipofectamine RNAiMAX (Life Technologies) following standard procedures. HeLa cells were systematically plated in DMEM with 10% FBS using a CombiDrop (Thermo Scientific) to ~60% density. 45-48hrs post siRNA treatment, cells were stained with Hoescht and fixed with 5% formaldehyde. Imaging occurred within one week of fixation.

Imaging and Data Analysis

Genetic interaction screening plates were imaged at room temperature with a 10x objective on an Image Xpress Micro (Molecular Devices) using MetaExpress software. Images were taken either at the Berkeley Screening Facility or at the Berkeley Stem Cell Facility (with special thanks to Mary West, Trish Burk, and Indro Fernando). Nine non-overlapping images were taken per co-depletion condition. Images were segmented using Cell Profiler and imported into Cell Profiler Analyst, where software was trained in an unbiased fashion to distinguish interphase, mitotic or dead, and unfocused cells. An individual training set was prepared for each screen to account for cell density and background. Using the non-biased training set, the numbers of interphase, mitotic or dead, and unfocused cells were prepared for each image taken. A Python script was written to filter out images that had 40% or greater unfocused cells, to compile all of the images taken of a given co-depletion experiment, and to calculate the mitotic index per co-depletion (*See Appendix A for sample Python script*). Further calculations were performed using Microsoft Excel.

siRNA depletion experiments

siRNA transfection experiments that were not used for screening or video microscopy purposes (see respective sections) were performed by forward transfection. Cells were plated at ~50% cell density, and incubated until ~70% confluency was reached, or approximately 18 hours. Transfections were performed using the standard protocol for Lipofectamine RNAiMAX (Life Technologies) reagent, with each oligo added at 4-20nM final concentration. For double or triple depletion experiments, oligos were combined at equimolar concentrations and the final oligo concentration per treatment was always constant within an experiment.

FACS analysis

FACS analysis performed as described (Meyer and Rape, 2014). Briefly, HeLa cells were transfected with siRNA at 10nM siRNA and harvested 48 hours later. Cells were washed, resuspended in PBS with 2% FBS, fixed with 75% cold

ethanol, and stained with 50µg/ml propidium iodide (Sigma-Aldrich) in 3.8mM sodium citrate containing RNase A. Stained cells were filtered prior to FACS analysis. A Beckman-Coulter EPICS XL Flow Cytometer (575nm band pass filter) was used to determine the cell cycle profile. The Berkeley Flow Cytometry facility instrumentation was used.

Production of Lentiviruses and Transduction

mCherry-tagged-histone H2B was cloned into pEF-1alpha/pENTR vector and recombined into pLenti XI DEST by LR recombination. Viruses were produced by 293T cells that had been transfected with packaging plasmids (Addgene) and the lentiviral constructs for 48-72 hours as described (Song, et al., 2014). Viral supernatant was collected, filtered through a 0.2µM pore and frozen at -80°C until use. Aliquots were thawed only once.

Immunofluorescence

Cells were plated in 6-well or 12-well dishes upon coverslips at ~40-60% density. Transfection or infection was performed as described. 48 hours after transfection or infection, cells were fixed for immunofluorescence imaging with at room temperature with one of the following methods: cold Methanol for 4-7min, PTEMF buffer (20mM PIPES, pH6.8; 10mM EGTA; 1mM MgCl₂; 0.2% Triton X-100; 4% formaldehyde) for 10min, or TBS with 4% formaldehyde and 0.1% Triton X-100. Fixed cells were rinsed with wash buffer (0.1% Triton X-100 in TBS). Methanol- and formaldehyde-fixed cells were permeabilized in TBS with 0.4% Triton X-100. For all treatments, cells were blocked in Abdil buffer (2% Bovine serum albumin, 0.1% Triton X-100 in TBS) and stained with primary antibodies diluted in Abdil buffer overnight at 4°C. The following day, cells were moved to room temperature, washed 5x, and stained with secondary antibodies coupled to Alexa488 and/or Alexa561 (Molecular Probes) and Hoescht in Abdil buffer for 45min in the dark. After washing, coverslips were mounted with ProLong Gold Antifade reagent (Invitrogen) and dried at room temperature overnight in the dark. Cells were visualized at 100x using MetaMorph software on an Olympus IX81 epifluorescence microscope.

Immunoprecipitations

When indicated, HeLa cells were treated with siRNA and grown asynchronously, or synchronously with thymidine/nocodazole or STLC protocol enacted four to six hours after transfection as described. Cells were resuspended in 50mM HEPES (pH 7.5), 1.5mM MgCl₂, and 5mM KCl, and further lysed by freeze/thaw cycles in liquid nitrogen and multiple passages through a 25G5/8 needle. Cell debris was pelleted by centrifugation, and the remaining lysates were normalized by their absorption at 280nm. Normalized lysates were incubated with mouse IgG, αCdc20-antibody, or αCdc27-antibody coupled to protein G agarose at 4°C for 3-5hours, rotating continuously. Beads were then carefully washed and bound proteins were eluted by addition of SDS buffer and 10min incubation at 95°C. Analysis was performed by Western blotting using specific antibodies. See section on mass spectrometry for flag immunoprecipitation protocol.

Video microscopy

HeLa cells that stably express mCherry-histone H2B and GFP-tubulin were reverse-transfected with equimolar oligo concentrations (8-12nM final concentration) with Lipofectamine RNAiMAX using standard procedures. HeLa cells were transfected following the same procedure, and were additionally infected with mCherry-histone H2B in the presence of 6µg/ml Polybrene four hours after transfection. 20-24 hours post transfection, media on cells was changed to fresh DMEM –phenol red with 10% FBS. For chemical inhibition of the SAC, reversine was added prior to imaging. Cell lines were imaged at a single focal plane every three minutes for the indicated time periods beginning 20-24 hours post transfection with siRNA and continuing for 18-24hr, at 37°C with 5% CO₂. Images were taken with a 0.95 NA 40x objective on an Olympus Revolution XD spinning disc confocal microscope equipped with a charged-couple device camera (Andor Technology) and a Yokogawa spinning disk. Movies were assembled using Metamorph and further analyzed with Photoshop.

Taxol titration screen

Screening was performed in sterile, black-bottomed 96well plates (Corning). HeLa cells were reverse-transfected with siRNA as follows using Lipofectamine RNAiMax (Invitrogen). Query oligos were spotted in equimolar concentrations per well, and master mix containing Lipofectamine RNAiMax in OptiMem was added per well. HeLa cells were plated in DMEM10% FBS at ~60% density. Cells were incubated at 37°C with 5% CO₂ for 24hr. Taxol was added at a range of 0-75nM, with the DMSO solvent making up less than 5% of the total volume, and cells were incubated for a further 24hr. Cells were stained with Hoescht (VWR International) and fixed with 5% formaldehyde. Imaging occurred within one week of fixation.

Purification of ubiquitin conjugates from cells

Protocol was modified from previous work (Meyer and Rape, 2014). HeLa S3 cell extract was prepared from cells treated with thymidine/nocodazole. Extract was pre-incubated with or without okadaic acid [9-10µM] for 30min at 30°C, shaking at 400 rpm. Extract was stimulated for APC/C activity by addition of energy mix, Ube2C, and his-ubiquitin or his-ubiquitin (K11R), as an APC/C amplification control (Meyer and Rape, 2014; Wickliffe, et al., 2011) for ten minutes at 37°C. Zero time points were immediately placed on ice after APC/C stimulation. Reactions were denatured by 8M Urea and ubiquitin conjugates were purified via NiNTA agarose (Qiagen). Ubiquitylated APC/C endogenous geminin was identified via Western blot using the geminin antibody.

HeLa Cell Extract Degradation Assays

HeLa cell extract *in vivo* degradation assays were performed as described (Song, et al., 2014; Song and Rape, 2010; see also Appendices B-C). When okadaic acid was present in the reactions, the extract was brought to room temperature before drug was added and was pre-incubated for 5min at 30°C before activating

the APC/C with Ube2C, ubiquitin, and energy mix. Degradation reactions were performed at 30°C or 37°C and were stopped with gel loading buffer.

Phosphatase assay

Endogenous CDC20 immunoprecipitation of HeLa cells arrested in mitosis was performed as described (see immunoprecipitation section in this chapter). pThr peptide (K-R-pT-I-R-R) was added to the washed Cdc20-bound fraction, and dephosphorylation was allowed to proceed via phosphatases bound to CDC20. The dephosphorylated samples were incubated with phosphate detection dye, and read at A630_{nM} using a fluorescence plate reader. The protocol for detection and dephosphorylation were obtained from the PP2A immunoprecipitation phosphatase assay kit (EMD Millipore). Buffers were routinely tested for the presence of contaminating phosphates, and a positive control in the form of a PP2A IP was performed as validation of the kit. When indicated, okadaic acid was added at the indicated concentrations prior to the addition of the pThr peptide.

Preparation, Quantification, and Analysis of Microtubule Cold Stability

HeLa cells were plated on 12well Corning dishes upon glass coverslips and treated with siRNA as described in Chapter 1. Each condition for each replicate of the assay was performed in the same dish. 48hours after siRNA, cells were subjected to DMEM+10%FBS media cooled to 4°C, and the dish was immediately placed at 4°C for 15min. After 15min, the cells were removed from 4°C and fixed with cold methanol. Immunofluorescence preparation was performed as described in Chapter 1.

Imaging and analysis protocols were based upon a published method (DeLuca, 2010). Using 60x objective on an Olympus IX81 epifluorescence microscope running Metamorph software, individual mitotic cells were chosen through the DAPI channel in pre-determined sections of a slide to avoid bias. Once chosen, stacks with .2uM steps (200nM) 10 above the plane, 10 below (20 images) were taken. The total tubulin fluorescence of the stack was summed using Metamorph. An ellipse was drawn that encompassed just the mitotic spindle area; a second was drawn that was approximately twice the area of the first and encompassed the first. The total integrated tubulin fluorescence of both ellipses was determined using Metamorph. To calculate the total % of microtubules remaining for the cell area, the percentage of tubulin fluorescence due to non-microtubule background was calculated for the given area and subtracted from the sum total (DeLuca, 2010). Fluorescence values were logged with Metamorph, parsed using the Python script included in Appendix D, and transferred to Excel (Microsoft) in order to perform calculations and graphical analysis. Special thanks to Dr. Ling Song (currently of Novartis) for assistance with the Excel box and whiskers plot template.

Microtubule Flux and Kinetochore Oscillation assays

Microtubule flux calculations were performed by Sarah Young and Julie Welburn of the Welburn Lab at the Wellcome Trust Centre in Edinburgh, Scotland. Kinetochore oscillation calculations were performed as previously described (Jaqaman, et al., 2010).

Mass Spectrometry Sample Preparation

Samples for mass spectrometry analysis were prepared from 25-35 15cm tissue culture dishes (Corning) of transfected HeLa cells per condition. Transfections of maxi-prepped (Qiagen) plasmid DNA: cDNA5/TO-FLAG-CDC20 with or without pcs2-Ube2C(C114S; dominant negative) were performed using calcium phosphate (HBS: HEPES, NaCl, Dextrose, KCl, Na₂HPO₄(7H₂O) with CaCl₂) at 60-80% cell density. The morning after transfection, fresh media was added to stimulate uptake of the transfected DNA. Approximately eight hours later, thymidine was added to 2mM. 20-24hrs after thymidine addition, cells were washed in fresh media, incubated for 3hrs, and S-T-L-C was added to 5µM for 12 hours. When indicated, MG132 (20µM; UBPBio) or DMSO was added for an additional three hours. Cells were harvested by scraping, washed with PBS, and resuspended on ice in swelling buffer (50mM HEPES (pH 7.5), 1.5mM MgCl₂, 5mM KCl, 0.1% TritonX-100 (Thermo Fisher), and protease inhibitor cocktail tablet (Roche)) for 30min. Cells were further lysed by freeze/thaw cycles in liquid nitrogen and multiple passages through a 25G5/8 needle. Cell debris was pelleted by centrifugation, and NaCl was added to 5M. Extract was pre-cleared with protein G agarose for 30min 4°C, rotating continuously. Cleared cell lysate was incubated with washed flag M2 agarose resin (Sigma-Aldrich) and incubated for 3-5hours at 4°C, rotating continuously. Flag resin was washed in swelling buffer with 150mM NaCl and 0.1% TritonX-100, and further with swelling buffer with 150mM NaCl only. Proteins bound to flag resin were eluted with flag peptide (500µg/ml in PBS + 0.1% TritonX-100; Sigma Aldrich) in three steps. Eluates were pooled, and TCA (Thermo Fisher) was added to 20% for overnight precipitation at 4°C. Pellets were washed with ice cold 0.01M HCl/90% acetone solution three times, centrifuged, and allowed to air dry. The pellet was resuspended directly in 100mM Tris (pH 8.5) with 8M Urea for trypsin digestion. Samples were reduced by 100mM TCEP (Sigma-Aldrich), alkylated by iodoacetamide (Sigma-Aldrich), and trypsin-digested in the presence of 100mM CaCl₂. Samples were trypsinized (Fisher Scientific) overnight at 37°C, shaking continuously, in the dark. Trypsinization was completed by addition of formic acid (Fisher Scientific) to 5%. Mass spectrometry and data collection were performed at the Proteomics/Mass Spectrometry Laboratory at UC Berkeley.

Mass Spectrometry parsing and data analysis

Raw mass spectrometry interaction data were filtered through a statistical software program, referred to as CompPASS, in which a given interaction set was assigned a variety of confidence values based upon a database of previous data. The database used for comparison was a compilation of work from Ling Song, Aileen Kelly, and myself (Song, et al., 2014; Kelly, et al., 2014).

Programming for the Rape Lab CompPASS database was performed by Indro Fedrigo based upon the work of the Harper Lab, who originally published and wrote instructions for the analysis (Sowa, et al., 2009). Two Python scripts used for data parsing and analysis are included in Appendix D.

Results

APC/C is essential when kinetochore-microtubule interactions are disrupted

To identify mitotic processes that require Ube2S function, we designed a siRNA-based screening approach to identify mitotic proteins that genetically interact with Ube2S (Fig. 1A). We reasoned that by elucidating a mitotic genetic interactome for the E2 enzyme, we could uncover evidence supporting the necessity of K11-linked ubiquitin chains in specific pathways (Frost, et al., 2012; Luo, et al., 2009; Measday, et al., 2005; Roguev, et al., 2008). In asynchronous HeLa cells, we performed either mock or Ube2S depletion, combined with siRNA targeting one mitotic regulator. After depletion, we determined the mitotic index, or percentage of cells in mitosis condition by high-throughput immunofluorescence against DNA and automated image analysis, and calculated a Ube2S genetic interaction index by subtracting the mitotic index resulting from depletion of the mitotic regulator alone from the mitotic index of its co-depletion with Ube2S (Fig. 1A). In this manner, we screened for dozens of potential Ube2S genetic interactors with functions spanning multiple mitotic processes (Table 3.1).

The top genetic interacting proteins were both interesting and unpredicted. We found strong genetic interactions between Ube2S and Kif18A, as well as between Ube2S and Knl1, Hec1, Sgo1, and MAPK (Fig. 1B, red). MAPK functions in a pathway that has been implicated in SAC silencing. Therefore, the genetic interaction between Ube2S and MAPK may indicate two separate challenges to silencing, and thus a prolonged mitosis (Lee, et al., 2010). The additional putative genetic interactors play important roles in early mitosis, particularly in the regulation of microtubule plus ends and kinetochore-microtubule dynamics (Jaqaman, et al., 2010; Stumpff, et al., 2008). Additionally, all have previously been linked to the regulation of or are subject to regulation by mitotic protein phosphatases (Hong, et al., 2013; Meadows, et al., 2011).

These interactors were unexpected, as in early mitosis, APC/C is dynamically maintained in a low activity state though the inhibitory binding of the MCC (Chapter 1; Crane and Rape, 2013), rendering its ubiquitylation activities targeted mainly toward substrates that are invisible to the mitotic checkpoint or toward the removal of MCC by auto-ubiquitylation of Cdc20 (Den Elzen and Pines, 2001; Hayes, et al., 2006). Interestingly, the next cluster of top hits also represented proteins with roles in prometaphase, ch-TOG, RanGAP1, KNL1, and Nup107 (Fig. 1B, yellow). In addition, we noted a suppression of the Ube2S siRNA mitotic arrest phenotype when known activators of the SAC were depleted, such as Mad1 and Mad2 (Fig.1B, blue). Taken together, this genetic interactome suggests that Ube2S and branched ubiquitin chains may play an important role in early mitosis.

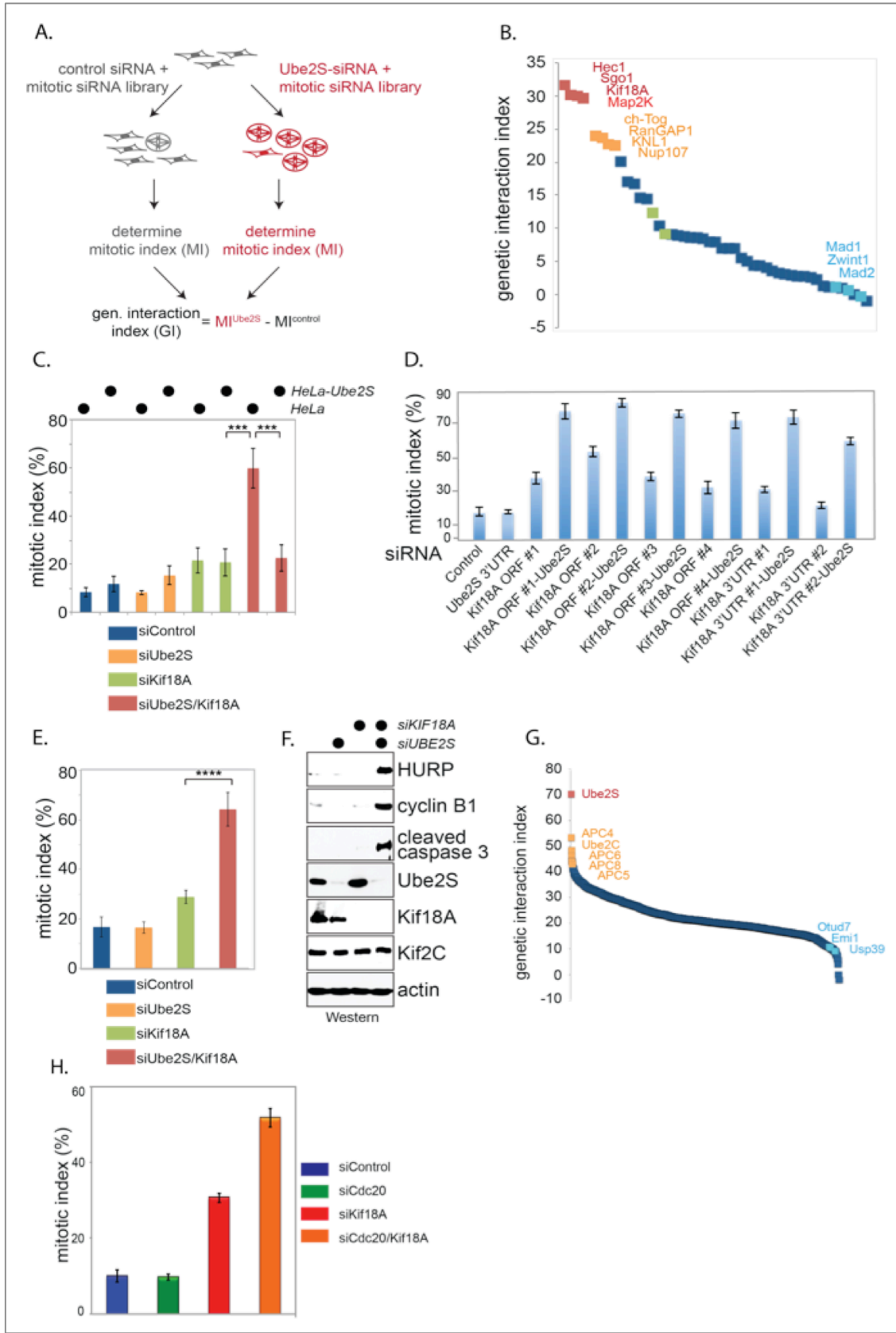


Figure 1. The APC/C genetically interacts with regulators of kinetochore-microtubule dynamics. (A) Schematic of genetic interaction scheme experimental design. (B) Ube2S genetic interaction screen identifying regulators of kinetochore-microtubule dynamics as tops hits. (C) Synergistic mitotic arrest resulting from depletion of Ube2S and a genetic interactor is dependent upon loss of Ube2S. (D) Multiple oligos targeting a genetic interactor, Kif18A, confirm the genetic interaction. Loss of Ube2S in addition to Kif18A siRNA from six different oligos causes a synergistic increase in mitotic index as compared to the Kif18A single depletions. (E) FACS confirms the synergistic mitotic arrest resulting from co-depletion of Ube2S and Kif18A. (F) Cells co-depleted of Ube2S and Kif18A exhibit both the presence of mitotic proteins and evidence that apoptosis is active, suggesting that the co-depletion results in synthetic lethality. (G) A Kif18A genetic interaction screen was performed using an siRNA library targeting the ubiquitin genome; Ube2S and APC/C score as top hits, while loss of an APC/C inhibitor and SAC-promoting ubiquitin proteins cause suppression. (H) Ube2S genetic interactors are also APC/C genetic interactors, as verified by evidence that co-depletion of Cdc20 and Kif18A cause a significant increase in mitotic index as compared to either single depletion.

We more closely examined the mitotic phenotype that results from co-depletion of Ube2S and a genetic interactor, Kif18A. Kif18A is a mitotic kinesin that regulates kinetochore microtubule length by destabilizing microtubule plus-ends, and assists in chromosome alignment by attenuating centromeric movements (Stumpff, et al., 2012; Weaver, et al., 2011). We were particularly interested in Kif18A as we had previously predicted the protein to be a novel APC/C substrate through a bioinformatics screen; we later confirmed this hypothesis through relevant biochemistry (Chapter 2; subsequently published in Sedgwick, et al., 2013). The synergistic mitotic arrest was specific to loss of Ube2S and Kif18A, as co-depletion in a HeLa cell line that expressed siRNA-resistant Ube2S rescued the mitotic index of the double depletion to that of the Kif18A single depletion phenotype (Fig. 1C). Also, multiple combinations of siRNA oligos resulted in statistically significant mitotic arrest in the double depletion conditions (Fig. 1D).

The validation experiments shown in Figures 1C and 1D both rely upon the same phenotypic analysis as the initial screen. Therefore, we also confirmed the synthetic interaction through two additional methods. First, we analyzed the cell cycle state of the various depletions through FACS (Fig. 1E), which further confirmed the synergistic mitotic arrest due to Ube2S and Kif18A co-depletion. Second, we generated HeLa cell lysate from each of the various conditions, and assayed for the presence of cleaved-caspase 3, a marker of apoptosis. We only identified a substantive presence of cleaved caspase-3 in the co-depletion condition, which importantly was the only condition in which we were able to detect the presence of proteins, HURP and cyclin B, that are expressed only in late G2 and mitosis (Fig. 1F). The presence of both mitotic proteins and a marker for apoptosis in the double depletion support the hypothesis that co-depletion of Ube2S and Kif18A cause a synthetic arrest in mitosis, and also synthetic lethality, as conditions that cause a prolonged or permanent mitotic block are often subject to apoptosis after cohesion fatigue (Daum, et al. 2011; Stevens, et al., 2011).

Similar genetic interactions are additionally seen in reverse: when a genetic interactor (Kif18A) was screened against either a ubiquitin siRNA library (Fig. 1G) or a cell cycle-based siRNA library (data not shown), Ube2S and the

APC/C were top hits. Notably, the reciprocal screen against the ubiquitin genome suggested that the synthetic lethality is due to loss of APC/C activity, not just Ube2S, in addition to a genetic interactor. To address this more directly, we determined that synthetic mitotic arrest also occurs when a genetic interactor is co-depleted with CDC20 (Fig. 1H).

APC/C is required for progression through prometaphase when a kinetochore or microtubule plus-end regulator is depleted

If Ube2S is responsible for a novel role in early mitosis, we predicted that co-depletion of the E2 enzyme with a genetic interactor should result in a early mitotic block. Thus far, our screening mechanisms quantified total mitotic cells, but we were unable to identify exactly when the arrest occurred. Fixed immunofluorescence was helpful in the initial examination of these cells, but imperfect, as we had no idea of how long cells had been arrested prior to fixation. Therefore, the phenotypes we identified via fixed microscopy may have been secondary consequences of cohesion fatigue due to prolonged arrest (Daum, et al. 2011; Stevens, et al., 2011).

To circumvent this challenge and to identify when cells subjected to co-depletion arrest in mitosis, we used confocal video microscopy platform in addition to fixed immunofluorescence. We generated HeLa cells that had been transfected with mock, Ube2S, Kif18A, or Ube2S/Kif18A siRNA, and further transduced with mCherry-H2B for cell cycle visualization. 24 hours after the transfection, we imaged the cells in culture every three minutes for 20-24 hours (Fig. 2A). We analyzed every cell in each of the four conditions that entered mitosis, and determined how what percentage of cells entered anaphase within a four-hour window. While less than five percent of the Ube2S and Kif18A siRNA-treated cells remained arrested in mitosis, the double depleted cells exhibited close to 70% that remained in a pre-anaphase state for at least four hours (Fig. 2A-2B). Additionally, cells experienced classic symptoms of cohesion fatigue after extended arrest, such as dramatic sister chromatid scattering and spindle rotation (Fig. 2A and additional data not shown).

Fixed immunofluorescence against Hec1 (marking the outer kinetochore) and HURP (to visualize kinetochore-fibers) corroborated our finding by illustrating that kinetochore-microtubule attachments appeared perturbed under conditions in which Ube2S and a selected genetic interactor were co-depleted. While kinetochores in the mock and single depletion conditions appeared relatively well aligned at the metaphase plate, kinetochores in the siUbe2S/Kif18A condition were tracked along the kinetochore fibers, and did not appear well aligned (Fig. 2C).

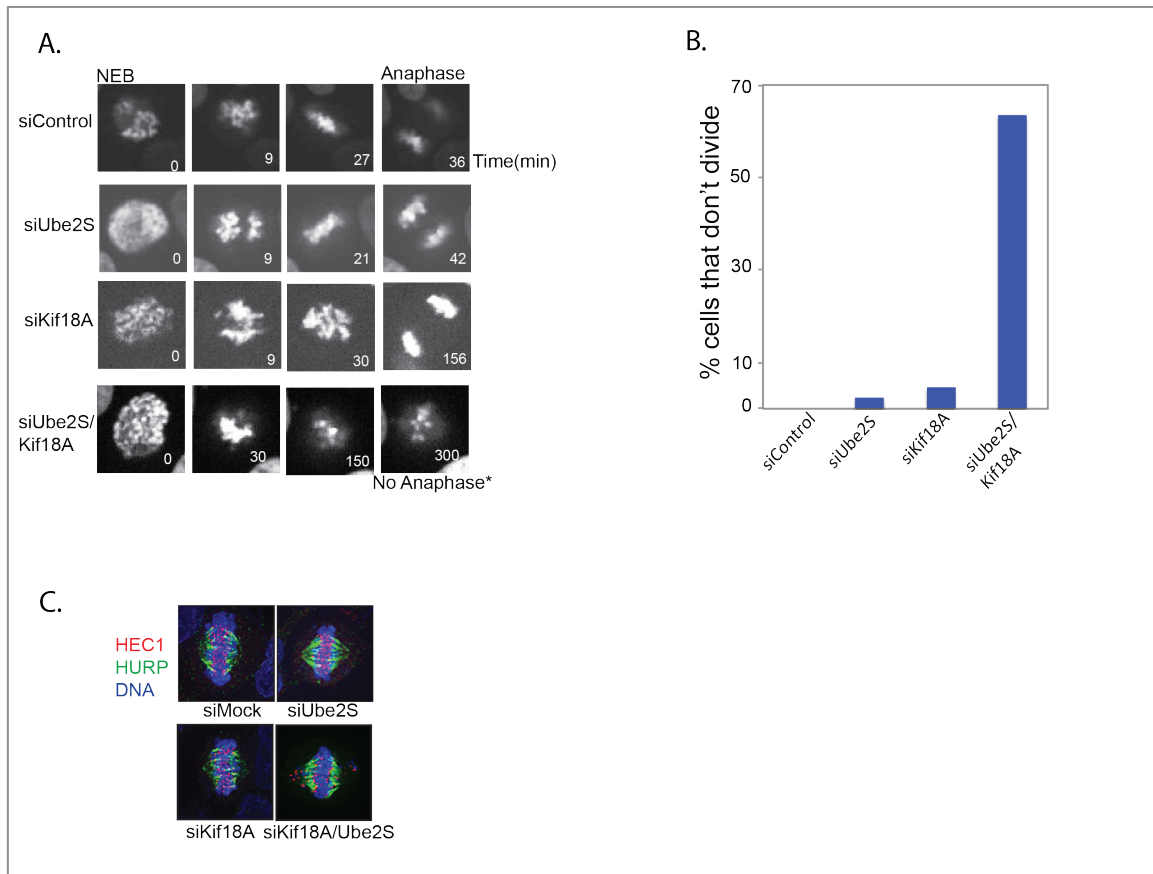


Figure 2. The APC/C genetically interacts with regulators of kinetochore-microtubule dynamics in order to promote progression through metaphase. (A-B) Video microscopy was performed upon HeLa cells treated with mock, Ube2S, Kif18A, or Ube2S/Kif18A siRNA. Filming was begun 24hr after siRNA transfection, and images were taken every 3minutes. While greater than 95% of cells in the control or single depletion conditions successfully initiated anaphase, close to 70% of the cells co-depleted of Ube2S/Kif18A remained arrested in a pre-anaphase state, and/or died after prolong arrest. (C) Fixed immunofluorescence demonstrates defects in kinetochore-microtubule attachments, demonstrated by Hec1 staining tracking along microtubules. This is further evidence to suggest that pre-anaphase defects are caused by co-depletion of Ube2S and Kif18A.

Synergistic mitotic arrest requires the spindle assembly checkpoint

During prometaphase, aberrant attachment of spindle microtubules to mitotic chromosomes activates the spindle assembly checkpoint, which in turn results in low APC/C activity and a block to cell division. The effector complex of the spindle assembly checkpoint is the mitotic checkpoint complex composed of BubR1, Bub3, and Mad2. This complex directly binds the APC/C co-activator Cdc20 and causes a conformational change in the APC/C that makes substrate binding less efficient. Interestingly, while the mitotic checkpoint complex is bound, the APC/C can autoubiquitylate Cdc20: this autoubiquitylation results in removal of the mitotic checkpoint complex from the core ubiquitylation machinery, opening the possibility of having free Cdc20 bind apo-APC/C in order

to proceed with cell division, or, alternatively, the mitotic checkpoint complex can re-bind to halt anaphase progression.

Further, if mitotic arrest occurred prior to anaphase, we would expect to see evidence of active SAC signaling. To visualize SAC signaling we analyzed cells in each of the depletion conditions for the presence of Mad1 foci (Mad1 antibody was a gift from A. Musacchio). For each condition, mitotic cells scored positive for the presence of at least one Mad1 focus, indicative of an active SAC (Ballister, et al., 2014; Kuijt, et al., 2014; Maldonado and Kapoor, 2011) (Fig. 3A). Therefore, the double depletion of Ube2S along with Kif18A arrests cells prior to anaphase with evidence for an active mitotic checkpoint.

We began our examination of the role of the SAC by analyzing whether or not core APC/C associates with members of the mitotic checkpoint complex. We detected association of the mitotic checkpoint complex with APC/C in all siRNA conditions when cells had been transfected with siRNA and subsequently arrested in mitosis with nocodazole (Fig. 3B). While these Western blots are not quantitative, we did not notice large differences in the amount of SAC proteins Mad2 and BubR1 associating with APC/C in the double depletion compared to the other depletion conditions. This result both confirms that the checkpoint is active in co-depleted cells – may also reflect that they are more in mitosis (Fig. 3B). In cells that were treated with siRNA but not synchronized with a spindle poison, SAC proteins co-associated with the APC/C in only the double depletion condition, confirming our screening results that detected a synergistic mitotic arrest only in the co-depletion condition (data not shown).

Is the checkpoint required for a Ube2S-dependent cell cycle arrest that occurs in response to altered MT dynamics? To address this question, we examined if cells divided by live video microscopy when treated with a chemical inhibitor of the spindle assembly checkpoint, Reversine (Santaguida, et al., 2010). All cells treated with mock siRNA, regardless of drug or vehicle treatment, that entered mitosis also entered anaphase (Fig. 3C-D). However, HeLa cells that were first depleted of Ube2S and Kif18A only divided in the presence of Reversine. Close to 100% of cells remained arrested in mitosis when the vehicle control was used (Fig. 3C-D).

To address drug specificity concerns, as Reversine may also target other protein kinases in mitosis, we also performed co-depletion experiments in which we removed Ube2S and Kif18A by siRNA, and further depleted components of the mitotic checkpoint complex, BubR1, Mad2, or Mps1, all essential spindle assembly checkpoint signaling proteins. Under triple depletion conditions, the cells did not arrest in mitosis, and showed significant differences in mitotic index as compared to the Ube2S/Kif18A co-depletion (Fig. 3E).

As expected, cells that are co-depleted of Ube2S, a genetic interactor, and spindle assembly checkpoint signaling inappropriately enter anaphase and exhibit lagging chromosomes, anaphase bridges, and multinucleation. Cells depleted of Ube2S and a genetic interactor remain arrested in mitosis (Fig. 3F). Based upon these results, we infer that perturbing both APC/C activity and kinetochore-microtubule dynamics concurrently results in a permanent

prometaphase arrest dependent upon signaling of the spindle assembly checkpoint.

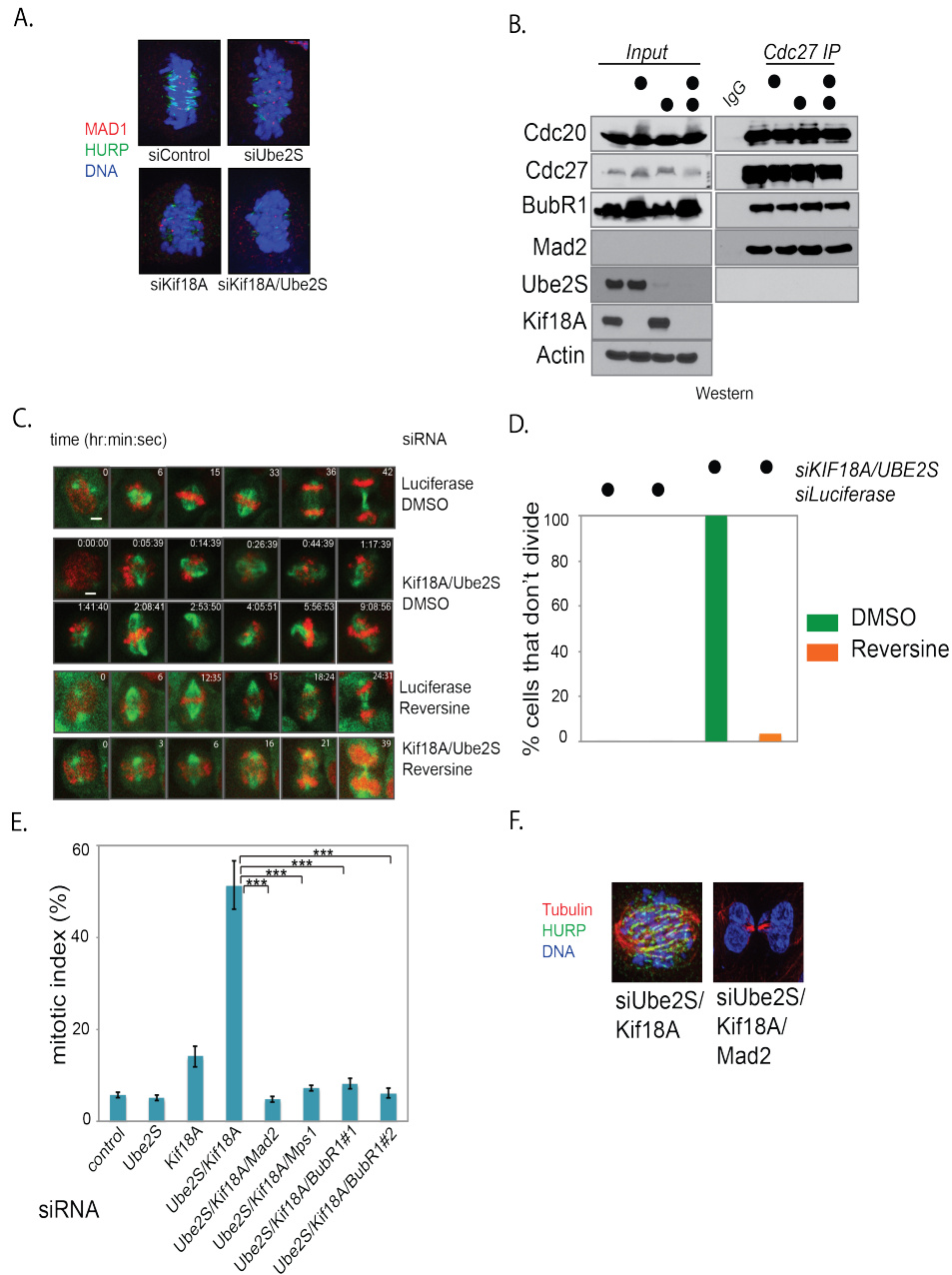


Figure 3. Spindle Assembly Checkpoint (SAC) signaling is required for maintaining the mitotic arrest caused by co-depletion of Ube2S and Kif18A. (A) At least one Mad1 focus is present in cells depleted in each condition, indicative of an active spindle assembly checkpoint (SAC). (B) Depletion of Kif18A and/or Ube2S does not change protein composition of the APC/C. Cells were transfected with siRNA and arrested in mitosis by thymidine-nocodazole. Extract was prepared from the conditions and APC/C or IgG was precipitated and assayed for co-purifying proteins by Western blot. In all conditions, the APC/C associates with MCC members BubR1 and Mad2. (C) SAC signaling is required to maintain the mitotic arrest caused by co-depletion of Ube2S and Kif18A. HeLa cells stably expressing GFP-tubulin and mCherryH2B were transfected with luciferase (mock) or Ube2S/Kif18A siRNA, and incubated for 24hr. Cells were then incubated with

DMSO or reversine (which inhibits SAC signaling) for 1hr, and were then subjected to video microscopy for the next 24hr. All cells divided in the luciferase condition, regardless of drug status, while the cells subjected to Ube2S/Kif18A siRNA only divided in the presence of reversine. (D) Quantification of the percentage of cells that fail to divide during the time course of the movie. (E) SAC activators Mad2, Mps1, and BubR1 are each required for the synergistic mitotic arrested caused by co-depletion of Ube2S and Kif18A siRNA. While Ube2S/Kif18A siRNA cause over 50% of cells to arrest in mitosis, loss of Mad2, BubR1, or Mps1 significantly decrease the mitotic index back to baseline mitotic index as exemplified in the mock condition. (F) Immunofluorescence of cells treated with Ube2S/Kif18A siRNA identified mitotic cells with chromosome alignment and spindle defects. When Mad2 was reduced in combination, cells were able to degrade HURP (green), indicating an active APC/C, and divided with lagging chromosomes, indicative of a defective SAC. HURP is shown in green, DNA in blue, and tubulin in red. In all conditions of each experiment, the total amount of siRNA added to cells was constant.

Ube2S regulates microtubule flux and promotes kinetochore oscillations

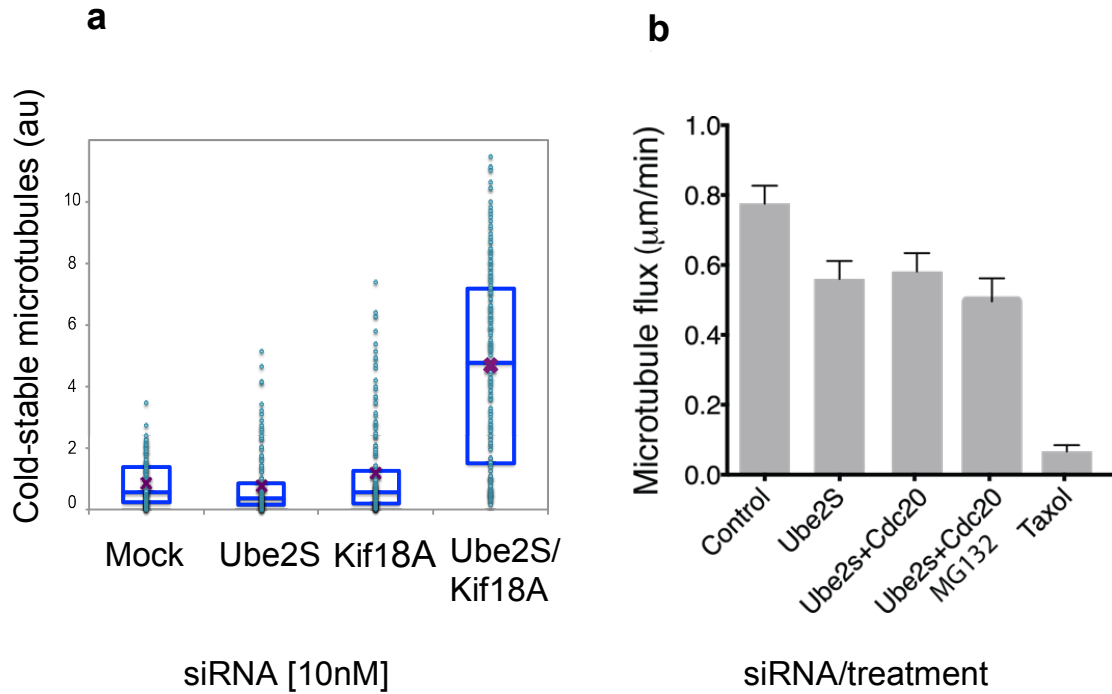
Ube2S and the APC/C genetically interact with regulators of microtubule dynamics in early mitosis. Co-depletion of Ube2S with a genetic interactor result in prolonged mitotic arrest prior to metaphase. This led us to ask whether Ube2S also played a role in regulating spindle assembly. If so, we hypothesized that loss of Ube2S's regulatory function in combination with depletion of a genetic interactor could result in inability to enter anaphase through a direct or indirect block to MCC disassembly.

We began by analyzing how cells depleted of Ube2S responded to an additional challenge to microtubule dynamics by the addition of taxol, a drug that stabilizes microtubules and therefore abolishes proper spindle dynamics, leading to mitotic arrest (Yvon, et al., 1999; Waters, et al., 1996; Figure 1C). These results, not shown here due to their preliminary nature, suggested that cells depleted of Ube2S specifically are sensitized to taxol treatment.

Taxol stabilizes microtubules and abolishes microtubule flux. We wondered if Ube2S also changed the stability of microtubules in mitosis. In order to examine this possibility, we quantified the percentage of microtubules remaining after cold treatment, which depolymerizes labile microtubules at a faster rate than the more stable kinetochore fibers (DeLuca, 2010). We expected that if Ube2S also stabilized spindle microtubules, we would see a higher amount of cold stable microtubules after treatment. However, depletion of Ube2S did not significantly increase the amount of cold stable microtubules (Figure 4A). Unexpectedly, however, we did observe a significant increase in cold stable microtubules after co-depletion of Ube2S and Kif18A (Figure 4A). This effect was synergistic in nature, as neither Ube2S nor Kif18A depletion alone resulted in an increase in cold stable microtubules, but the combined depletion led to enhancement.

Why would loss of Ube2S lead to sensitivity to spindle defects? While several potential explanations exist, we wished to frame our understanding in light of the genetic interaction profile detailed earlier in the chapter. It has been shown that taxol treatment lead to a reduction in the distance between two sister kinetochores of a pair (Waters, et al., 1996; Khodjakov and Kapoor, 2005), likely

as a result of altered microtubule dynamics. We therefore asked if Ube2S may also play a role in regulating kinetochore dynamics. This could explain both the genetic interactions with kinetochore-microtubule dynamics regulators and the taxol sensitivity data. We began by imaging kinetochore dynamics in a LAP-GFP-CENPA cell line (gift from Iain Cheeseman) in cells depleted of Ube2S or Ube2S/Ube2C. We qualitatively observed that, while kinetochores aligned at the metaphase plate in cells lacking APC/C E2 activity, the alignment at the metaphase plate appeared less dynamic as compared to mock cells (data not shown), and perhaps showed a defect in oscillation about the metaphase plate.



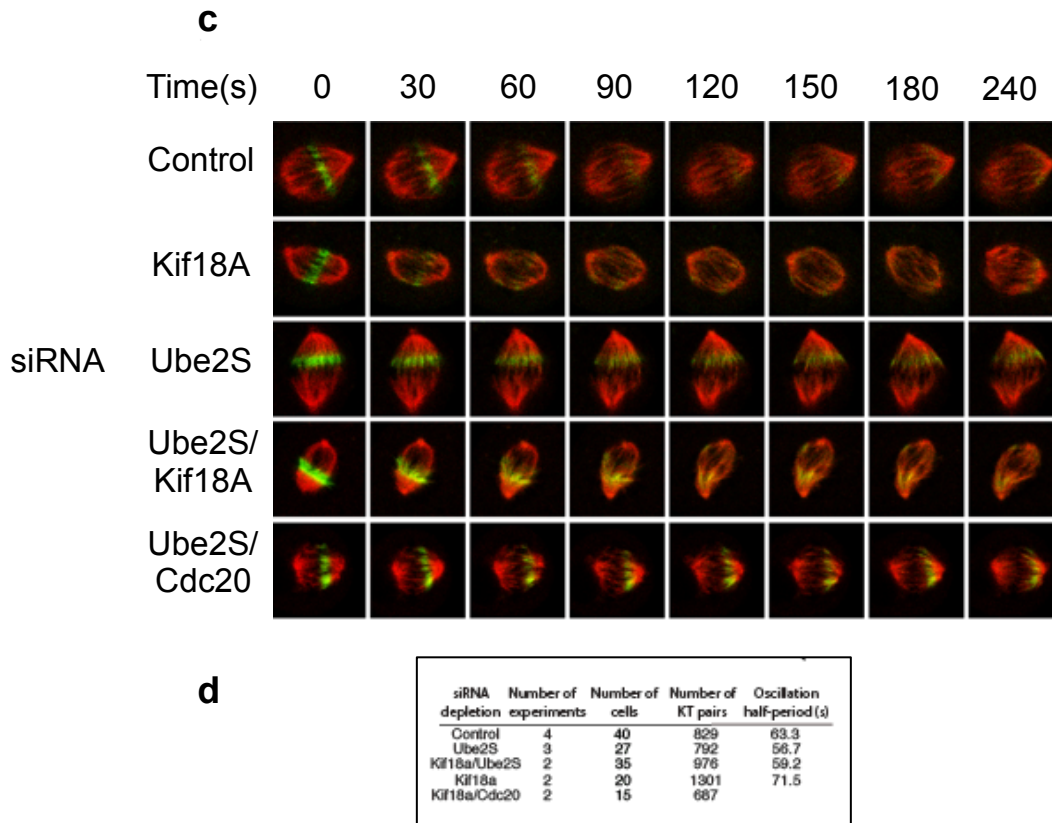


Figure 4. Ube2S is important for proper microtubule spindle dynamics. (A) Concurrent loss of Ube2S and Kif18A results in a significant increase in the amount of stable microtubules that withstand 15min at 4°C, which induces depolymerization of labile microtubules. (B) Ube2S-depleted cells experience a significant decrease in prometaphase microtubule flux. Prometaphase U2OS cells expressing mCherry-tubulin and photo-activatable GFP-tubulin were exposed to laser light at the microtubule plus ends, and the movement (flux) of the photoactivated region (on one half of the spindle) toward the spindle pole was tracked over time. (C) Representative microscopy images of cells quantified in (B). (D) Ube2S depletion significantly dampens kinetochore oscillations about the metaphase plate. Kinetochore oscillations were measured as previously described (Jaqqaman, et al., 2010).

However, to gain an in depth understanding of how Ube2S could control kinetochore dynamics, we first examined microtubule flux in prometaphase cells. Utilizing a U2OS cell line expressing both mCherry tubulin and photo-activatable GFP tubulin, we measured the amount of poleward directed microtubule flux after depletion of various factors. Interestingly, Ube2S depletion alone resulted in a significant decrease in flux (Figures 4B-4C). However, this effect was not enhanced by further depletion of APC/C activity by Cdc20 siRNA, suggesting that this effect was caused by stabilization of a protein substrate that requires Cdc20 for its degradation. Strikingly, this suggests a direct effect of Ube2S depletion on

spindle dynamics in prometaphase, although the functional consequence of this regulation is not yet clear.

We wished to know if our qualitative observation of kinetochore oscillation defects in the absence of Ube2S was correct. Again using a GFP-CENPA cell line, we quantified the dynamics of kinetochore oscillations under various conditions. Quantitative analysis of Ube2S depletion demonstrated a significant dampening of kinetochore oscillations. The dampening of kinetochore oscillations in Ube2S depleted cells suggested that the APC/C plays an important role regulating kinetochore dynamics; while the APC/C has been implicated in MCC dynamics and some protein degradation during prometaphase, these processes do not explain why loss of Ube2S would affect kinetochore oscillations. While we speculate further on the causes and consequences that APC/C activity has upon prometaphase kinetochore oscillations, we do not currently understand the significance of this result. However, these data did promote us to think about how limiting APC/C activity in prometaphase and analyzing the consequences could help us better understand important functional roles of the APC/C in prometaphase.

Identification of the early mitotic APC/C interactome

We decided to take a proteomics approach to identify novel possibilities of APC/C function in early mitosis. As APC/C activity is low in prometaphase, we decided to examine the APC/C interactome when APC/C activity is limited. We took two approaches to limiting APC/C activity; first, we expressed dominant negative Ube2C, the APC/C initiation E2; second, we inhibited the proteasome by MG132 treatment. Both of these approaches were used in HeLa cells that were persistently arrested in mitosis with a monopolar spindle through the addition of STLC (Ogo, et al., 2007). The APC/C^{Cdc20} interactome was generated by mass spectrometry, and the increase in interactors when APC/C was inhibited was compared to wildtype APC/C prometaphase interactors with the help of statistical analysis through CompPASS (Sowa, et al., 2009; Figure 5A).

As expected, limiting APC/C activity resulted in increased MCC and SAC binding (Figure 5B), as well as that of known interactors, such as Cyclin A. Unexpectedly, however, we also identified the SAC effector KNL1 and all three members of the PP2A^{B⁵⁶} complex bind APC/C in an enhanced fashion when ubiquitylation activity was further limited in prometaphase (Figure 5B, see also

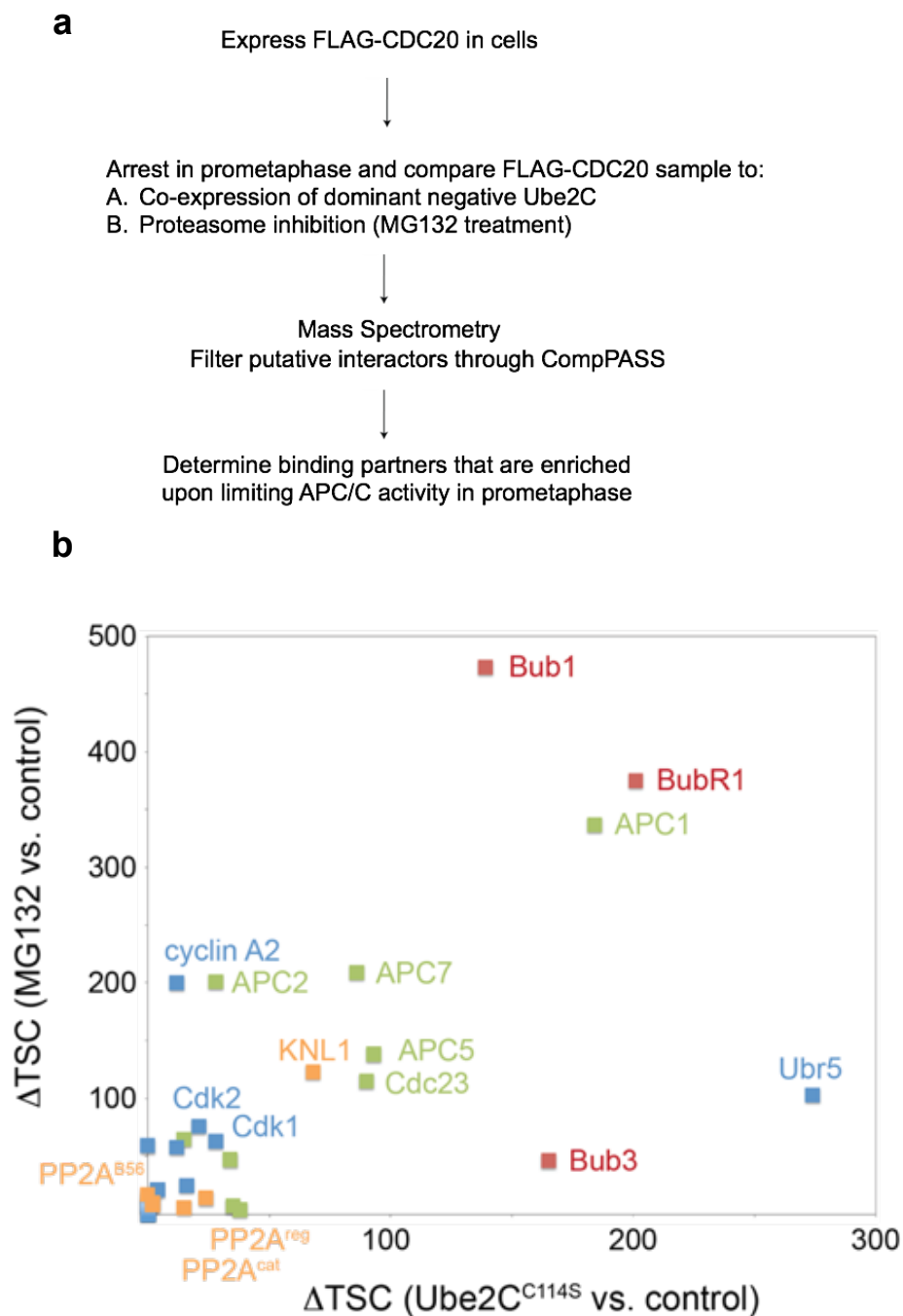


Figure 5. Identification of the early mitotic APC/C interactome. (A) Schematized experimental design. HeLa cells transiently expressing FLAG-CDC20 were subjected to limited APC/C activity by either 1) co-expression of dominant Ube2C enzyme (C114S), or 2) proteasome inhibition by MG132, and arrested in early mitosis by thymidine/STLC treatment. FLAG-CDC20 interactors determined by mass spectrometry were assigned confidence values and filter through the

statistical software database CompPASS (Sowa, et al., 2009). The abundance of high confidence interactors in each of the limited APC/C activity samples was compared to a FLAG-CDC20 IP with wildtype APC/C activity. Factors that are highly enriched or only detected in C114S or MG132 samples are likely novel and/or important factors of the APC/C prometaphase interactome. (B) Samples were collected from at least two independent IP/mass spectrometry runs per condition. The change in total spectral count from the FLAG-CDC20 interactome was compared to the absolute value of the limited APC/C activity interactome. Enriched proteins encompass known and unexpected protein families: MCC (red), APC/C components (green), APC/C substrates and known interactors (blue), as well as all three components of the PP2A^{B56} complex and the phosphatase-MCC linker protein, KNL1 (orange).

Figure 6B). The enhancement of PP2A^{B56} binding was confirmed through endogenous Cdc20 validation experiments (Figure 6A), as well as to an alternative immunoprecipitation approach to generating endogenous APC/C (Figure 6C). This suggests that phosphatases and the APC/C interact during prometaphase. While APC/C has previously been linked to phosphoregulation in early mitosis (Peters, 2006), to our knowledge, PP2A^{B56} binding was not known. It had, however, recently been linked to binding of BubR1 (Suijkerbuijk, et al., 2011), and had been known to re-localize to the kinetochore once tension was present (Foley, et al., 2011).

To begin to develop an understanding of why PP2A interacts with the APC/C, we wanted to know if the interacting pool represented an active fraction. Again, we generated prometaphase APC/C^{Cdc20} with limited activity through MG132 treatment, and we analyzed whether phosphatase activity was present through incubation of the immunopurified APC/C with a threonine phosphopeptide, and measurement of the amount of free phosphate generated. Results mirrored that of the PP2A^{B56} binding assay, as immunoprecipitation of Cdc20+MG132 resulted in a strong, dose-dependent amount of phosphate removed from the peptide (Figure 7A).

As this assay does not distinguish between PP2A, PP1, or other phosphatases that could be present in the reaction, we performed the same Cdc20 immunoprecipitation in the presence of STLC and MG132, and incubated the binding reaction with increasing amounts of the phosphatase inhibitor, okadaic acid. The IC₅₀ for the reaction was 4.65nM okadaic acid. This value is more consistent with published data in which PP2A is completely inhibited near 2nM in mammalian tissue extracts, whereas greater than 1000nM was required for complete inhibition of PP1 (information obtained from media.cellsignal.com and Cohen, et al., 1989) (Figure 7B).

However, the binding of PP2A to APC/C^{Cdc20} was not stable over time. We discovered that if we generated APC/C^{Cdc20} bound to PP2A on beads, and incubated the complex at room temperature, PP2A was quickly lost from the complex (Figure 7C). Also, performing washes of immunoprecipitations of APC/C^{Cdc20} and PP2A resulted in loss of phosphatase (data not shown). This suggests that phosphatase activity either weakly binds to the complex intrinsically, or possibly that its activity results in release. The amount of MCC bound appeared to be relatively stable, through the assessment of BubR1 binding, suggesting that loss of PP2A binding was not linked to MCC

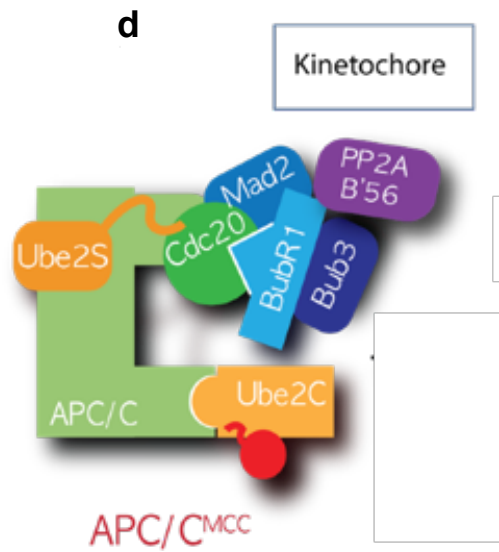
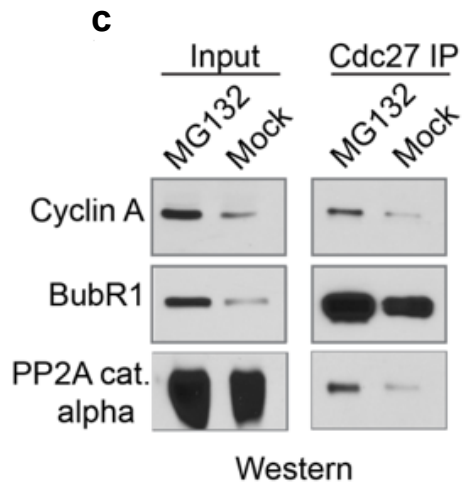
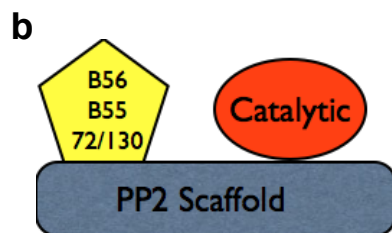
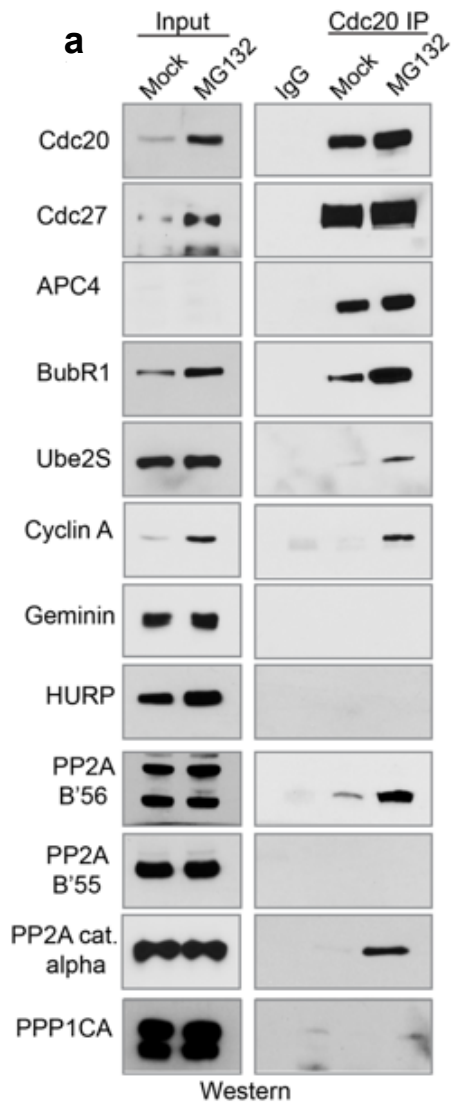
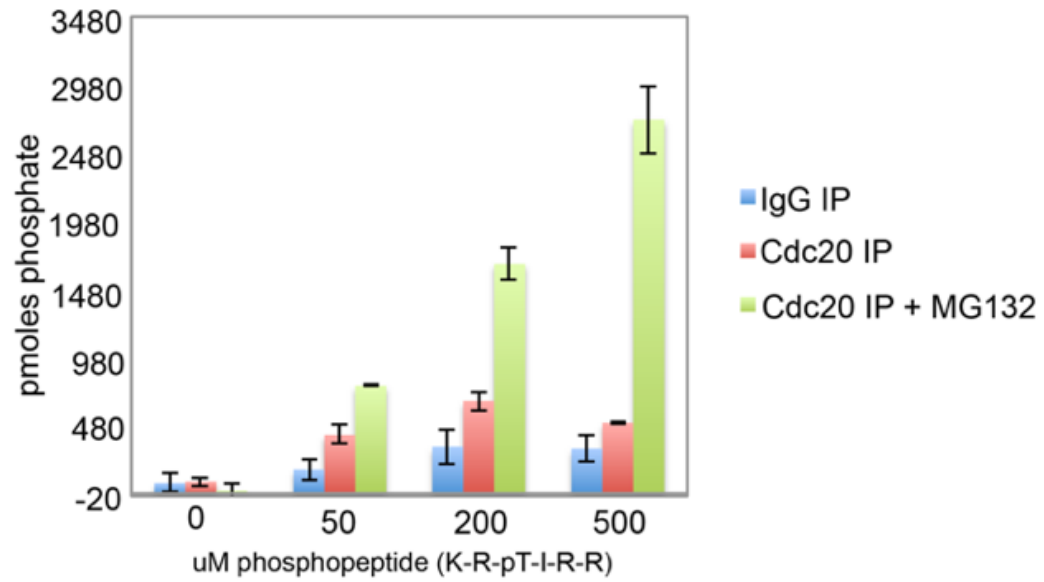
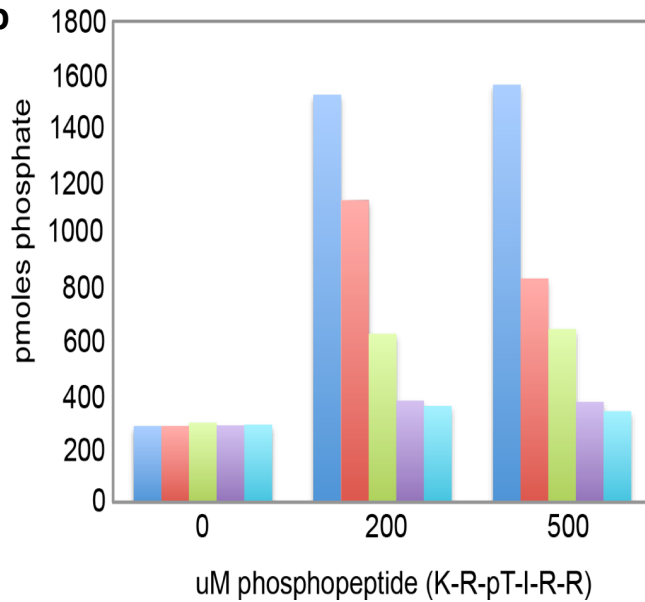
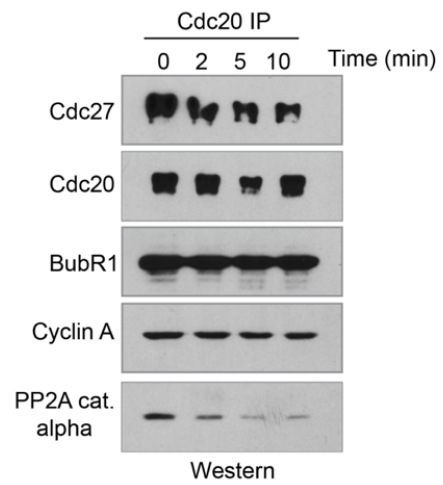


Figure 6. APC/C^{CDC20} interacts with PP2A^{B'56} in prometaphase. (A) Validation of FLAG-Cdc20 interaction data by endogenous Cdc20 IP from cells treated with STLC in the presence of absence of MG132. Cdc20 and Cyclin A inputs are stabilized by MG132. As substrates known to be degraded in prometaphase, this validates the presence of proteasome inhibition in prometaphase. Substrates degraded at metaphase, however, such as geminin and HURP (Song, et al., 2014), are not affected by proteasome inhibition in STLC-treated cells. In addition, Cdc20 binds known interactors: APC/C and MCC components, and the interaction between Cdc20 and the PP2A^{B'56} complex is validated. As specificity controls, we assayed for binding to the PP1 catalytic subunit and a different PP2A substrate recognition protein, B'55. Neither bound Cdc20 in this assay, suggesting a specific interaction between Cdc20 and PP2A^{B'56}. (B) Schematic of the PP2A complex, composed of catalytic, regulatory, and substrate adaptor subunits. Multiple isoforms of each complex member exist. While multiple isoforms were detected in our FLAG-Cdc20 mass spectrometry assay, only the B'56 substrate adaptor (and not B'55, 72, or 130) was detected. (C) APC/C^{CDC20} interacts with PP2A in a proteasome-dependent manner. (D) Schematic of novel APC/C^{CDC20} prometaphase interactome data, depicting the PP2A B'56 complex and the kinetochore.

disassociation (Figure 7C). We have not yet followed up on this role, although the implications for this observation *in vivo* could be very fruitful.

We detected PP2A^{B'56} binding to APC/C^{Cdc20} through immunoprecipitation of either Cdc20 or Cdc27, a core APC/C subunit. However, it has also been reported to bind BubR1 (Suijterbuijk, et al., 2012). If bound to Cdc20 directly or if brought to APC/C through MCC binding, the presence of Cdc20 would be required. Indeed, if we depleted Cdc20 via siRNA, and pulled down endogenous APC/C from mitotic HeLa cells, both MCC and PP2A binding were lost, while the core composition of APC/C was unaffected (Figure 8A). This suggests that PP2A^{B'56} could bind Cdc20 directly, or most likely, could bind via BubR1 contained within the MCC in order to associate with APC/C^{Cdc20}. Regardless of the direct binding partner, these data suggest that PP2A^{B'56} specifically interacts with APC/C^{Cdc20} (and not APC/C^{Cdh1}, which is the predominant form of the ligase in anaphase and G1).

We also expected that if APC/C activity was limited by Ube2S depletion, that we would detect an increase in PP2A activity associating with APC/C^{Cdc20}. Interestingly, this was not the case (Figure 8B). While Ube2S was depleted from cells (Figure 8C), the amount of phosphatase activity that associated with APC/C^{Cdc20} was not significantly higher in the absence of Ube2S. Though initially puzzling, this result could be informative, as it could suggest that loss of ubiquitin amplification through Ube2S is not the mechanism by which PP2A associates with the APC/C. A second explanation is that Ube2C must also be depleted in order to stabilize PP2A upon the APC/C; we have preliminary evidence via a separate assay monitoring PP2A binding to the APC/C suggesting that this may be the case.

a**b****c**

[okadaic acid]

Figure 7. PP2A phosphatase activity co-precipitates with APC/C^{CDC20}. (A) Endogenous Cdc20 or IgG was IP'ed from cells arrested in thymidine/STLC minus or plus proteasome inhibition by MG132. Cells were harvested and normalized to total protein levels prior to IP. FLAG resin bound to protein interactors was thoroughly washed, and incubated with a threonine phosphopeptide (K-R-pT-I-R-R) at increasing concentrations and incubated to allow for Cdc20-bound phosphatases to dephosphorylate. A phosphate indicator dye was added to each reaction, and the amount of free phosphate was quantified by fluorescent plate reading of the detection dye at A_{630nm}, and compared to a phosphate standard curve. Results from at least three independent experiments are shown. (B) Cdc20-bound phosphatase activity can be attributed to PP2. HeLa cells treated with thymidine/STLC/MG132 were IP'ed for Cdc20 and treated as described in (A). However, the phosphatase inhibitor okadaic acid [0-100nM] was added to reactions prior to addition of the phosphothreonine peptide. The IC₅₀ for the reaction was 4.65nM okadaic acid, which is closer to the published IC₅₀ for PP2 inhibition (0.1nM, completely inhibited near 2nM in mammalian tissue extracts), but much further from the levels of drug needed for PP1 inhibition (IC₅₀: 15-20nM, complete inhibition >1000nM in mammalian tissue extracts) (information obtained from media.cellsignal.com and Cohen, et al., 1989). (C) PP2A binding to Cdc20 is unstable. HeLa cells were arrested with thymidine/STLC and MG132 was added to enrich phosphatase binding to the APC/C. Endogenous Cdc20 was IP'ed and incubated at room temperature, shaking, for 0, 2, 5, or 10min. Cdc27, BubR1, and Cyclin A are stably bound over this timecourse, but PP2A binding to Cdc20 decreases dramatically over time.

The possibility of two independent functions for Ube2S and PP2A^{B'56} was very intriguing. As the role of Ube2S as an APC/C E2 is well documented (Kelly, et al., 2014; Meyer and Rape, 2014; Wickliffe, et al., 2009; Wickliffe, et al., 2011), we wished to examine whether PP2A^{B'56} also participates in APC/C activation. We first generated HeLa mitotic extract in which APC/C was inhibited. We pre-incubated the extract with or without okadaic acid, and then induced APC/C activity by the addition of Ube2C, energy mix, and ubiquitin. While substrates were degraded with expected kinetics in the solvent control, blocking phosphatase activity by okadaic acid resulted in stabilization of the same substrates (Figure 9A). Notably, substrates, as well as Cdc27, experienced a migratory shift in the okadaic acid samples, as well.

This result suggested that phosphatases may act to promote APC/C activity in prometaphase. To confirm this, we examined the ubiquitylation of a well-characterized, metaphase APC/C substrate, geminin. We generated mitotic HeLa extract, preincubated with vehicle or okadaic acid, and charged the APC/C in the presence of his-ubiquitin, energy mix, and exogenous Ube2S. A his-ubiquitin K11R mutant that cannot participate in amplified K11 chains was used as an APC/C control. After incubation, we performed a denaturing NiNTA pulldown and examined the endogenous modification of geminin through western blot. Similar to our degradation assay results (Figure 9A), inhibiting phosphatase activity resulted in loss of geminin ubiquitylation by the APC/C (Figure 9B).

Our results demonstrate integration of ubiquitylation and phosphatase activity in order to promote rapid and efficient APC/C activation at prometaphase.

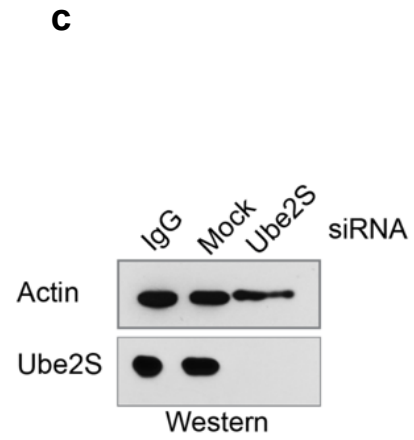
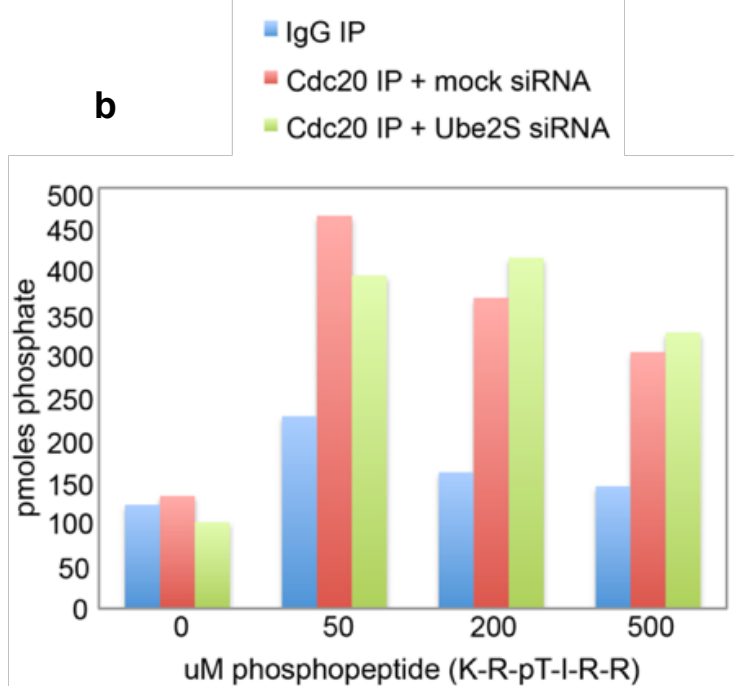
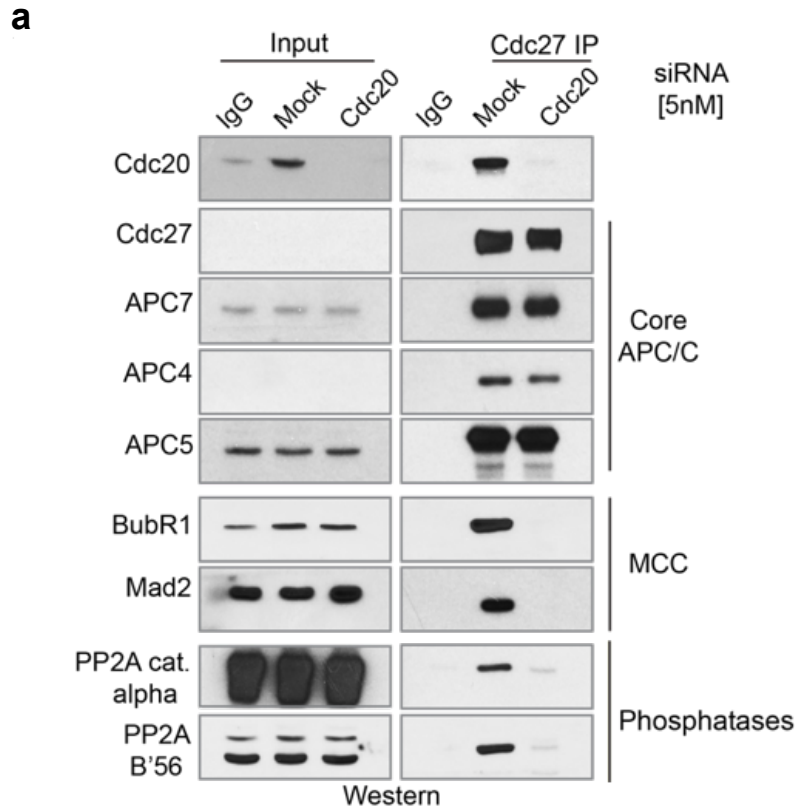


Figure 8. Cdc20, but not Ube2S, is required for PP2A association with APC/C in prometaphase. (A) Depletion of Cdc20 results in loss of MCC and PP2A^{B'56} from the APC/C interactome. HeLa cells were treated with mock or Cdc20 siRNA and arrested in mitosis by thymidine/STLC. Extract was prepared and normalized, and either IgG or APC/C (via endogenous Cdc27) was IP'ed from

each condition. APC/C components (Cdc27, APC7, APC4, and APC5) were unaffected by loss of Cdc20; however, MCC components BubR1, Mad2, and PP2A^{B56} were lost from the APC/C. (B) Ube2S depletion does not increase phosphatase activity that co-precipitates with the APC/C. Cells were treated with mock or Ube2S siRNA and arrested in mitosis by thymidine/STLC. IgG or Cdc20 was IP'ed from the normalized extract. After careful washes of the binding reactions, phosphothreonine peptide was incubated with the reaction, and phosphatase activity was assayed by presence of a phosphate detection dye and absorbance reading at A_{630nm}. (C) Inputs for the phosphatase reaction in (B).

Discussion

In this chapter, we provide evidence that Kif18A, Knl1, Hec1, and Sgo1 are novel APC/C genetic interactors. We originally identified these proteins as genetic interactors of Ube2S in a screen aimed at further elucidating the role of Ube2S-catalyzed ubiquitin chains on proper cell cycle progression. Interestingly, the genetic interactors have multiple commonalities: first, they play important roles in prometaphase near the site of kinetochore-microtubule attachment. Kif18A, a plus-end directed kinesin, concentrates at the plus ends of microtubules where it regulates the stability of microtubule plus ends by regulating the movement of centromeres (Jaqaman, et al., 2010; Stumpff, et al., 2008; Stumpff, et al., 2012). Hec1 and Knl1 are components of the outer kinetochore that help regulate microtubule-kinetochore attachment (DeLuca, et al., 2005; Welburn and Cheeseman, 2008), and Sgo1 is found at the centromere and protects sister chromatid cohesion (Hong, et al., 2013).

Second, due to their important prometaphase functions, the genetic interactors are important for proper chromosome segregation and timely completion of cell division. Third, they all have links to protein phosphatase 1 and 2 activities in prometaphase. For example, Sgo1 and PP2A directly interact to ensure sister chromatid cohesion (Clift, et al., 2009; Hong, et al., 2013; Xu, et al., 2009). Knl1 has been shown to bind PP1 in a manner important for spindle assembly checkpoint silencing (Liu, et al., 2010; Rosenberg, et al., 2011). In yeast, Kif18A was shown to interact with PP1 via a motif conserved in metazoans (Meadows, et al., 2011). Intriguingly, PP1 and PP2 subunits also scored as weak APC/C genetic interactions. Taken together, we have found that prometaphase regulators of the microtubule plus end/kinetochore interface and phosphatases are essential when APC/C activity is depleted.

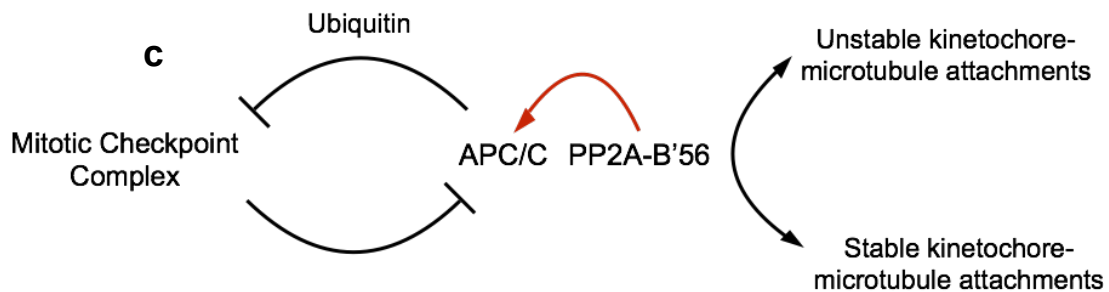
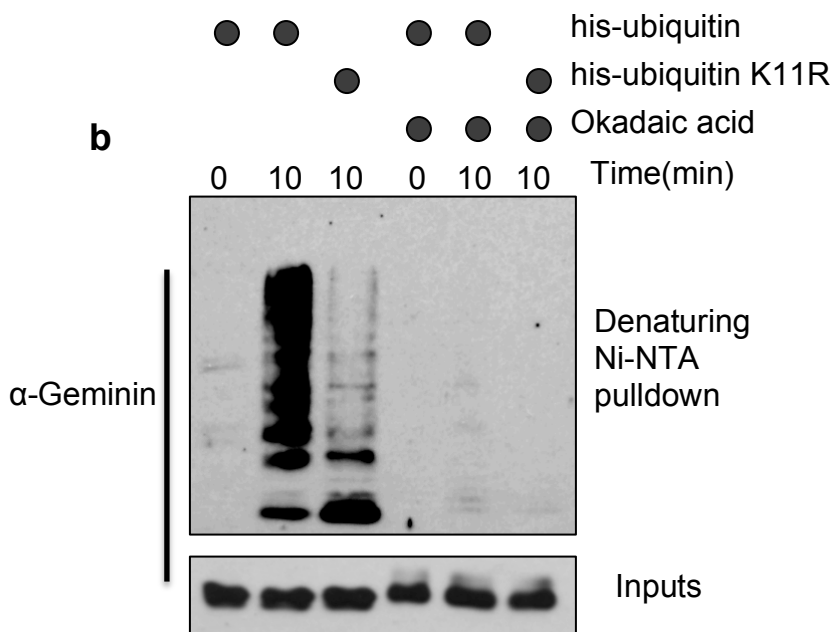
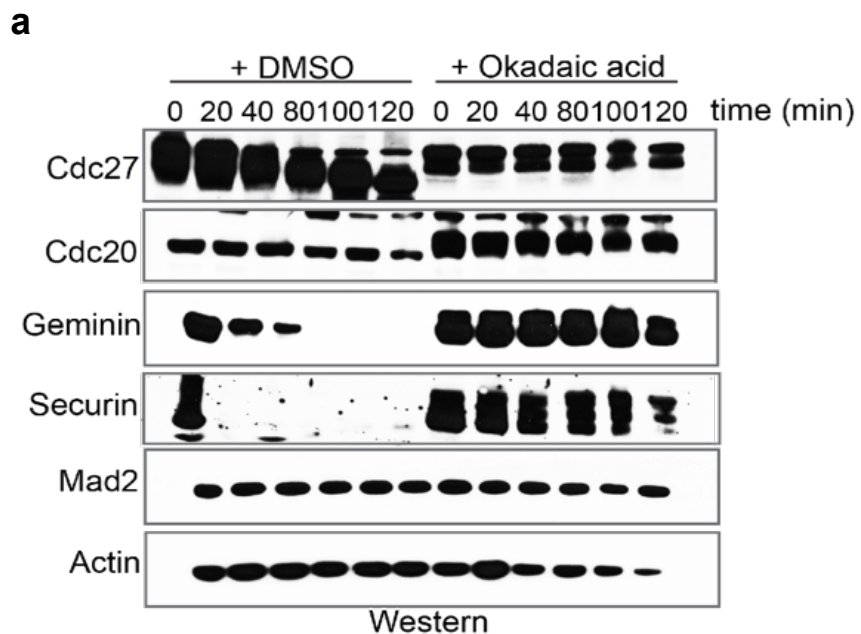


Figure 9. Phosphatase activity is required for efficient APC/C activation. (A) HeLa cell mitotic extract (thymidine/STLC) was pre-incubated with either DMSO or okadaic acid for 30min, and APC/C was activated by addition of ubiquitin, Ube2C, and energy mix. Protein stability was assayed in a timecourse assay. Cdc20, geminin, and securin were degraded in the DMSO reaction, but largely stabilized in the okadaic acid pre-treated cell extract. Efficient dephosphorylation of Cdc27, and a shift in protein mobility in Cdc20, geminin, and securin in the DMSO, but not okadaic acid, treated extract provided a control for the okadaic acid treatment. (B) Geminin is not efficiently ubiquitylated by APC/C that is treated with phosphatase inhibitor. HeLa cell extract (thymidine/nocodazole) was prepared and pre-incubated with either DMSO or okadaic acid for 30min. APC/C activity was stimulated by addition of his-ubiquitin, Ube2C, and energy mix for 0 or 10min. As an APC/C control, his-ubiquitin-K11R was added in place of wildtype ubiquitin. The K11R mutant does not allow for ubiquitin chain elongation through K11 by Ube2S. A denaturing his-ubiquitin pulldown was performed, and geminin ubiquitylation status was analyzed by Western blot. Geminin is robustly ubiquitylated by his-ubiquitin as compared to the K11R ubiquitin mutant in the DMSO treated samples. However, preincubation with okadaic acid resulted in loss of efficient ubiquitylation of geminin. (C) Model of APC/C activation by Ube2S and PP2A^{B⁵⁶}. In early mitosis, the mitotic checkpoint complex and the APC/C dynamically regulate one another through ubiquitylation, requiring Ube2S. PP2A^{B⁵⁶}, which monitors the stability of kinetochore-microtubule attachment status, contributes to APC/C activation, and provides a direct link between checkpoint expiration, APC/C activation, and the attachment status of kinetochore-microtubules.

In support of this hypothesis, we observed that cells arrest permanently in a pre-anaphase state when Ube2S and a genetic interactor are co-depleted. The arrest is characterized by evidence of an active SAC, microtubule spindle defects, and misalignments of kinetochores. Why does attenuating APC/C activity cause a permanent pre-anaphase arrest when kinetochore-microtubule dynamics are disturbed? Pre-anaphase, APC/C activity is believed to be low due to its dynamic inhibition by the mitotic checkpoint complex (MCC) (Reddy, et al., 2007; Varetti, et al., 2011), which blocks the APC/C co-activator, CDC20, from recognizing its substrates. Therefore, the only APC/C substrates thought to be robustly degraded in early mitosis are those that are 'invisible' to the MCC inhibition, including Nek2A (Hames, et al., 2001), Cyclin A (den Elzen and Pines, 2001; Geley, et al., 2001), and CDC20 itself (Reddy, et al., 2007; Uzunova, et al., 2012; Foster and Morgan, 2012; Varetti, et al., 2011). In this work, however, we demonstrate an important role for ubiquitylation prior to removal of SAC signaling and anaphase onset.

Several different mechanisms could explain these data. First, we may have uncovered evidence for novel 'MCC-invisible' substrates. As the APC/C genetic interactors play important roles at the plus ends of spindle microtubules, our interactome data may suggest that novel APC/C substrate(s) exist primarily at the spindle pole, and/or regulate microtubule minus ends. These putative substrates would increase in abundance when APC/C activity is diminished by depletion of Ube2S (Meyer and Rape, 2014; Williamson and Wickliffe, et al., 2009), disrupting forces on microtubule dynamics. Further loss of microtubule plus-end regulators would further disrupt the balance of forces, leading to a synergistic block to proper cell division. Supporting this potential explanation,

previous works have shown that perturbations at one end of the microtubule spindle can be at least partially ameliorated by a corresponding perturbation at the opposing end to restore the balance of forces (Cai, et al., 2009; Stumpff, et al., 2012). If this hypothesis was correct, by identifying and artificially lowering the substrate(s) abundance, we should significantly rescue the deleterious effects of the co-depletion of Ube2S and a plus end genetic interactor.

A related explanation for the synergistic mitotic arrest is that Ube2S and the APC/C target important protein substrates for ubiquitylation, but that the ubiquitin marks play a structural rather than proteolytic function in early mitosis. In this case, the protein substrates would be more difficult to extract, as tuning the level of the protein substrate down would not rescue the synthetic mitotic arrest due to the co-depletion. However, we may expect to see localization changes of these substrate(s), or differences in the components of different regulatory complexes.

In the process of exploring the mitotic arrest caused by co-depletion of Ube2S and Kif18A, we did discover proteins that, when depleted in a Ube2S/Kif18A-siRNA background, caused suppression of the arrest. All but one of these suppressor proteins identified were integral components of the MCC and SAC. Analysis and experimentation regarding the additional suppressor protein is discussed in Appendix A. Regarding the SAC suppressor proteins, our data demonstrate that active SAC signaling is required for maintenance of the mitotic arrest caused by Ube2S and Kif18A siRNA. However, we were unable to discover evidence that the persistence of these proteins increased due to co-depletion conditions, or that increased presence was necessary for the arrest.

The SAC suppressor proteins identified, Mad2, MPS1, BubR1, are not believed to be APC/C substrates. However, they do participate integrally in the inhibition of APC/C in early mitosis. It is likely is that loss of the SAC proteins suppresses the mitotic arrest because cells are unable to pause anaphase. A second, and not mutually exclusive possibility is that our genetic interaction profile has uncovered new links between APC/C activity and kinetochore-microtubule dynamics in early mitosis. While SAC signaling is necessary for the mitotic arrest, it may also be the case that SAC inhibition or removal is also affected under conditions in which APC/C activity and a genetic interactor have been depleted.

Multiple lines of evidence had previously caused us to consider a direct role for Ube2S in spindle-microtubule dynamics. We began by investigating whether or not depletion of Ube2S would sensitive cells to an additional challenge to spindle microtubule dynamics. We reasoned that if Ube2S played a spindle regulatory role, a drug such as taxol might result in synergistic effects, similar to those observed when Ube2S was co-depleted with a genetic interactor. Indeed, cells depleted of Ube2S were sensitized to the drug, as at an equivalent concentration of taxol, cells depleted of Ube2S exhibited a larger pool of cells arrested in mitosis, while depletion of Ube2S itself shows no significant difference in mitotic index compared to mock depletion when only vehicle is added (data not shown). While this result again suggested that Ube2S plays a role in spindle

dynamics, it does not elucidate a particular function for the protein or for the APC/C complex in a specific process.

We have also qualitatively observed that cells depleted of Ube2S or Ube2S/Ube2C experienced a lag in completion of metaphase (data not shown; Meyer and Rape, 2014), punctuated by kinetochores that appeared static (data not shown). This suggested that Ube2S could either play a role in regulating the movement of kinetochores themselves, or perhaps could regulate microtubule flux or plus end dynamics. Both regulatory processes could also serve as an explanation for how Ube2S genetically interacts with proteins such as Sgo1, Hec1, and Kif18A. Additionally, it has been shown that kinetochore-microtubule attachment stability is significantly less stable in prometaphase when compared to the same cell in metaphase (Kabeche and Compton, 2013). We reasoned that Ube2S could promote this attachment stability transition so we examined these qualitative observations in quantitative detail.

Precise measurements of microtubule flux in prometaphase and kinetochore oscillations in metaphase showed roles for Ube2S in the regulation of both processes. Both microtubule flux and kinetochore oscillations were significantly dampened when Ube2S is depleted. While we expected that Ube2S and the APC/C might have an effect in one or both of these processes, we were still struck by these results, as they have demonstrated that Ube2S, indeed, has underlying roles in microtubule dynamics. Neither prometaphase microtubule flux nor kinetochore oscillations are strictly required for progression through mitosis (Jaqaman, et al., 2010), while they both likely contribute to the fidelity of sister chromatid separation and segregation. These results help explain why depletion of Ube2S in an otherwise unchallenged mitosis leads to a mitotic delay, but no overt effects (Meyer and Rape, 2014). Compensatory mechanisms to regulate these early mitotic events exist, likely by APC/C genetic interactors, and loss of both the functions of Ube2S and the APC/C, as well as one of their genetic interactors, would therefore be required to cause dramatic mitotic consequences.

MCC, phosphatases, and receptors accumulate on APC/C^{Cdc20} when autoubiquitylation is blocked in prometaphase

While defining a precise role for Ube2S on kinetochore function was both exciting and explanatory, it still does not explain the mechanism through which Ube2S and the APC/C regulate early mitotic processes. We decided to further investigate the mechanism of action, and took to a proteomics approach to examine what proteins accumulated upon the APC/C when its activity was limited in early mitosis, such as by proteasome inhibition. Excitingly, when we limited APC/C activity, we found that proteins involved in kinetochore-microtubule attachment regulation (KNL1 and PP2A^{B⁵⁶}) and MCC both accumulated. Interactions were dependent on the presence of Cdc20, and the interaction was validated by both endogenous binding assays, as well as phosphatase assays. Interestingly, the binding of PP2A to the APC/C was not stable. If a pool of PP2A-bound APC/C was generated, the amount of PP2A was found to rapidly decrease over the timespan of several minutes.

It would be important, however, to complete an analysis of MCC disassociation from the APC/C in prometaphase. It is possible that the increase of PP2A upon APC/C^{Cdc20} when dominant negative Ube2C is present or the proteasome is inhibited is due to loss of MCC dynamic on/off rates. Perhaps Ube2S depletion, while critical for degradation of MCC-invisible substrates, does not significantly change the dynamics of MCC binding and release. On the other hand, the opposite scenario could be true. For example, Cdc20 must be ubiquitylated in order for MCC to disassociate (Reddy, et al., 2007). If Cdc20 ubiquitylation is dependent upon Ube2S as suggested earlier (Meyer and Rape, 2014), it is possible that the MCC dynamics are even more static than during either of the other methods of limiting APC/C^{Cdc20} activity. A third possibility is that Ube2S may promote the activation of PP2A activity, perhaps upon the APC/C. We favor the model in which Ube2S depletion causes a change in the dynamics of MCC binding to APC/C in prometaphase, therefore interrupting the timely initiation of anaphase. With an additional challenge to inactivating the checkpoint, such as interfering with kinetochore-microtubule dynamics, the cell is unable to proceed with proper sister chromatid segregation.

PP2A^{B'56} and Ube2S link kinetochore-microtubule attachment status to efficient checkpoint expiration by promotion of ubiquitylation

What transitory effect could PP2A^{B'56} have upon APC/C^{CDC20} binding? As PP2A has recently been shown to interact with BubR1, we wondered if it was possible that the MCC delivered PP2A^{B'56} to the APC/C, where it could then promote MCC disassembly by either direct or indirect means. As PP2A^{B'56} has been shown to counteract Aurora B, it seemed likely that PP2A^{B'56} would antagonize, rather than promote SAC signaling. We tested the role of PP2A in altering APC/C activity. Strikingly, when the APC/C was activated, but when dephosphorylation was blocked, the degradation and ubiquitylation of APC/C targets was significantly decreased (9A-9B).

PP2A^{B'56} counteracts Aurora B phosphorylation of important kinetochore targets in order to promote kinetochore-microtubule attachment stabilization (Foley, et al., 2011). In addition, it is known to interact with MCC complex members, potentially in order to help control its localization to the kinetochore (Suijkerbuijk, et al., 2012). However, in this work, we have discovered that not only does PP2A^{B'56} promote kinetochore-microtubule attachment stabilization, it also cooperates with Ube2S in order to promote full activation of the APC/C (Figures 6A-B).

Therefore, taken together, this work illustrates that both the APC/C and other regulators of kinetochore-microtubule dynamics, such as PP2A, regulate spindle dynamics and APC/C activity, and thus represent integration points for MCC disassembly and amphitelic attachment sensing. One interesting observation that is not fully explained by this model is the effect that Ube2S has on dampening chromosome oscillations. Is it possible that MCC turnover itself can oscillate? The dynamic regulation of MCC turnover has been hypothesized to contribute to the efficient turnover of MCC so that APC/C can be

rapidly activated in order to promote the timely completion of mitosis (Craney and Rape, 2013; Reddy, et al., 2007, Varetti, et al., 2011). However it could also serve an additional role in helping to regulate the dynamics of microtubules plus ends themselves, perhaps by allowing for dynamic association and disassociation of proteins that regulate alter the phosphorylation status of the kinetochore.

Previously, both APC/C^{Cdc20} and PP2A^{B'56} have been shown to monitor and promote the stability of kinetochore-microtubule attachments between prometaphase and metaphase (Foley, et al., 2011: through antagonizing Aurora B; Kabeche and Compton, 2013: through degradation of Cyclin A). We and others have also demonstrated previously that Ube2S promotes the activity of APC/C in order to rapidly process the modification of the many APC/C substrates in mitosis (Meyer and Rape, 2014; Wickliffe, et al., 2009). This work adds a new link between APC/C^{Cdc20} activation and the monitoring of kinetochore-microtubule attachments through PP2A^{B'56}.

Our genetic interaction screen has revealed novel links between the mitotic ubiquitylation machinery and mechanisms that regulate microtubule dynamics and attachment status. These results support a mechanism by which the signal to initiate anaphase is coordinated by a sensor of the microtubule-kinetochore attachment interface via PP2A^{B'56} and activation of the APC/C by both Ube2S and PP2A^{B'56}. Further work to elucidate the specific targets of PP2A^{B'56} will be very important. For example, does dephosphorylation of certain marks on APC/C itself signify initiation of anaphase? Or, does PP2A^{B'56} regulate the stability of Cdc20 binding to the MCC in order to help distinguish between pools of APC/C^{Cdc20} and APC/C^{MCC}? Further research upon this mechanism will be both useful and fruitful in determining the precise mechanics of MCC disassembly at the kinetochore.

Table 1. Genes targeted by the mitotic siRNA library utilized for the Ube2S genetic interactome (see also Fig 1A-1B).

Gene Name	Protein Description
1. Kif11	Kinesin family member 11
2. Plk1	Polo-like kinase 1
3. Cdca8	Borealin
4. Birc5	Survivin
5. AurkB	Aurora kinase B
6. Stk6	Aurora kinase A
7. Incenp	Inner Centromere Protein
8. Kif2C	Kinesin family member 2C
9. CenpE	Centromere protein E
10. Kif2	Kinesin family member 2
11. Kif18A	Kinesin family member 18A
12. Ube2S	Ubiquitin-conjugating enzyme E2S
13. Ube2C	Ubiquitin-conjugating enzyme E2C
14. Fzr1	Cell division cycle 20
15. Kif22	Kinesin family member 22
16. Bub1B	Bub1 mitotic checkpoint serine/threonine kinase B (BubR1)
17. Mad2	Mitotic arrest deficient-like 2
18. Mad1	Mitotic arrest deficient-like 1
19. Bub1	Bub1 mitotic checkpoint serine/threonine kinase
20. Ttk	TTK protein kinase (MPS1)
21. Dlg7	Discs, large (Drosophila) homolog-associated protein 5 (HURP)
22. Pcaf	Histone acetyl transferase
23. CenpA	Centromere protein A
24. Cdca1	NDC80 kinetochore complex component (NUF2)
25. Spc24	NDC80 kinetochore complex component (SPC24)
26. Spc25	NDC80 kinetochore complex component (SPC25)
27. Kntc2/Hec1	NDC80 kinetochore complex component (NDC80)
28. Ppp1CA	Protein phosphatase 1, catalytic subunit
29. Nup214	Nucleoporin 214KDa
30. Mis12	Mis12 kinetochore complex component
31. Mapre1	Microtubule-associated protein, RP/EB family, member 1 (EB1)
32. RanBP2	Ran binding protein 2
33. Fam22A	Nut family member 2A

34. C13orf3	Spindle and kinetochore associated complex subunit 3
35. ZW10	Zeste white 10 homolog
36. CenpF	Centromere Protein F
37. Dctn1	Dynactin 1
38. Rab5A	Member RAS Oncogene Family
39. Casc5	Cancer susceptibility candidate 5
40. Wapl	Wings apart-like homolog
41. Sept7	Septin 7
42. Nup160	Nucleoporin 160kDa
43. Nup88	Nucleoporin 88kDa
44. Nup107	Nucleoporin 107kDa
45. Sgo1	Shugoshin 1
46. Kntc1	Kinetochore associated 1 (ROD)
47. Clasp1	Cytoplasmic Linker Associated Protein 1
48. Ch-TOG	Cytoskeleton associated protein 5
49. RanGap1	Ran GTPase activating protein 1
50. Cdc34	Cell division cycle 34
51. Esp1	Separin
52. Cdc2	Cell division cycle 2
53. Pttg1	Securin
54. CenpH	Centromere protein H
55. CenpB	Centromere protein B
56. Zwint	ZW10 interacting kinetochore protein
57. Xpo1	Exportin 1
58. Ube2I	Ubiquitin-conjugating enzyme E2I
59. Ppp2R4	Protein phosphatase 2A regulatory subunit B'
60. Dnah1	Dynein, axonemal, heavy chain 1
61. Map2K1	Mitogen-activated protein kinase

Chapter 2:

The mitotic spindle regulates APC/C-dependent degradation of spindle assembly factors (SAFs)

Song, L., Craney, A., and Rape, M. 2014. Microtubule-dependent regulation of mitotic protein degradation. *Molecular Cell*. **53**(2): 179-192.

Overview

Chapter 2 consists of a reproduction of a recent manuscript. This project depicts a major focus of my graduate work, the development of a video microscopy platform to enhance both the scope of my work and that of others in the lab. My contributions to the manuscript are as follows: I developed the immunofluorescence protocol and performed the experiments in Figure 3E. The video microscopy platform that I developed is featured in Figures 5-7 and S6. For the work described in this paper, I performed trouble-shooting and helped set up the confocal hardware; developed the protocols for the software, hardware, and cell-based experiments; identified appropriate materials, performed training, and assisted in the execution and data analysis of the video microscopy experiments.

As a graduate student, I was lucky to work closely with Dr. Ling Song, who pioneered a complex investigation of how APC/C regulates spindle assembly factors (SAFs) in mitosis. Ling and I have collaborated formally on this project and another (Appendix B), but we collaborated informally on many, if not all, aspects of our cell cycle work. Chapters 1 and 2 of this thesis examine the genetic interactions of APC/C and different mitotic regulators, including SAFs. Many of Ling's suggestions and protocols are embedded in these chapters, and the topics and analyses are complementary. This work connects to the first chapter by adding a more biochemical layer of understanding as we continue to uncover more important functions of APC/C throughout mitosis.

Abstract

Accurate cell division depends on tightly regulated ubiquitylation events catalyzed by the anaphase-promoting complex. Among its many substrates, the APC/C triggers the degradation of proteins that stabilize the mitotic spindle, and loss or accumulation of such spindle assembly factors can result in aneuploidy and cancer. Although critical for cell division, it has remained poorly understood how the timing of spindle assembly factor degradation is established during mitosis. Here, we report that active spindle assembly factors are protected from APC/C-dependent degradation by microtubules. In contrast, those molecules that are not bound to microtubules are highly susceptible to proteolysis and turned over immediately after APC/C-activation. The correct timing of spindle assembly factor degradation, as achieved by this regulatory circuit, is required for accurate spindle structure and function. We propose that the localized stabilization of APC/C-substrates provides a mechanism for the selective disposal of cell cycle regulators that have fulfilled their mitotic roles.

Introduction

Posttranslational modification with ubiquitin is widely used to regulate protein stability or activity, and it is essential for cell division in all eukaryotes (Komander and Rape, 2012). Substrates are selected for ubiquitylation by E3 ligases, many of which play important roles in cell cycle control (Deshaies and Joazeiro, 2009). Among the ~600 human E3s, the anaphase-promoting complex (APC/C) is of particular interest as it controls essential steps in mitosis (Peters, 2006).

The APC/C was originally identified based on its role in triggering the degradation of cyclin B1, an activating subunit of Cdk1 (reviewed in (Peters, 2006)). It is now known to ubiquitylate a large number of cell cycle regulators, thereby orchestrating progression of cells through mitosis and G1. Substrates are delivered to the APC/C by the WD40-repeat proteins Cdc20 and Cdh1, which recognize degron motifs referred to as D- or KEN-boxes (Buschhorn et al., 2011; da Fonseca et al., 2011; Tian et al., 2012; Visintin et al., 1997). Following substrate recognition, the APC/C-specific E2s Ube2C and Ube2S synthesize ubiquitin chains that are recognized by the proteasome (Garnett et al., 2009; Rape and Kirschner, 2004; Williamson et al., 2009; Wu et al., 2010; Yu et al., 1996). Depletion of Cdc20 or Ube2C and Ube2S stabilizes APC/C-substrates and arrests cells prior to anaphase (Manchado et al., 2010; Williamson et al., 2009; Wolthuis et al., 2008).

As full activation of the APC/C leads to sister chromatid separation, it has to be delayed until all chromosomes have achieved bipolar attachment to the mitotic spindle. To this end, the APC/C is inhibited during spindle formation by a signaling network referred to as the spindle checkpoint (Kim and Yu, 2011; Musacchio and Salmon, 2007). The checkpoint components Mad2, BubR1, and Bub3 associate with Cdc20 to form the mitotic checkpoint complex, which binds the APC/C and blocks recognition of most of its substrates (Chao et al., 2012; Herzog et al., 2009; Schreiber et al., 2011). Once the spindle has been built and all chromosomes have been aligned at the metaphase plate, checkpoint complexes are disassembled, APC/C^{Cdc20} is activated, and sister chromatid separation ensues (Foster and Morgan, 2012; Reddy et al., 2007; Uzunova et al., 2012; Varetta et al., 2011). Thus, by virtue of the checkpoint, the spindle indirectly controls the stability of most APC/C-substrates.

Spindle formation is a highly dynamic process that depends on a large number of proteins referred to as spindle assembly factors. Several of these factors, such as HURP, NuSAP, or Tpx2, associate with and stabilize microtubules, the main constituents of the spindle apparatus (Gruss et al., 2001; Koffa et al., 2006; Ribbeck et al., 2006; Sillje et al., 2006; Wittmann et al., 2000; Wong and Fang, 2006). Spindle assembly factors also recruit regulators of spindle formation: Tpx2, for example, promotes the spindle association of Aurora A and Eg5, thus controlling spindle pole integrity or spindle bipolarity (Gable et al., 2012; Kufer et al., 2002). After their activation in prometaphase, spindle assembly factors continue to play important roles during ana- and telophase, when they stabilize kinetochore fibers, drive spindle elongation, or establish a

microtubule-dense spindle midzone (Goshima et al., 2007; Uehara and Goshima, 2010).

Befitting their role in cell division, complete loss of spindle assembly factors leads to embryonic lethality or female infertility (Aguirre-Portoles et al., 2012; Tsai et al., 2008), whereas their overexpression can result in tumorigenesis (Aguirre-Portoles et al., 2012; Gulzar et al., 2013; Hu et al., 2012; Tsou et al., 2003). These observations imply that cells need to control the abundance of spindle assembly factors, and indeed, HURP, NuSAP, and Tpx2 are turned over during mitosis by APC/C-dependent ubiquitylation and proteasomal degradation (Song and Rape, 2010; Stewart and Fang, 2005). HURP, NuSAP, and Tpx2 are also regulated by proteins of the importin family, which restrict their association with microtubules and prevent their recognition by the APC/C (Gruss et al., 2001; Gruss et al., 2002; Koffa et al., 2006; Kufer et al., 2002; Ribbeck et al., 2006; Sillje et al., 2006; Song and Rape, 2010). A consequence of this dual regulation, the dissociation of importin-b by GTP-bound Ran not only activates spindle assembly factors, but also allows their APC/C-dependent inactivation. However, despite the importance of spindle formation for cell division, it has remained unclear how cells can sufficiently delay the degradation of HURP, NuSAP, and Tpx2 to allow these proteins to fulfill their critical roles in regulating spindle structure and function.

Here, we have discovered that spindle microtubules protect HURP, NuSAP, and Tpx2 from APC/C-dependent degradation. By contrast, those spindle assembly factor molecules that are not associated with microtubules are highly susceptible to proteolysis and degraded instantaneously after APC/C-activation in early anaphase. The proper timing of spindle assembly factor degradation, as achieved by this regulatory circuit, is critical for mitosis, and inappropriate stabilization of spindle assembly factors disrupts spindle structure and function. Our findings suggest that localized stabilization of APC/C-substrates enables the selective disposal of cell cycle regulators that have fulfilled their mitotic roles, in this case coupling the activity and stability of important spindle assembly factors.

Materials and Methods

Plasmids, siRNAs, antibodies and proteins

cDNAs encoding APC/C-substrates were cloned into pCS2 for IVT/T and into pCS2-HA and pcDNA5/FRT/TO (Invitrogen) for expression in cells and stable cell line generation. A N-terminal Flag-tag was introduced into pcDNA5/FRT/TO by PCR. MBD1 consisted of residues 65-174 of HURP, and MBD2 consisted of the first 69 residues. HURP^{MBD1*} & HURP^{MBD2*} were generated by replacing the following residues with Ala: MBD1*: K105, K107, R110, K112, K114, R115; MBD2*: R20, K22, R26, K27. HURP^{APC} was prepared by mutating D-, KEN-, and TEK-boxes in HURP as described (Song and Rape, 2010). The geminin^{MBD1} fusion was generated by fusing the first 101 residues of geminin to the MBD1 by hybrid PCR. For recombinant proteins, cDNAs were cloned into pMAL and pET28 for expression in *E.coli*, and the purification procedures for MBP-tagged and 6xHis-tagged proteins were as described (Song and Rape, 2010).

ON-TARGETplus Human Cdc20 siRNA-SMARTpool was purchased from Dharmacon.

The following antibodies were used: α HURP & α importin β (polyclonal; Bethyl Laboratories); α NuSAP (polyclonal; ProteinTech Group); α Tpx2 (polyclonal; Novus); α Cdc27 [AF3.1], α Cdc20/p55CDC [E-7], α C-Myc [9E10] (monoclonal; Santa Cruz Biotechnology); α cyclin B1, α geminin, α securin, aGFP & α ANAPC2 (polyclonal; Santa Cruz Biotechnology); α Ube2S (polyclonal; Novus); α MBP (monoclonal; NEB Biolab); α tubulin [DM1A] (monoclonal; Calbiochem); α Flag M2 (monoclonal), α Flag (polyclonal) & α γ tubulin (monoclonal) (Sigma); α HA [C29F4] (monoclonal; Cell Signaling); α centrin [20H5] (monoclonal; Millipore); α Mad2 (monoclonal; BD Biosciences); α β -tubulin (Developmental Studies Hybridoma Bank); Goat anti-rabbit Alexa488 (Invitrogen); Donkey anti-mouse DyLight 549, Goat anti-mouse DyLight 549 (Jackson Laboratories).

***In Vitro* Degradation Assays**

In vitro degradation assays were performed as described (Song and Rape, 2010). To test microtubule-dependent stabilization of substrates, 20 μ M paclitaxel/taxol (Sigma) was added to HeLa S3 extracts (pre-warmed to 30 °C) to promote microtubule polymerization; where indicated, 140 μ M nocodazole (Sigma) was added to destabilize microtubules. To deplete Cdc20, 400 μ l mitotic extract was depleted twice at 4°C for 1h with 2 μ g monoclonal α Cdc20 antibody.

***In Vitro* Ubiquitylation Reactions**

APC/C- or SCF^{bTrCP}-dependent ubiquitylation of ³⁵S-labeled substrates was performed as described (Song and Rape, 2010; Wickliffe *et al.*, 2011). As indicated, 1mg microtubules were pre-incubated with purified substrates (Williamson *et al.*, 2011) at 25°C for 5min before being added to ubiquitylation reactions. For ubiquitylation of recombinant HURP, ~0.25mM Flag-tagged HURP¹⁻²⁸⁰ was used.

HURP-Microtubule interaction assays

Taxol-stabilized microtubules were prepared by incubating pre-warmed porcine brain tubulin with 80mM taxol at 37°C for 10min. Polymerized microtubules were stabilized by bringing the final concentration of taxol to 160 μ M. Subtilisin-treated microtubules were prepared by incubating taxol-stabilized microtubules with 200 μ g/ml subtilisin (gift from Eva Nogales) at 37°C for 30min. The reaction was stopped by 2mM PMSF. Microtubules were spun down at room temperature (RT) at 14K rpm for 20min, and pellets were resuspended in binding buffer consisting of 1xBRB80 (80mM PIPES, 1mM MgCl₂, 1mM EGTA, pH 6.8), 1mM DTT, 5% sucrose and 20 μ M taxol.

For co-pelleting experiments, 250nM ^{MBP}MBD1 was incubated with control or subtilisin-treated microtubules in a 20 μ l reaction for 10min at RT. Reactions were spun at 14K rpm for 20min at RT. The supernatant and pellet fractions were

solubilized in 2x Laemmli buffer. 10% of supernatant and pellet were subjected to α MBP immunoblot or Coomassie.

For monitoring the HURP-microtubule interaction by microscopy, MBP^{HURP} was labeled with Oregon Green 488 iodoacetamide (Invitrogen), cleaned by PD SpinTrap G-25 columns (GE Healthcare), and mixed with rhodamine-labeled microtubules. As indicated, ^{6xHis}importin-b was pre-incubated with labeled HURP at equal molar ratio for 5min. Images were taken using 60x magnification on an Olympus IX81 microscope, and processed using ImageJ.

Cell culture, transfection, and immunofluorescence

HeLa cells were cultured in DMEM containing 10% FBS. For plasmid transfection, cells were plated on coverslips and transfected using TransIT-LT1 (Mirus). For siRNA, cells were transfected with 50nM oligos using RNAiMAX (Invitrogen). Cells were fixed 48h post transfection for immunofluorescence or subjected to live cell imaging 24h post transfection. For drug treatment, cells were treated with 20 μ M MG132, 20 μ M proTAME (Boston Biochem; gift from Randy King) or 20 μ M importazole (gift from Rebecca Heald) for 6~8h before fixation. Cells were fixed with cold methanol (-20 °C) for 3min or 3.7% formaldehyde for 20min. Images were taken using Zeiss LSM 710 confocal microscope or Olympus IX81 microscope, deconvolved using Metamorph, and processed using ImageJ.

Flp-In T-REx 293 cells to stably express Flag-tagged HURP were generated following manufacturer's manual (Invitrogen). For immunofluorescence, cells were plated on coverslips coated with poly-D-lysine and induced with 0.5 μ g/ml doxycycline for 48h before fixation.

Production of Lentiviruses and Transduction

eGFP-tagged HURP and mCherry-tagged histone H2B were cloned into pEF-1 α /pENTR vector and recombined into pLenti X1 DEST by LR recombination to generate lentiviral expression constructs. Lentiviruses were produced in 293T cells by co-transfection of lentiviral constructs with packaging plasmids (Addgene) for 48~72 hours. Transduction was carried out by infecting ~50% confluent HeLa cells with lentiviruses in the presence of 6 μ g/ml Polybrene (Sigma).

Live Cell Imaging

HeLa cells that stably express mCherry-H2B and GFP-tubulin (gift from Rebecca Heald) or LAP-tagged CenpA (gift from Iain Cheeseman) were maintained in DMEM-phenol red media containing 10% FBS at 37 °C with 5% CO₂, and imaged at a single focal plane every 3min for the indicated time periods beginning 4h post drug treatment. Images were taken with a 0.95 NA 40x objective on an Olympus Revolution XD spinning disk confocal microscope equipped with a charged-couple device camera (Andor technology) and a Yokogawa spinning disk. Movies were assembled using Metamorph and analyzed with Photoshop.

Cell synchronization, immunoprecipitation and pulldown assays

Cell synchronization, immunoprecipitation and MBP pull-down assays were performed as previously described (Song and Rape, 2010).

Results

Microtubules protect spindle assembly factors from degradation

As most spindle assembly factors accumulate on the spindle during mitosis, we wished to determine whether their localization affected their stability. To this end, we tested whether microtubules, the main constituents of the spindle, influence the efficiency of spindle assembly factor degradation by the APC/C. We first generated extracts of prometaphase HeLa cells that contained inactive APC/C and soluble tubulin. We then supplemented these extracts with taxol to induce microtubule formation; GTP-charged Ran^{Q69L} to release spindle assembly factors from their inhibitors of the importin family; and p31^{comet} to activate the APC/C. Without microtubules, these extracts supported the efficient degradation of spindle assembly factors and other known APC/C-substrates, and depletion of the essential APC/C-activator Cdc20 or addition of the APC/C^{Cdc20}-specific inhibitor Mad2 underscored the specificity of these reactions (Figure 1A; Figure S1A, B). By contrast, when microtubules were present, HURP, NuSAP and Tpx2 were protected from degradation, whereas soluble APC/C-substrates remained unstable (Figure 1A). The effects of microtubules on the stability of spindle assembly factors were reversible, as HURP was rapidly turned over once microtubules had been depolymerized with nocodazole (Figure 1B). Thus, microtubules protect multiple spindle assembly factors from degradation through APC/C^{Cdc20} in early mitotic extracts.

During cytokinesis and G1, the APC/C is activated by Cdh1 (Visintin et al., 1997). To determine whether microtubules stabilize spindle assembly factors against APC/C^{Cdh1}, we generated extracts of HeLa cells that were synchronized in G1. We supplemented these extracts with taxol and Ran^{Q69L} and then measured the stability of radiolabeled APC/C-substrates. As we had seen for APC/C^{Cdc20}, microtubules protected the spindle assembly factor HURP, but not soluble cyclin B1, from APC/C-dependent degradation (Figure 1C). Soluble HURP was stabilized by the APC/C^{Cdh1}-inhibitor Emi1, which attests to the specificity of these reactions.

Prompted by these observations, we tested whether microtubules interfered with the ubiquitylation of spindle assembly factors by the APC/C. Indeed, the APC/C^{Cdc20}- and APC/C^{Cdh1}-dependent ubiquitylation of HURP, NuSAP, and Tpx2 were blocked by microtubules (Figure 2A, B; Figure S1C, D), with an efficiency comparable to that of Mad2, an established APC/C^{Cdc20}-inhibitor (Figure S1E). Microtubules also ablated the ubiquitylation of a bacterially purified HURP-domain that contained all APC/C-degrons and microtubule-binding domains (Figure 2C), whereas unpolymerized tubulin did not impede these reactions (Figure S1F). In contrast to their effects on spindle assembly factors, microtubules did not affect the modification of soluble APC/C-substrates, such as cyclin B1 (Figure 2D), nor did they interfere with the ubiquitylation of

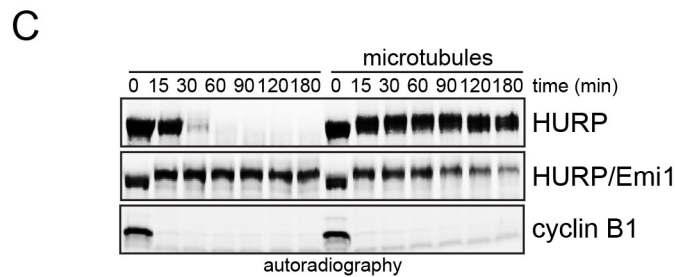
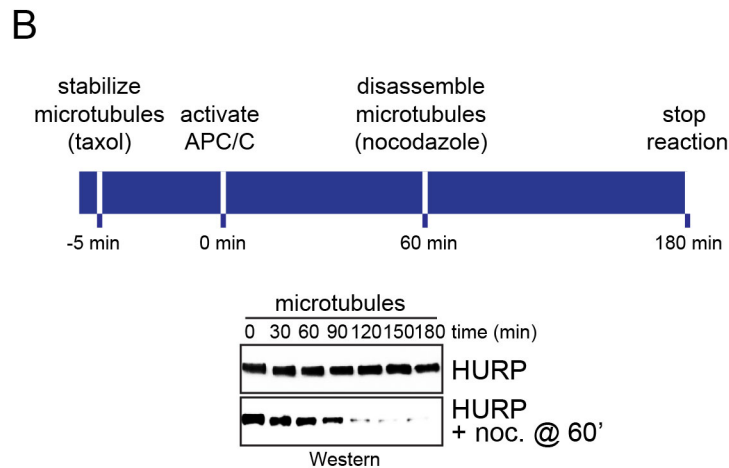
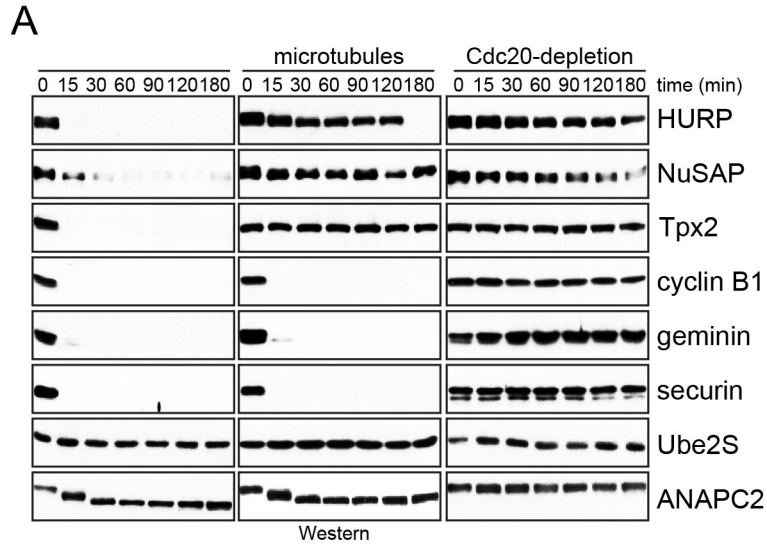


Figure 1: Microtubules stabilize spindle assembly factors. A. Microtubules protect spindle assembly factors from APC/C^{Cdc20}-dependent degradation in extracts. Extracts of prometaphase HeLa cells were subjected to p31^{comet} to activate APC/C^{Cdc20}, and Ran^{Q69L} to release spindle assembly factors from importin inhibitors. As indicated, extracts were treated with taxol to stabilize microtubules. Control extracts were depleted of Cdc20, and the stability of endogenous substrates was monitored by immunoblotting. **B.** Microtubule-dependent stabilization of spindle assembly factors is reversible. Mitotic extracts were treated with taxol and Ran^{Q69L}. As indicated, nocodazole was added after 60min to depolymerize microtubules. **C.** Microtubules prevent APC/C^{Cdh1}-dependent degradation of spindle assembly factors. ³⁵S-labeled HURP or cyclin B1 was added to G1-extracts of HeLa cells with active APC/C^{Cdh1} and treated with taxol and Ran^{Q69L}.

As control, the APC/C^{Cdh1}-inhibitor Emi1 was added, and substrate stability was monitored by autoradiography. See also Figure S1.

substrates of other E3s (Figure S1G). We conclude that microtubules protect spindle assembly factors from APC/C-dependent ubiquitylation and degradation *in vitro*.

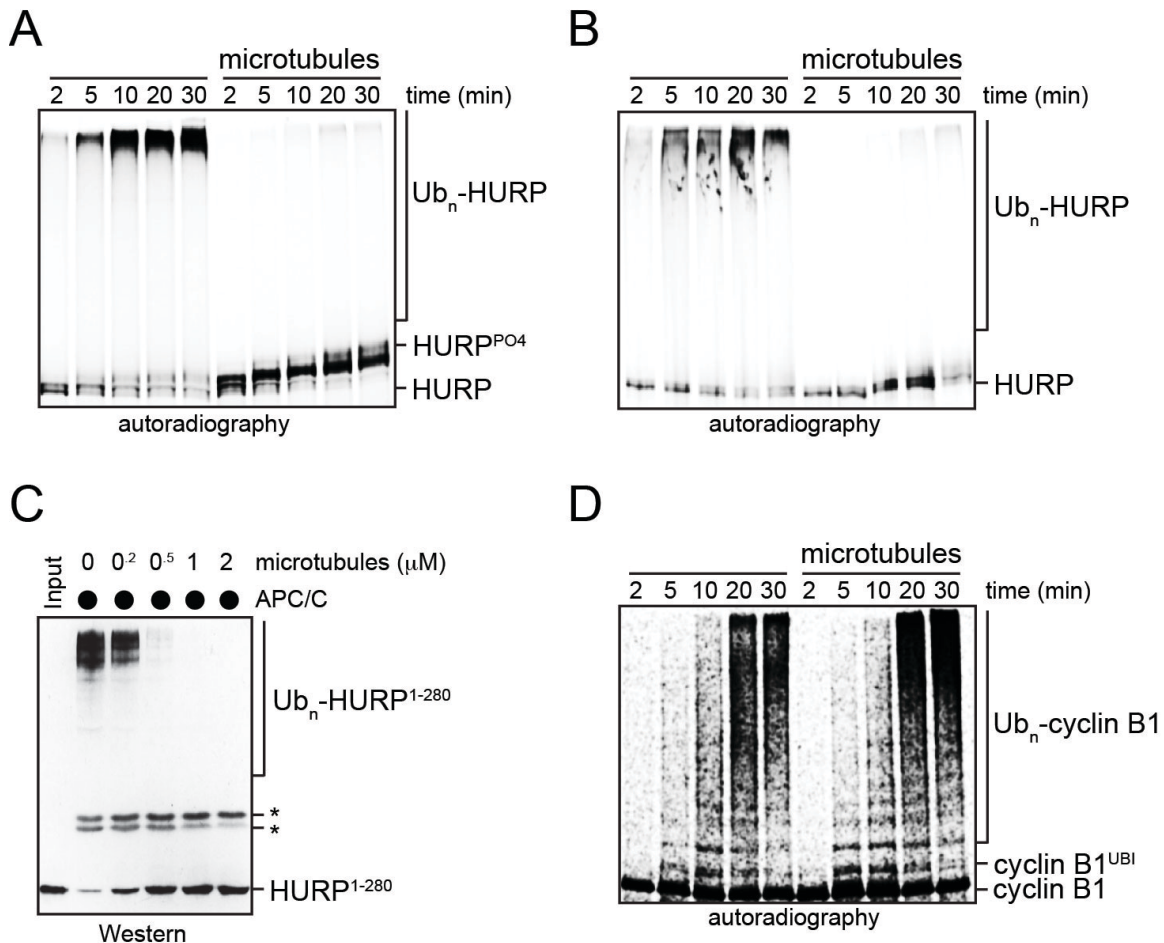


Figure 2: Microtubules prevent ubiquitylation of spindle assembly factors by the APC/C. **A.** Microtubules inhibit ubiquitylation of HURP by APC/C^{Cdc20}. ³⁵S-labeled HURP was synthesized *in vitro*, purified, incubated with Ran^{Q69L} and subjected to ubiquitylation by APC/C^{Cdc20}. As indicated, HURP was pre-bound to microtubules. Reactions were monitored by autoradiography. **B.** Microtubules inhibit ubiquitylation of ³⁵S-labeled HURP by APC/C^{Cdh1} isolated from HeLa cells synchronized in G1. Reactions were analyzed in the presence of microtubules as described. **C.** Microtubules prevent the ubiquitylation of bacterially expressed HURP. HURP¹⁻²⁸⁰, which contains all degrons and microtubule-binding domains, was incubated with microtubules (0, 0.2, 0.5, 1, or 2 μM) and subjected to APC/C-dependent ubiquitylation. Reactions were analyzed by Western. The asterisks mark crossreactive bands. **D.** Microtubules do not affect the ubiquitylation of ³⁵S-labeled cyclin B1 by APC/C^{Cdc20}. See also Figure S1.

HURP contains two microtubule-binding domains

Multiple lines of evidence suggest that HURP, NuSAP, and Tpx2 are regulated by similar mechanisms: all proteins localize to a subset of spindle microtubules, the kinetochore fibers; their association with microtubules is inhibited by importins (Kalab and Heald, 2008); and their microtubule-regulated degradation is dependent upon the APC/C, which targets these spindle assembly factors at similar times during mitosis (Song and Rape, 2010; Stewart and Fang, 2005). Unfortunately, for none of these proteins were microtubule-binding domains sufficiently characterized to generate inactive mutants, a prerequisite for understanding how their degradation is controlled. Given the similarities in regulation, we decided to use HURP as a model substrate to define its microtubule-binding domains. We then introduced inactivating mutations into the respective domains to gain insight into the mechanism of microtubule-dependent APC/C-regulation.

Previous work had located a microtubule-binding domain within the first 280 residues of HURP (Wong et al., 2008). By testing fragments that covered this region, we found a smaller motif, the MBD1, which associated with microtubules with similar affinity as the full-length protein (Figure 3A, B) (Wong and Fang, 2006). The interaction between microtubules and the MBD1 was disrupted by mutation of positively charged residues in the MBD1 or treatment of microtubules with subtilisin, which removes the negatively charged C-terminus of tubulin. Thus, the MBD1 is a microtubule-binding motif that likely recognizes the C-terminal tail of tubulin.

To test whether the MBD1 was essential for the binding of HURP to microtubules, we generated Oregon Green-labeled HURP^{MBD1*}, in which positively charged residues of the MBD1 were replaced with alanine. We incubated HURP^{MBD1*} with rhodamine-labeled microtubules and monitored the interaction between the two partners by fluorescence microscopy. In these assays, mutation of the MBD1 strongly reduced the capacity of HURP to bundle, but not to bind, microtubules (Figure 3C, D), suggesting that a second domain provides an additional interaction surface. Indeed, a motif that we refer to as the MBD2 and that overlaps with the importin-b-binding site in HURP was enriched in positively charged residues, a common feature of microtubule-binding domains. When these charged residues were mutated in the background of HURP^{MBD1*} (HURP^{MBD1/2*}), all microtubule-binding of HURP was lost (Figure 3C, D). The MBD2, but not the MBD1, also bound importin-b *in vitro* and in cells (Figure S2A, B), and accordingly, importin-b inhibited the capacity of the MBD2 to associate with microtubules (Figure S2C). Thus, the MBD1 provides a constitutive high-affinity binding site for microtubules, whereas the weaker interaction between the MBD2 and microtubules is regulated by importin-b.

The results of our biochemical analyses were confirmed *in vivo*: when expressed during interphase, HURP and HURP^{MBD2*} co-localized with microtubules, indicative of a functional interaction (Figure 3E, F). This association was strongly reduced by mutation of the MBD1 or simultaneous inactivation of

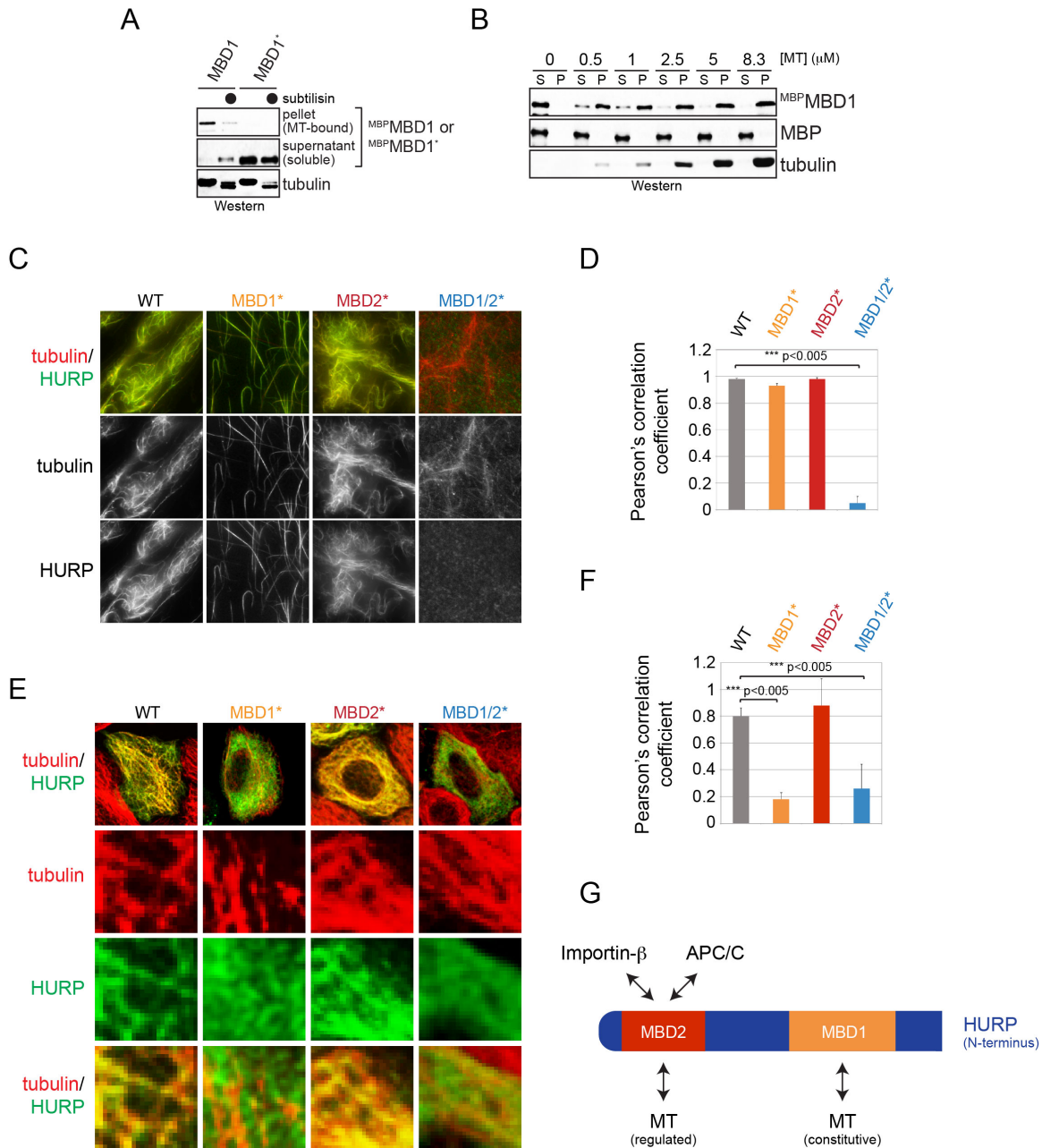


Figure 3: HURP contains two microtubule-binding motifs. **A.** Taxol-stabilized microtubules were incubated with ^{MBP}MBD1 or mutant ^{MBP}MBD1* in which positively charged residues were exchanged to alanine. As indicated, microtubules were treated with subtilisin. Binding reactions were centrifuged through a sucrose cushion, and microtubule-bound and soluble fractions were analyzed by Western. **B.** The MBD1 binds microtubules with similar affinity as full-length HURP. ^{MBP}MBD1 was incubated with taxol-stabilized microtubules and subjected to sucrose gradient centrifugation. **C.** The MBD1 and MBD2 both mediate microtubule-binding of HURP. Recombinant full-length HURP or mutants in its MBD1 or MBD2 were labeled with Oregon Green and incubated with rhodamine-labeled microtubules. Binding was analyzed by fluorescence microscopy. **D.** Quantification of HURP- and microtubule co-localization *in vitro*. Green (HURP) and red (tubulin) signals were correlated using ImageJ and JACoP, resulting in a Pearson's

correlation coefficient. **E.** MBD1 mediates microtubule-binding of HURP in interphase. HeLa cells were transfected with ^{FLAG}HURP or mutants in its MBDs and analyzed by immunofluorescence microscopy (green: HURP; red: b-tubulin). **F.** Pearson's correlation coefficient to quantify the colocalization between HURP-mutants and microtubules in interphase cells. **G.** Overview of binding motifs in the N-terminal domain of HURP. The MBD1 provides a constitutive binding site for microtubules; MBD2 overlaps with APC/C-degrons and the importin- β -binding site (Song and Rape, 2010). The asterisks mark residues mutated to alanine in order to ablate the functions of the MBD1 (orange), MBD2 (red), or APC/C-degrons (green). See also Figure S2.

the MBD1 and MBD2. These findings show that during interphase, the MBD1 is the dominant microtubule-binding domain in HURP. As described later, the MBD2 contributes to microtubule-binding of HURP during mitosis (see below), indicating that both the MBD1 and MBD2 can mediate an interaction of the spindle assembly factor HURP to microtubules (Figure 3G).

Binding to microtubules is necessary and sufficient for HURP stabilization

Having mapped HURP's microtubule-binding motifs, we tested whether their integrity was required for the stabilization of APC/C-substrates by microtubules. We supplemented extracts containing APC/C^{Cdc20}, taxol, and Ran^{Q69L} with the respective HURP-mutants and monitored the degradation of these substrates over time. While microtubules stabilized HURP and HURP^{MBD2*}, this effect was lost if the constitutive binding motif MBD1 was mutated (Figure 4A). The degradation of HURP^{MBD1*} and HURP^{MBD1/2*} was dependent upon the APC/C, as both proteins were stabilized by depletion of Cdc20 (Figure S3A), addition of Mad2 (Figure S3B), or mutation of APC/C-degrons (Figure 4A). Accordingly, in contrast to wild-type HURP (Figure 2A), microtubules did not inhibit the ubiquitylation of HURP^{MBD1*} and HURP^{MBD1/2*} by the APC/C (Figure 4B; Figure S3C). We conclude that the MBD1, but not the importin- β -regulated MBD2, is required for the stabilization of HURP by microtubules.

To test whether the MBD1 is sufficient to impose this regulatory mechanism onto APC/C-substrates, we fused it to the N-terminal half of geminin, a protein that is turned over by the APC/C in the presence of microtubules. The fusion geminin^{MBD1}, but not WT-geminin, was targeted to microtubules *in vitro* and to the spindle in cells, confirming that the MBD1 mediates an interaction with microtubules during mitosis (Figure 4C, D). Importantly, degradation of geminin^{MBD1} in extracts and its ubiquitylation by the APC/C were strongly inhibited by microtubules (Figure 4E, F). Similar results were obtained in assays that monitored the stability of MBD1-fusions to various other APC/C-substrates. The mutation of positively charged residues within the MBD1 disrupted the spindle-binding of geminin^{MBD1} and ablated the regulation of its ubiquitylation and degradation by microtubules (Figures 4C, E; Figure S3D). Thus, the MBD1 is not only required, but also sufficient for the microtubule-dependent stabilization of HURP.

It is possible that any stable interaction might prevent the degradation of APC/C-substrates, or alternatively, this might be a function of the microtubule binding domains present in spindle assembly factors. To address this issue, we fused geminin to the N-terminal microtubule-binding domain of tau, a protein that

interacts with microtubules in interphase, but does not act as a spindle assembly factor during mitosis (Cleveland et al., 1977). Although this domain afforded a similar affinity to microtubules as HURP's MBD1 (Figure 4D), geminin^{TAU} was not protected from APC/C-dependent degradation by microtubules (Figure 4E). Geminin^{TAU} was also not stabilized if the MBD1 was added *in trans*, showing that the MBD1 needs to be in the same peptide as the APC/C-degrons. Moreover, locking geminin into dimeric complexes by fusing it to the leucine zippers of the

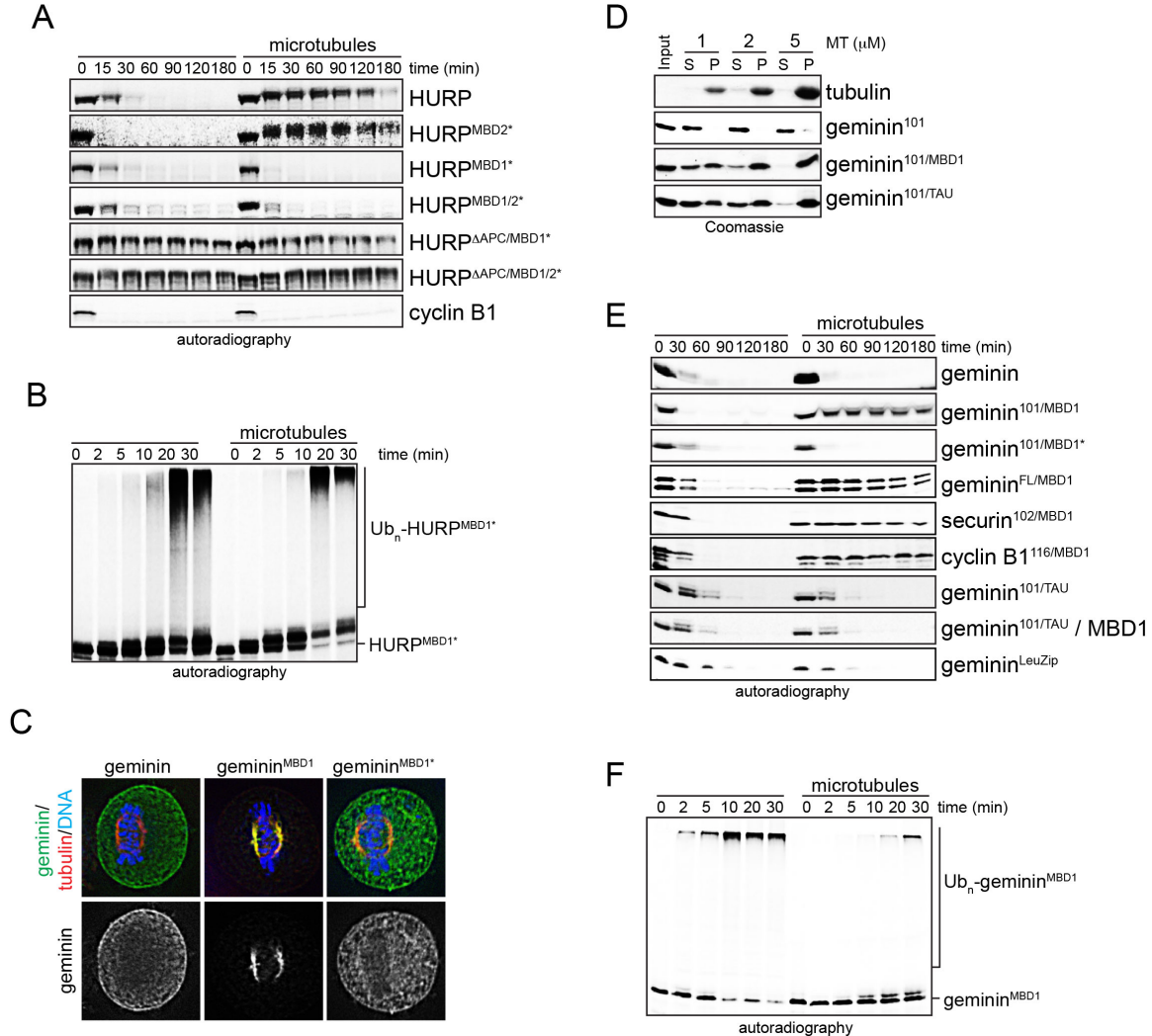


Figure 4: The MBD1 is required and sufficient for the regulation of HURP-stability by microtubules. **A.** MBD1-mutation allows degradation of HURP in the presence of microtubules. Mitotic extracts with APC/C^{Cdc20} and Ran^{Q69L} were supplemented with ³⁵S-labeled HURP, HURP-mutants (MBD1*, MBD2*, DAPC), or cyclin B1, and degradation was monitored by autoradiography. As indicated, microtubules were stabilized by taxol. **B.** The MBD1 is required for the inhibition of HURP-ubiquitylation by microtubules. ³⁵S-labeled HURP^{MBD1*} was incubated with buffer or microtubules, before being subjected to ubiquitylation by APC/C^{Cdc20}. Reactions were followed by autoradiography. **C.** The MBD1 targets a soluble APC/C-substrate to the spindle. HeLa cells were transfected with geminin, geminin^{MBD1} (residues 1-101 of geminin fused to the MBD1 of HURP); or geminin^{MBD1*} (charged residues in the MBD1 mutated to alanine), and localization was determined by immunofluorescence microscopy (green: geminin; red: tubulin;

blue: DNA/DAPI). The bottom panel shows the localization of the geminin proteins alone. **D.** Fusions of HURP's MBD1 or the N-terminal microtubule-binding domain of tau induce microtubule-binding of soluble APC/C-substrates with similar efficiency. Binding of recombinant proteins to microtubules was analyzed by sucrose gradient centrifugation (S: soluble fraction; P: microtubule-bound fraction). **E.** The MBD1 imposes microtubule-dependent regulation of degradation. ³⁵S-labeled substrates were added to extracts with APC/C^{Cdc20} and Ran^{Q69L} (MBD1: HURP's MBD1; TAU: N-terminal microtubule-binding domain of tau; LeuZip: leucine zippers of GCN4 transcription factor). As indicated, microtubules were stabilized by taxol or the ^{MBP}MBD1 was added to induce microtubule bundling. Reactions were monitored by autoradiography. **F.** Microtubules inhibit the ubiquitylation of geminin^{MBD1}. ³⁵S-labeled geminin^{MBD1} was incubated with buffer or microtubules and subjected to ubiquitylation by APC/C^{Cdc20}. Reactions were monitored by autoradiography. See also Figure S3.

transcription factor GCN4 did not prevent its APC/C-dependent degradation (Figure 4E). Together, these experiments indicate that stable interactions are not sufficient to protect HURP. Instead, a specific property of the MBD1, such as its capacity to bundle microtubules, might be required for its role in stabilizing HURP on microtubules.

Microtubules stabilize HURP during mitosis

We next wished to determine whether microtubules stabilize spindle assembly factors *in vivo*. To this end, we expressed low levels of GFP-tagged HURP or its microtubule-binding deficient mutants using lentiviruses (Figure S4A) and monitored the abundance of these variants in HeLa cells by video microscopy. In agreement with analyses of endogenous HURP (Koffa et al., 2006; Sillje et al., 2006; Wong and Fang, 2006), GFP-tagged HURP accumulated on the spindle until telophase, and was completely turned over only after all sister chromatids had been distributed into the two daughter cells (Figure 5A). By contrast, HURP^{MBD1*} bound the spindle with lower efficiency than WT-HURP, and HURP^{MBD1/2*} did not show significant enrichment at the spindle. Moreover, the degradation of HURP^{MBD1*} and HURP^{MBD1/2*} started much earlier than that of the wild-type protein, and both mutants were degraded beyond our detection limit shortly after sister chromatid separation had been initiated. Mutation of all APC/C-degrons stabilized HURP^{MBD1*} and HURP^{MBD1/2*} until G1, demonstrating that the premature degradation of these spindle assembly factor variants was carried out by the APC/C.

To independently assess whether microtubules protect spindle assembly factors from degradation, we measured the levels of microtubule-binding deficient mutants by immunofluorescence microscopy. As seen before, inactivation of the MBD1 or both the MBD1 and MBD2 caused a strong decrease in the abundance of HURP that was especially apparent shortly before anaphase (Figure 5B; Figure S4B, C). By contrast, HURP, HURP^{MBD1*}, and HURP^{MBD1/2*} were present at comparable levels in interphase when the APC/C was inactive (Figure S4B), or during mitosis, if the proteasome was inhibited, the APC/C^{Cdc20}-specific inhibitor Mad2 was overexpressed, or APC/C-degrons were mutated (Figure 5B; Figure S4C, D). In agreement with the premature degradation of soluble HURP, stable HURP^{DAPC/MBD1*}, but not HURP^{MBD1*}, was detected on

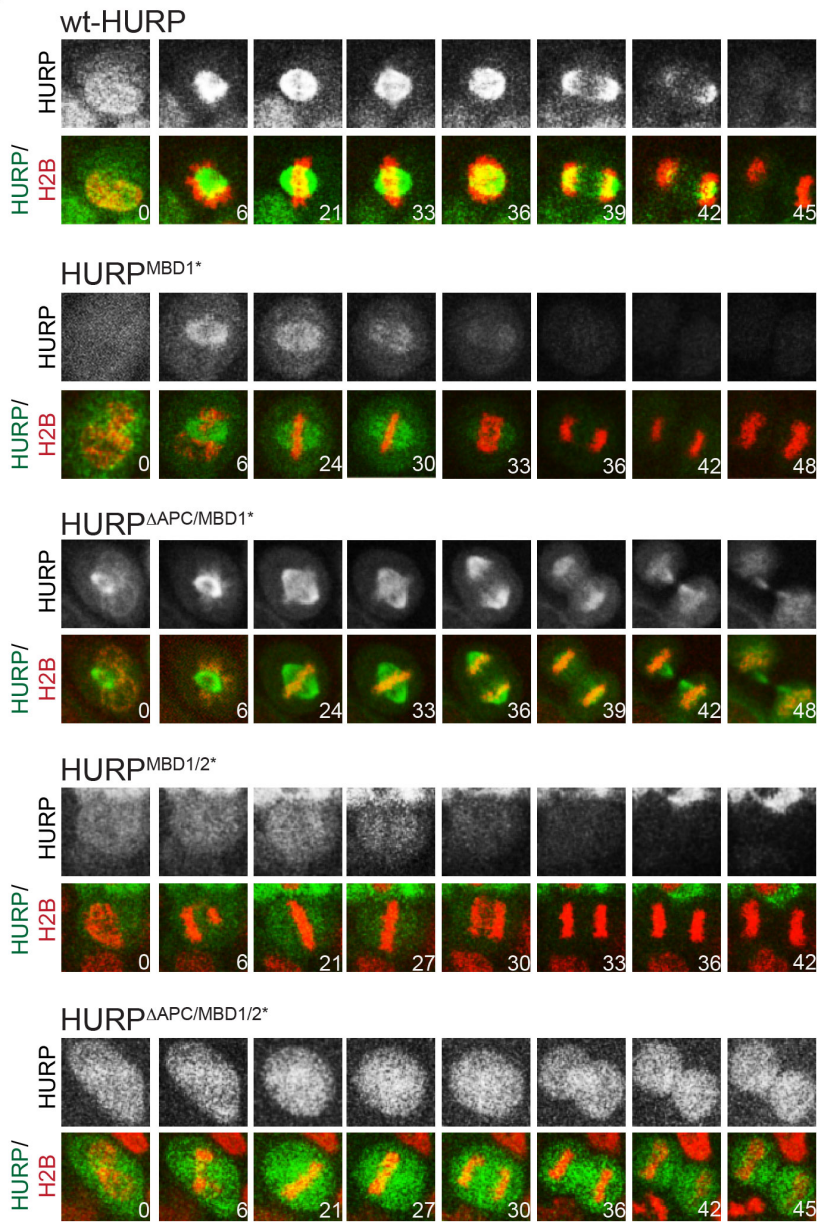
metaphase chromosomes, an observation that we also made for the GFP-tagged protein by live cell analysis (Figure 5A, B). Based on these findings, we conclude that microtubules prevent the premature degradation of HURP during mitosis. If this regulation is lost, the spindle assembly factor is highly susceptible to proteolysis and depleted from cells almost instantaneously after the APC/C has been activated.

The instability of microtubule-binding deficient HURP implied that the removal of spindle assembly factors contributes to robust spindle function. To test this hypothesis, we filmed cells that expressed HURP^{DAPC}, a stable mutant that lost all APC/C-degrons (Song and Rape, 2010), but retained its capacity to bind microtubules. Confirming APC/C's role in targeting HURP, GFP-HURP^{DAPC} was not degraded during any stage of mitosis, allowing it to persistently bind microtubules throughout mitosis (Figure 6A). The stabilization of HURP resulted in strong mitotic defects: HURP^{DAPC}, but not WT-HURP or inactive HURP^{DAPC/MBD1/2*}, impaired the assembly of a metaphase plate with completely aligned chromosomes, induced formation of multiple spindle poles, and delayed anaphase onset (Figure 6A-D). Immunofluorescence analysis against γ -tubulin and centrin showed that expression of HURP^{DAPC} triggered spindle pole fragmentation, rather than centrosome amplification (Figure S5A, B). In agreement with these results, inducible overexpression of HURP, but not inactive HURP^{MBD1/2*}, led to spindle defects, such as spindle elongation (Figure 6E). Thus, while losing its microtubule-dependent regulation caused premature degradation of HURP, the inappropriate stabilization of this spindle assembly factor interfered with accurate spindle function and, consequently, faithful cell division.

The APC/C and importin-b cooperate to ensure spindle structure and function

Contrary to the expression of HURP^{DAPC}, inhibition of the APC/C or the proteasome had little effects on spindle formation and only led to spindle breakdown after a prolonged metaphase arrest (Daum et al., 2011; Stevens et al., 2011; Zeng et al., 2010). The APC/C-dependent degradation of spindle assembly factors thus likely cooperates with another mechanism to ensure spindle function, and indeed, all microtubule-regulated APC/C-substrates studied here are also inhibited by members of the importin family. As HURP^{DAPC} was neither recognized by the APC/C nor importin-b (Figure S5C), the latter two regulators might cooperate in ensuring spindle function. To test this hypothesis, we inhibited the APC/C by depleting its activator Cdc20; importin-b by treating cells with importazole, a molecule that inactivates importin-b without stabilizing spindle assembly factors (Soderholm et al., 2011); or APC/C and importin-b by subjecting cells to siRNAs against Cdc20 and importazole at the same time. We then monitored cells that stably expressed ^{mCherry}histone H2B and ^{GFP}tubulin by video microscopy.

A



B

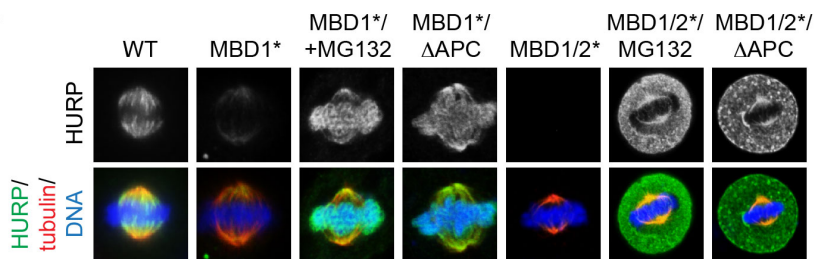


Figure 5: Microtubule-binding stabilizes HURP during mitosis. **A.** HeLa cells were transduced with lentiviruses expressing ^{mCherry} histone H2B and GFP-tagged HURP, HURP^{MBD1*}, HURP^{DAPC/MBD1/2*}, HURP^{MBD1/2*}, or HURP^{DAPC/MBD1/2*} (MBD1/2*: mutation of microtubule-binding motifs; DAPC: mutation of all degrons). Progression through mitosis was monitored by live cell imaging. The upper panels show the levels of the GFP-tagged HURP variant, whereas lower panels display GFP-HURP (green), mCherry-histone H2B (red), and the time post nuclear envelope breakdown. M: first frame with metaphase chromosome alignment; A: first frame with sister chromatid separation. **B.** HeLa cells were transfected with FLAG-HURP, FLAG-HURP^{MBD1*} or FLAG-HURP^{MBD1/2*}, where indicated, APC/C-degrons were mutated (FLAG-HURP^{DAPC/MBD1*}, FLAG-HURP^{DAPC/MBD1/2*}) or cells were treated with MG132. Cells were analyzed by immunofluorescence microscopy. *Upper panel:* HURP-proteins; *lower panel:* HURP (green); tubulin (red); DNA (blue). See also Figure S4.

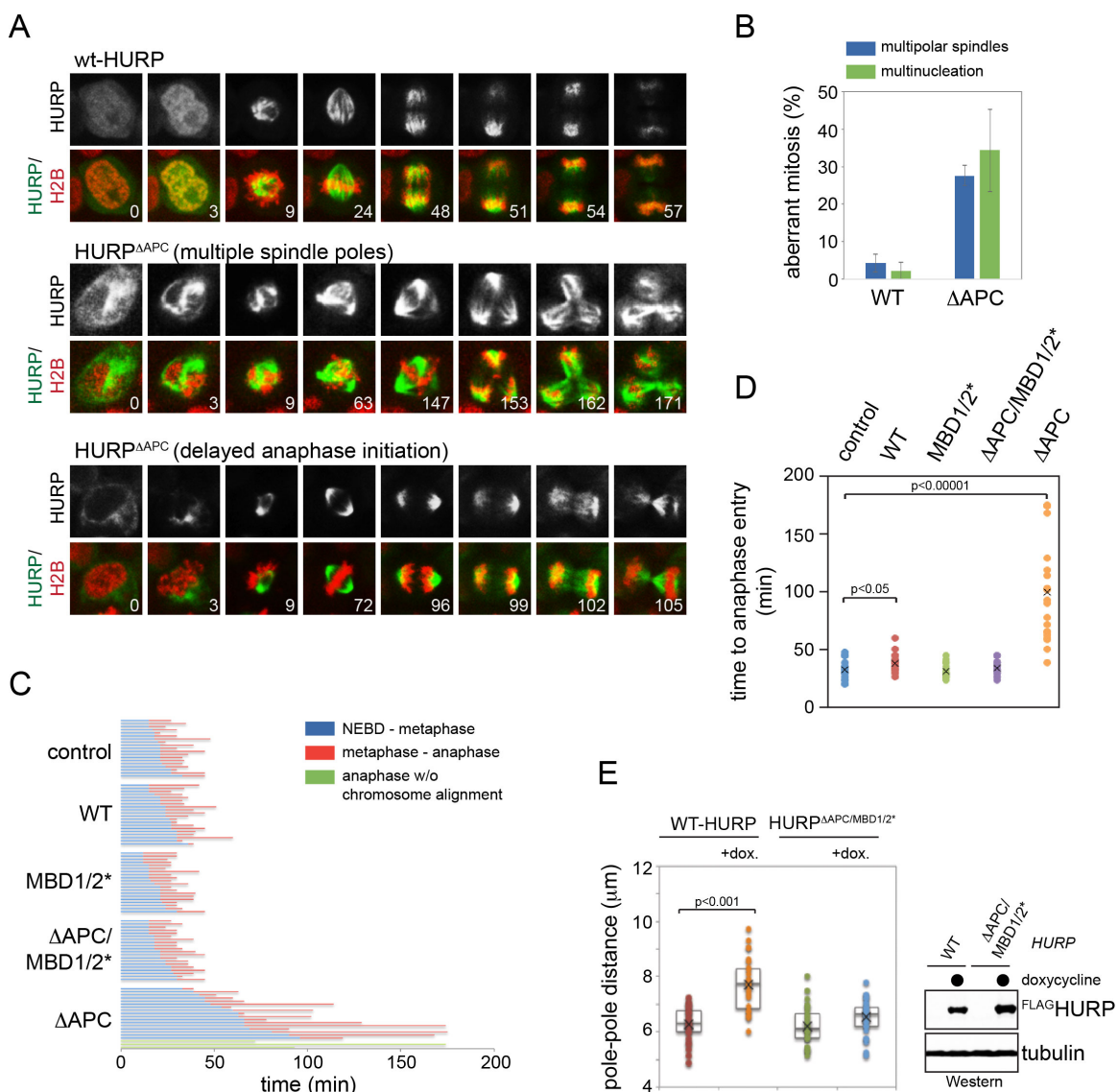


Figure 6: Stabilization of HURP interferes with spindle structure and function. A. Expression of stabilized HURP in mitosis leads to persistent microtubule-binding and mitotic defects. HeLa cells transduced with lentiviruses expressing m^{Cherry} histone H2B, and GFP-tagged HURP or HURP^{DAPC}, were filmed through mitosis. Upper panel: HURP; lower panel: GFP-tagged HURP (green), m^{Cherry} histone H2B (red), and the time post nuclear envelope breakdown. **B.** Stabilization of HURP results in multiple spindle poles and multinucleation. Cells expressing GFP-HURP or GFP-HURP^{DAPC} were filmed through mitosis and analyzed for >2 spindle poles or multinucleation. Results were from three independent experiments, including at least 50 dividing cells per condition and per experiment. **C.** Expression of HURP^{DAPC} delays the assembly of a metaphase plate with completely aligned chromosomes. HeLa cells expressing GFP-tagged HURP or mutants were filmed through mitosis. The time from nuclear envelope breakdown to assembly of a metaphase plate (blue) and from metaphase to anaphase initiation (red) are shown. Expression of HURP^{DAPC} frequently caused anaphase initiation after a profound delay, even though a metaphase plate had never been established (green). **D.** Quantification of the time required for anaphase entry in the presence of HURP proteins. **E.** Increased levels of active HURP cause spindle defects. Stable 293T cell lines expressing HURP or HURP^{DAPC/MBD1/2*} under an inducible promoter were treated with doxycycline, and spindle structures were analyzed by microscopy against α - and γ -tubulin. *Left panel:* pole-pole distance in the presence or absence of HURP; *right panel:* inducible expression of HURP-variants. See also Figure S5.

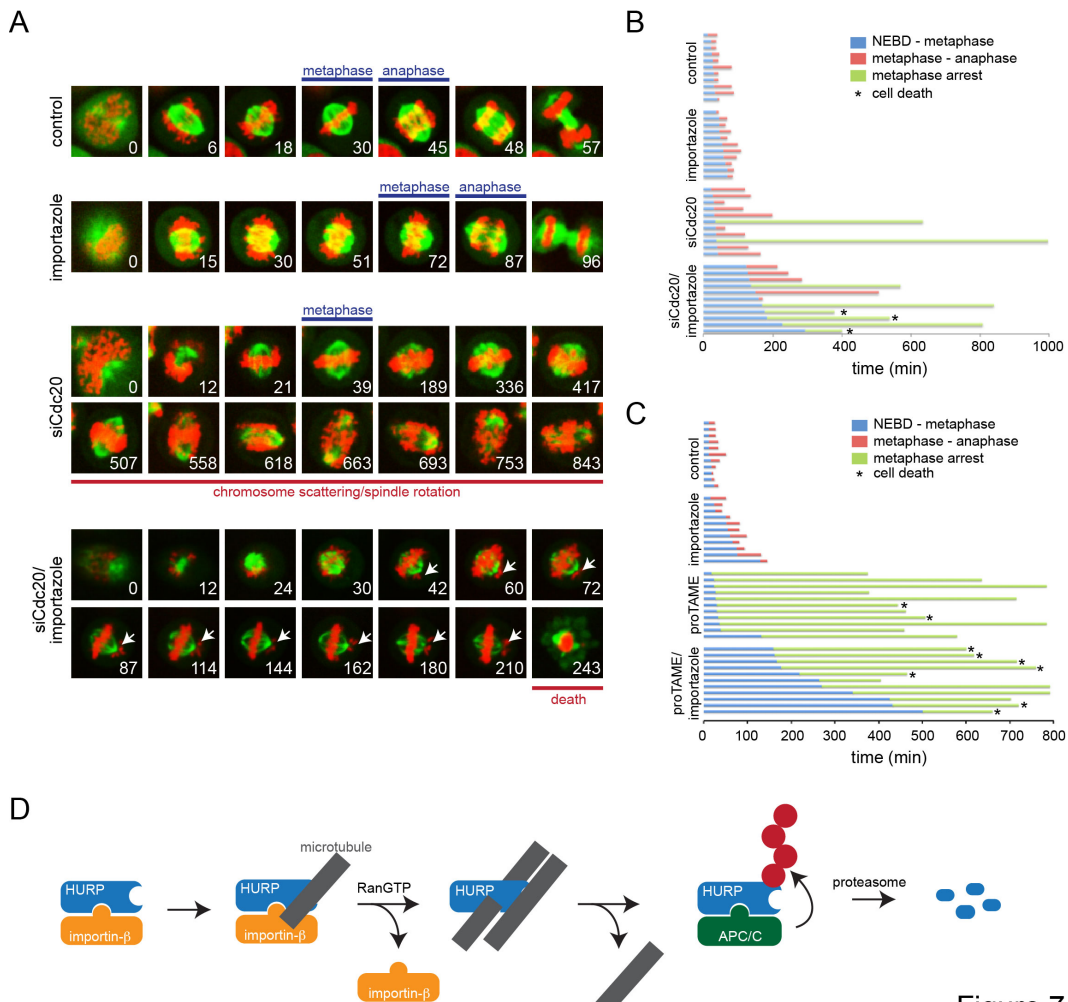


Figure 7

Figure 7: The APC/C and importin-b regulate spindle function. **A.** Simultaneous inhibition of the APC/C and importin-b results in cooperative defects in spindle structure and function. HeLa cells stably expressing ^{GFP}tubulin and ^{mCherry}histone H2B were treated with siRNAs against Cdc20, importazole, or siRNAs against Cdc20 and importazole at the same time. Progression of cells through mitosis was monitored by video microscopy (tubulin: green; histone: red; arrows: misaligned chromosomes). **B.** Quantification of the mitotic timing for HeLa cells expressing ^{mCherry}histone H2B and ^{GFP}tubulin, after being treated with siRNAs against Cdc20 or importazole, as shown on the left. *Blue*: time from nuclear envelope breakdown to completion of chromosome alignment; *red*: time from metaphase to anaphase initiation; *green*: cells permanently arrested prior to anaphase. The asterisk marks cells undergoing cell death. **C.** The Cdc20-inhibitor proTAME displays similar functional interactions with importin-b as Cdc20-siRNAs. HeLa cells stably expressing ^{mCherry}histone H2B and ^{GFP}tubulin were treated with proTAME, importazole, or both, and filmed through mitosis. Experiments were quantified as described. **D.** Model of microtubule-dependent regulation of APC/C-substrate degradation. Ran-dependent spindle assembly factors are inhibited by importin-b. As seen for HURP, importin-b does not ablate the microtubule-binding of a constitutive motif, the MBD1, indicating that spindle assembly factors might be loaded onto the spindle in their inactive state. Ran^{GTP}-dependent dissociation of HURP allows the MBD2 to engage microtubules, thereby activating the spindle assembly factor. Once HURP is not required, its release from microtubules results in rapid ubiquitylation by the APC/C and proteasomal degradation, a reaction that is required for maintaining proper spindle structure and function. See also Figure S6.

In agreement with earlier reports (Daum et al., 2011; Stevens et al., 2011; Zeng et al., 2010), inhibition of the APC/C had no apparent effect on spindle formation, but often caused a metaphase arrest followed by cohesion fatigue and chromosome scattering, spindle elongation, and spindle rotation (Figure 7A, B; Figure S6A). In other cases, cells depleted of Cdc20 were able to proceed into anaphase, albeit after a delay, which is consistent with reports that very low levels of Cdc20 are sufficient to support anaphase onset (Wolthuis et al., 2008). Also confirming published results (Soderholm et al., 2011), the inhibition of importin-b slightly delayed chromosome congression, yet cells eventually completed spindle assembly and initiated sister chromatid separation (Figure 7A, B). By contrast, when cells were concurrently treated with siRNAs against Cdc20 and importazole, a much larger fraction of cells arrested prior to anaphase, a metaphase plate with completely aligned chromosomes was rarely observed, and arrested cells died without visible chromosome scattering or spindle rotation (Figure 7A, B). Similar phenotypes were observed when importazole was combined with TAME (Figure 7C; Figure S6B, C), a compound that interferes with the activity of APC/C^{Cdc20} (Zeng et al., 2010), or MG132, a molecule that blocks proteasomal degradation (Figure S6D). These findings were independent of the reporter used to monitor cell division, as we made similar observations when the APC/C and importin-b were inhibited in cells that stably expressed the kinetochore marker ^{LAP/GFP}CenA (Figure S6E). Our experiments, therefore, confirm that neither the APC/C nor importin-b is essential for spindle formation. However, spindle function is highly compromised when the APC/C and importin-b are inhibited at the same time, a condition that simultaneously removes two players that restrict the activity of spindle assembly factors. We conclude that the rapid degradation of spindle assembly factors, a reaction that is tightly controlled by microtubules and importin-b, is a fundamental component of the control mechanisms that ensure the robustness and accuracy of metazoan cell division.

Discussion

In this study, we discovered localized stabilization as a mechanism that tightly controls the abundance of critical spindle assembly factors. At the heart of this regulatory circuit are microtubules, the main constituents of the mitotic spindle and direct binding partners of spindle assembly factors. When bound to microtubules, HURP, NuSAP, and Tpx2 are protected from APC/C-dependent degradation. By contrast, if these substrates are not associated with the spindle, they are highly susceptible to degradation and turned over shortly after the APC/C has been fully activated at the metaphase-anaphase transition. It is well established that spindle defects indirectly result in APC/C-inhibition by triggering the spindle assembly checkpoint, a signaling network that impedes the capacity of APC/C^{Cdc20} to recognize its substrates. Our current work suggests that the spindle also directly inhibits the turnover of specific APC/C-substrates, a mechanism that is important for accurate cell division.

Based on our findings, we propose a framework for the temporal and spatial regulation of spindle assembly factors (Figure 7D): HURP, NuSAP, or Tpx2 are initially sequestered by importins, which inhibit and stabilize Ran-dependent spindle assembly factors (Kalab and Heald, 2008; Song and Rape, 2010). As importin-b does not block HURP's high-affinity microtubule-binding domain, spindle assembly factors could be loaded onto the spindle in their inactive, importin-bound states. In contrast to surgical mutations in microtubule- and importin-b binding sites, expression of dominant negative importin- or Ran-variants displaces HURP from the spindle (Sillje et al., 2006), suggesting that the global interference with the Ran-gradient also has secondary effects upon spindle assembly factor targeting. In proximity to chromatin, Ran^{GTP} dissociates HURP from importin-b, thereby activating the spindle assembly factor by allowing its MBD2 to engage microtubules. Importantly, as the MBD1 is already bound to microtubules, the active spindle assembly factor remains protected from recognition by the APC/C. When HURP is no longer required, it will be released from the spindle, and - as suggested by the instantaneous degradation of soluble HURP upon APC/C-activation - rapidly degraded. In this model, only spindle assembly factors that have fulfilled their mitotic role are turned over: inactive spindle assembly factors are stabilized by importin-b, whereas those molecules that are engaged in spindle formation are protected by microtubules. The microtubule-dependent regulation of APC/C-substrate degradation, therefore, effectively couples the activity and stability of critical cell cycle proteins.

How microtubules stabilize specific APC/C-substrates requires further analyses, but our results indicate that a direct interaction with spindle assembly factors plays an important role: whereas microtubules stabilized HURP, NuSAP and Tpx2, they had no effects on soluble APC/C-substrates. Moreover, the mutation of HURP's MBD1 allowed the degradation of this spindle assembly factor in the presence of microtubules, while the transfer of the MBD1 to soluble APC/C-substrates was sufficient to impose this control mechanism. By associating with spindle assembly factors, microtubules could impede the

recognition of substrates by the APC/C or interfere with rate-limiting steps of the ubiquitylation reaction, such as chain initiation (Williamson et al., 2011). Potentially pointing towards the latter mechanism, the MBD1 does not overlap with the D-box, KEN-box or initiation motif in HURP (Song and Rape, 2010), and its transfer to other substrates allowed their stabilization even though these proteins had their degrons at distinct positions than HURP. These findings make it seem unlikely that microtubules simply shield a critical degron from recognition by the APC/C. Instead, we favor the idea that the MBD1 confers a property onto microtubules, such as bundling, that is not conducive to the build-up of ubiquitin chains by the APC/C. Indeed, all spindle assembly factors subject to this regulatory mechanism bundle microtubules, and HURP requires the MBD1 for this function. Moreover, a microtubule-binding domain that does not bundle microtubules failed to impose microtubule-dependent stabilization, even though it could target APC/C-substrates to microtubules with similar efficiency as the MBD1.

As microtubule-bundlers often accumulate on kinetochore fibers, but not astral microtubules, this mechanism of stabilization might be of particular relevance for the critical subset of spindle microtubules that mediate chromosome attachment and sister chromatid separation. Supporting this notion, the stabilization of HURP impaired the assembly of a metaphase plate with completely aligned chromosomes. This result is consistent with the finding that overexpression of spindle assembly factors can impair cell division and lead to tumorigenesis, and that it has been inversely correlated with therapeutic outcome (Aguirre-Portoles et al., 2012; Gulzar et al., 2013; Perez de Castro and Malumbres, 2012; Tsou et al., 2003). Without proper APC/C-activity, spindle assembly factors might accumulate over multiple cell cycles and exert their effects due to a gradual increase in their abundance. It is also possible that a fraction of spindle assembly factor molecules are degraded immediately after the last kinetochore has been attached to the spindle, a hypothesis that is consistent with the high processivity of HURP ubiquitylation (Rape et al., 2006; Song and Rape, 2010). Alternatively, spindle assembly factor molecules that were released from microtubules might need to be turned over even during spindle formation and checkpoint signaling, potentially to ensure microtubule dynamics. In agreement with this hypothesis, proteasome inhibition stabilized the microtubule-binding deficient HURP in mitotic cells that had retained high levels of kinetochore-bound Mad1 and BubR1 (data not shown), a condition that usually signals an active spindle checkpoint (Kim and Yu, 2011; Musacchio and Salmon, 2007).

Our work underscores the notion that two essential cell cycle regulators, the APC/C and Ran, cooperate in establishing a robust spindle that can effectively separate sister chromatids during mitosis. Similar to the misregulation of spindle assembly factors, aberrant activity of the APC/C or Ran has been linked to tumorigenesis (Garcia-Higuera et al., 2008; Jung et al., 2006; Kalab and Heald, 2008; Manchado et al., 2010; van Ree et al., 2010; Wagner et al., 2004). Understanding how ubiquitin-dependent proteolysis is integrated with other mitotic regulators, such as Ran, to allow faithful cell division and how this

interplay between multiple levels of cell cycle control is disrupted in disease will be an important avenue for future work.

Summary

This project examines how the APC/C and Ran systems are integrated in the regulation of mitotic spindle assembly and disassembly. Previously, our lab had characterized HURP as an APC/C substrate that was protected from degradation through importin binding (Song and Rape, 2010). In this work, we build upon those understandings, and further show that the Ran system, microtubules, and APC/C all play important roles in regulating HURP spatially and temporally. These data, and the underlying philosophy of generating a better understanding of APC/C activities in mitosis, connect directly to my previous chapters, in which we examine how the APC/C genetically interacts with a subset of prometaphase regulators. The techniques shown throughout are complementary; throughout the three chapters, my microscopy skills grew and developed, and techniques developed for this paper were used in my other work, and vice versa. Finally, two additional projects were undertaken as a result of the work, in which we examine similar types of SAF regulation (shown in Appendices B and C). While we originally thought that the substrates investigated in Appendices B and C would phenocopy HURP's regulation, we subsequently discovered that they possess both similar but distinct modes of regulation.

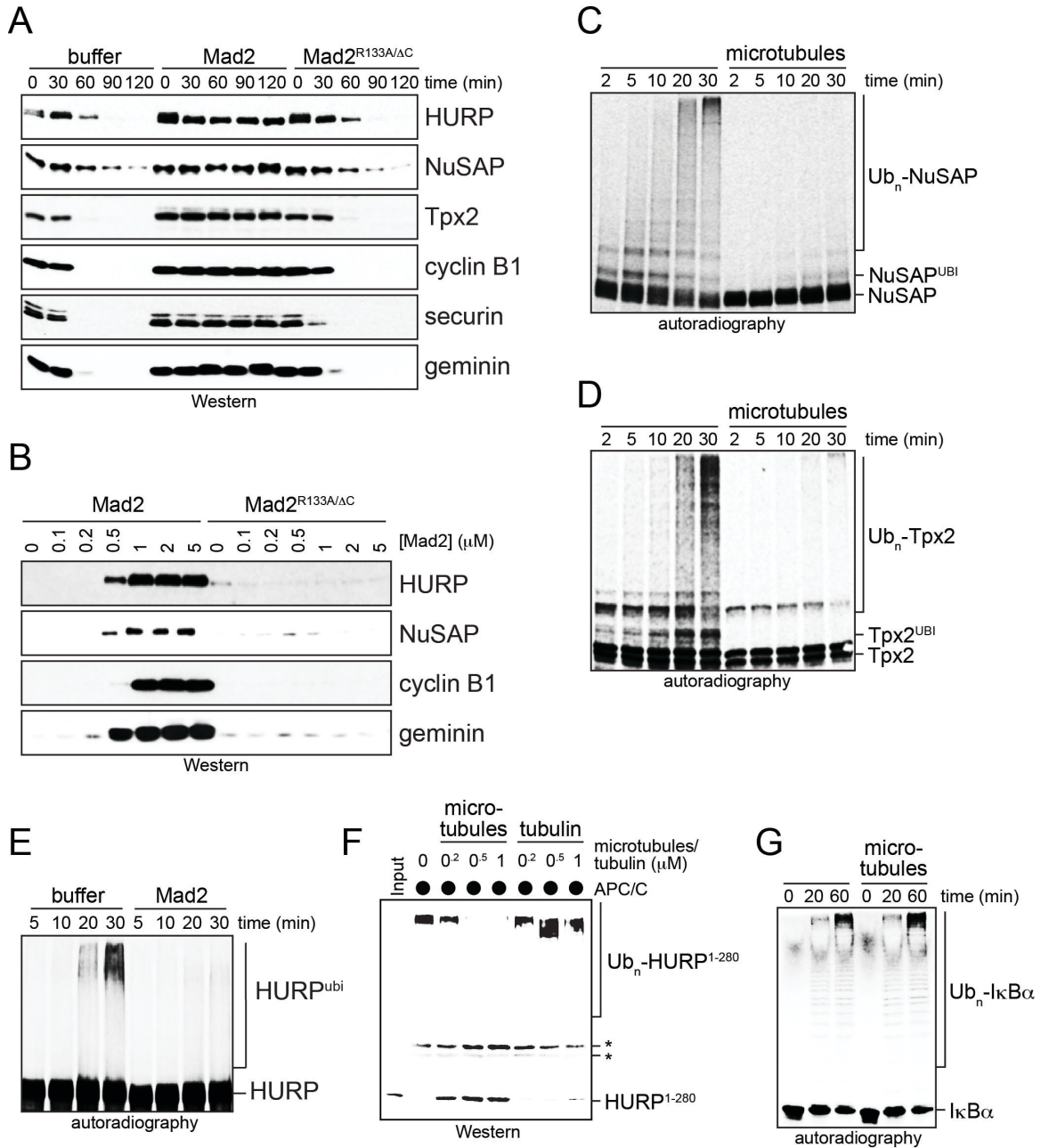


Figure S1 (related to Figures 1 and 2): Soluble spindle assembly factors can be targeted by APC/C^{Cdc20}. **A.** Extracts were prepared from prometaphase HeLa cells, treated with Ran^{Q69L} to dissociate spindle assembly factors from importins, and incubated with p31^{comet} to activate the APC/C. Where indicated, the APC/C^{Cdc20}-specific inhibitor Mad2 or an inactive variant of Mad2 (Mad2^{R133A/ΔC}) were added. The stability of endogenous APC/C-substrates in the extracts was monitored over time by Western blotting. **B.** Degradation assays were performed in the presence of increasing concentrations of Mad2 or inactive Mad2^{R133A/ΔC} and the abundance of APC/C-substrates after 120min of incubation was analyzed by Western blotting. **C.** Microtubules inhibit the APC/C^{Cdc20}-dependent ubiquitylation of NuSAP. ³⁵S-labeled NuSAP was purified and incubated with APC/C^{Cdc20} and a ubiquitylation cocktail. As indicated, microtubules were added prior to the ubiquitylation. Reactions were analyzed by autoradiography. **D.** Microtubules prevent APC/C^{Cdc20}-dependent ubiquitylation of Tpx2. The ubiquitylation of purified ³⁵S-labeled Tpx2 by APC/C^{Cdc20} was performed as described. **E.** Mad2 inhibits the ubiquitylation of HURP by

APC/C^{Cdc20}. ³⁵S-labeled HURP was synthesized *in vitro* and incubated with APC/C^{Cdc20} purified from early mitotic cells in the presence or absence of recombinant Mad2. Reactions were analyzed by autoradiography. **F.** Tubulin polymerization is required for effects on APC/C-dependent ubiquitylation. Equal concentrations of taxol-stabilized microtubules or tubulin were incubated with bacterially purified, recombinant HURP¹⁻²⁸⁰, APC/C, and a ubiquitylation cocktail. Reactions were analyzed by Western blotting of recombinant HURP. **G.** Microtubules do not inhibit SCF-dependent ubiquitylation. SCF^{βTRCP} purified from 293T cells was incubated with radiolabeled, phosphorylated, and purified IκBα. Ubiquitylation reactions contained microtubules where indicated. The reactions were analyzed by autoradiography.

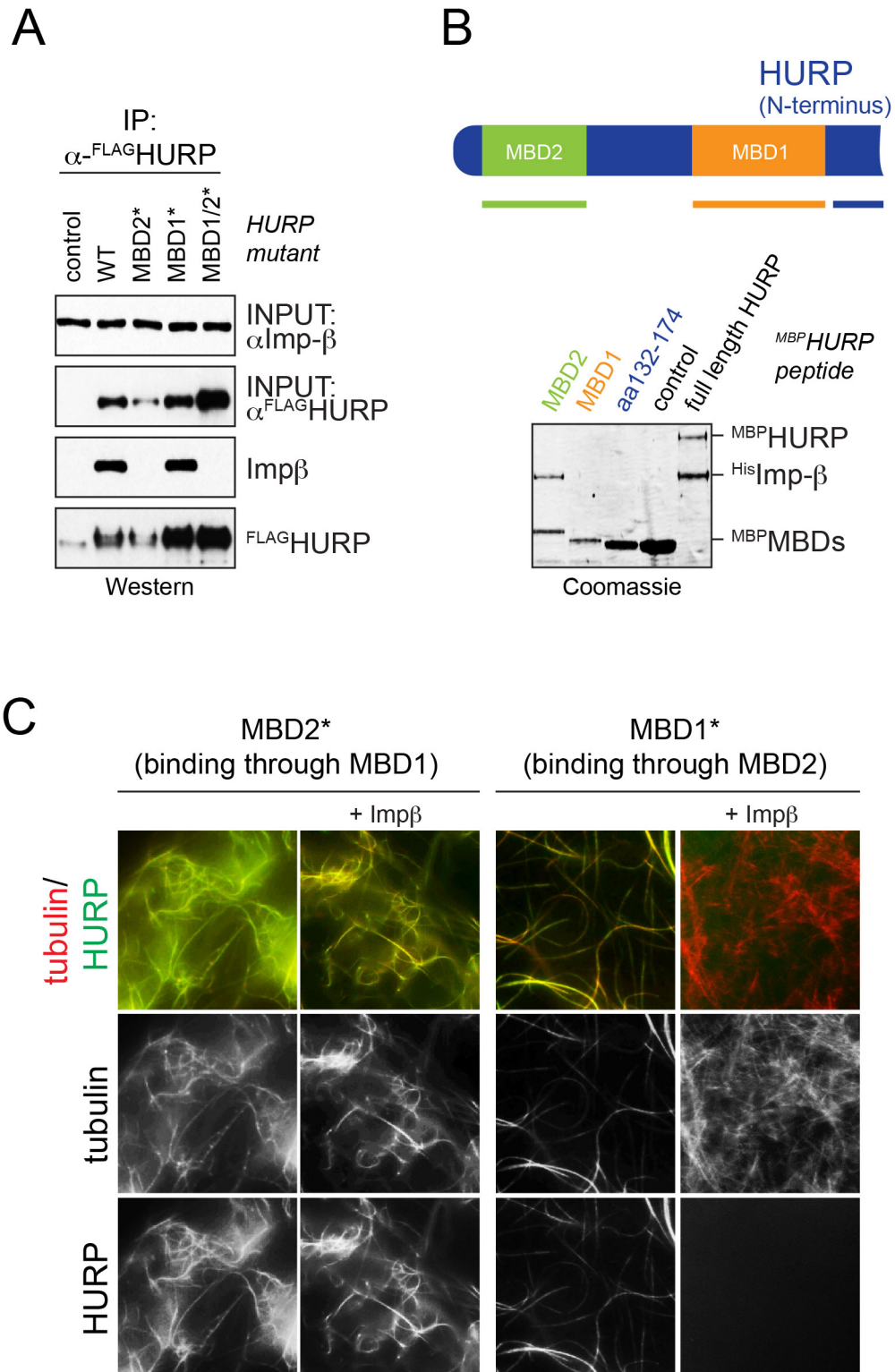


Figure S2 (related to Figure 3): Importin- β recognizes the MBD2 of HURP. A. Mutation of the MBD2 abolishes binding of importin- β to HURP in cells. 293T cells were transfected with FLAG-tagged HURP, mutants of its MBD1 or MBD2 (positively charged residues were changed to alanine), or a mutant that lacked both MBDs. Interphase cells were harvested and analyzed for interactions between HURP and importin- β by FLAG-affinity purification and Western blotting. **B.**

Importin- β binds the MBD2 of HURP. MBP-fusions to HURP, the MBD1, or the MBD2, were immobilized on amylose beads and incubated with recombinant importin- β . Following extensive washes, binding reactions were analyzed by Coomassie staining. **C.** Importin- β blocks the microtubule-binding of the MBD2. Rhodamine-labeled microtubules were incubated with recombinant Oregon 488-labeled HURP^{MBD1*} (functional MBD2) or HURP^{MBD2*} (functional MBD1). Where indicated, a two-fold molar excess of importin- β was added. Binding of labeled HURP-proteins to microtubules was visualized by fluorescence microscopy.

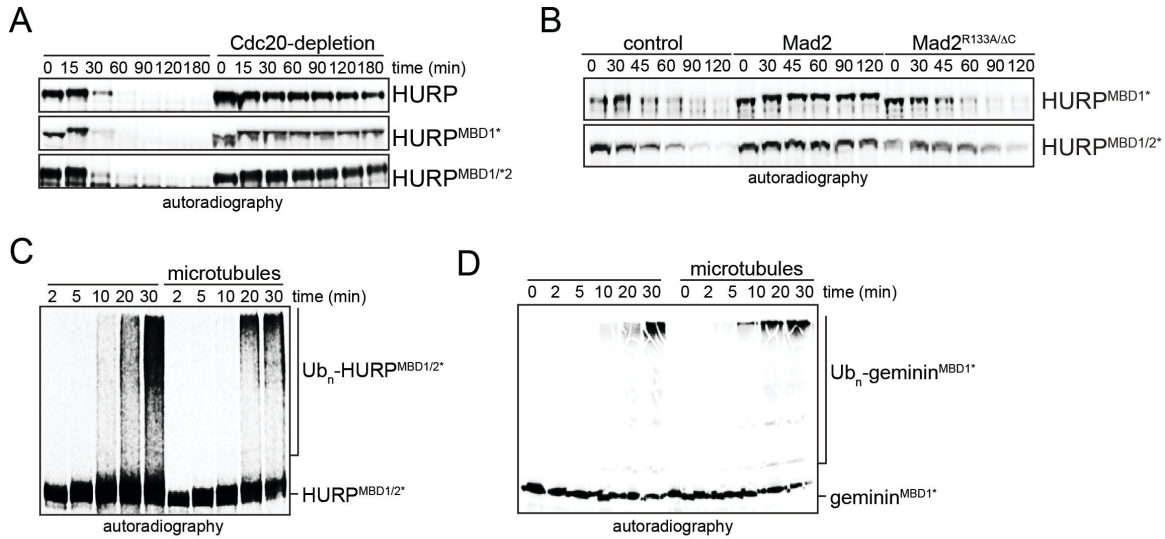


Figure S3 (related to Figure 4): Characterization of the effects of mutants and fusions of the MBD1 on APC/C-substrate ubiquitylation and degradation. **A.** Mutants in the MBD1 of HURP are degraded in an APC/C-dependent manner. Extracts of prometaphase HeLa cells were treated with Ran^{Q69L} to dissociate HURP from importin-β and supplemented with p31^{comet} to activate the APC/C. As indicated, Cdc20 was depleted from extracts using specific antibodies. The degradation of ³⁵S-labeled HURP, HURP^{MBD1*}, or HURP^{MBD1/2*} was monitored by autoradiography. **B.** Mutants in the MBD1 of HURP are stabilized by the APC/C^{CDC20}-inhibitor Mad2, ³⁵S-labeled HURP^{MBD1*} or HURP^{MBD1/2*} were added to mitotic extract with active APC/C either in the presence of recombinant Mad2 or an inactive variant, Mad2^{R133A/ΔC}. Substrate stability was monitored by autoradiography. **C.** Loss of microtubule-binding ablates any effects of microtubules upon HURP-ubiquitylation. ³⁵S-labeled ZZ/TEV-HURP^{MBD1/2*} was purified after *in vitro* transcription/translation over IgG-sepharose, eluted with TEV, and incubated with active APC/C either in the presence or absence of microtubules. Reactions were analyzed by autoradiography. **D.** Mutations in the MBD1 obliterate its effect on the ubiquitylation of a heterologous APC/C-substrate. A fusion between the first 101 residues of geminin and a mutant MBD1 of HURP was synthesized as a ³⁵S-labeled protein, purified over IgG-sepharose, eluted with TEV, and incubated with active APC/C either in the presence or absence of microtubules. Reactions were analyzed by autoradiography.

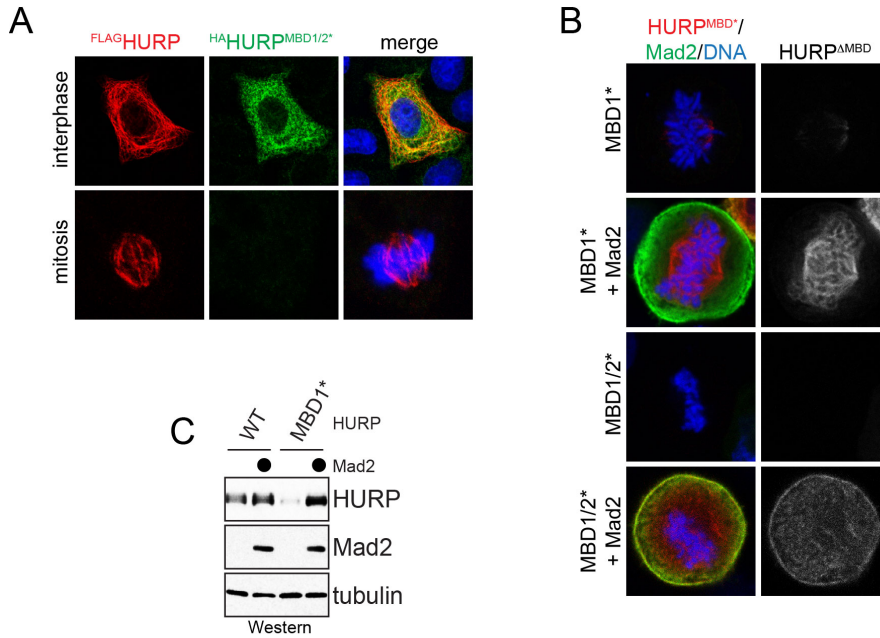


Figure S4 (related to Figure 5): Microtubules protect HURP from degradation. A. Levels of lentivirus-dependent expression of GFP-tagged HURP or microtubule-binding mutants. **B.** Loss of microtubule-binding reduces HURP-levels in mitosis. HeLa cells were simultaneously transfected with FLAG-HURP and HA-HURP^{MBD1/2*} and analyzed for HURP-expression at different cell cycle stages by immunofluorescence. **C.** Overexpression of the CDC20-inhibitor Mad2 stabilizes microtubule-binding deficient HURP-mutants in late metaphase/early anaphase. HeLa cells were transfected with FLAG-HURP^{MBD1*} or FLAG-HURP^{MBD1/2*} in the presence or absence of Mad2-overexpression. The levels of HURP proteins were detected by immunofluorescence microscopy (HURP: red; Mad2: green; DNA: blue). **D.** Microtubule-binding deficient HURP is stabilized in mitosis by Mad2 over-expression. Mitotic HeLa cells expressing HURP or HURP^{MBD1*} were harvested by shake-off and analyzed for HURP levels in the presence or absence of Mad2-overexpression by Western blotting.

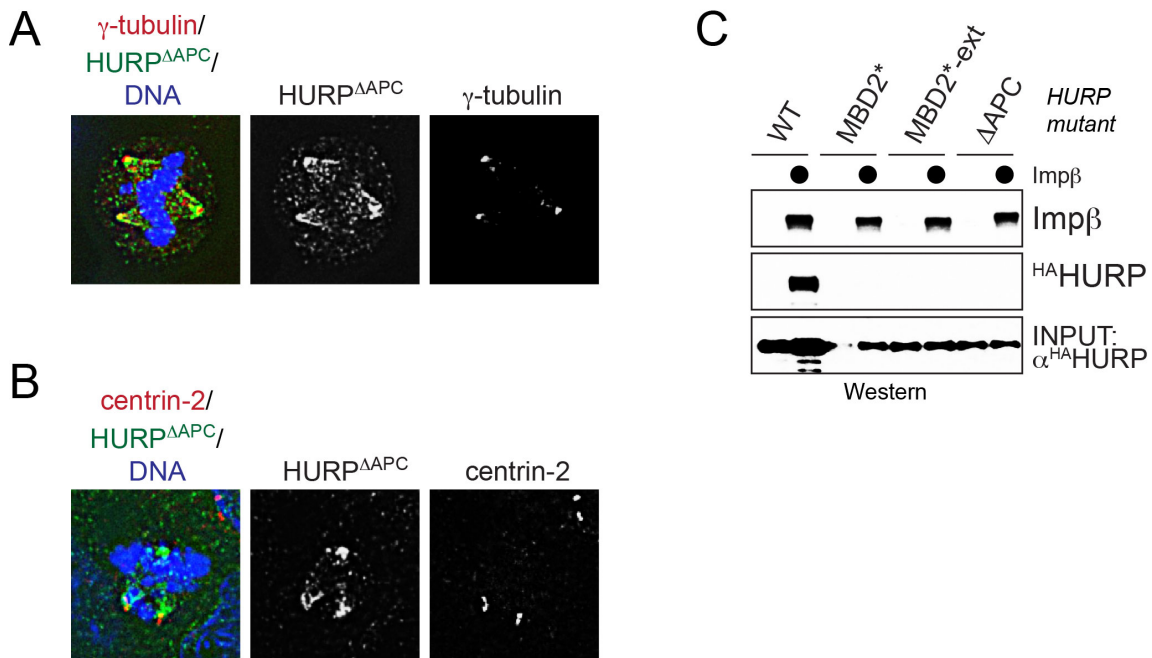


Figure S5 (related to Figure 6): Stabilization of HURP causes spindle pole fragmentation.
A. HeLa cells expressing GFP-tagged HURP Δ ^{APC/C} and having multipolar spindles were stained for GFP (green), γ -tubulin (red), and DNA (blue). **B.** HeLa cells expressing GFP-tagged HURP Δ ^{APC/C} and having multipolar spindles were stained for GFP (green), centrin-2 (red), and DNA (blue). **C.** HURP Δ ^{APC/C} is neither recognized by importin- β nor the APC/C. Lysates of HeLa cells expressing ^{myc}importin- β , ^{HA}HURP, or the indicated mutants were subjected to ^{myc}-affinity purification, and co-precipitating HURP was detected by Western blotting using specific antibodies.

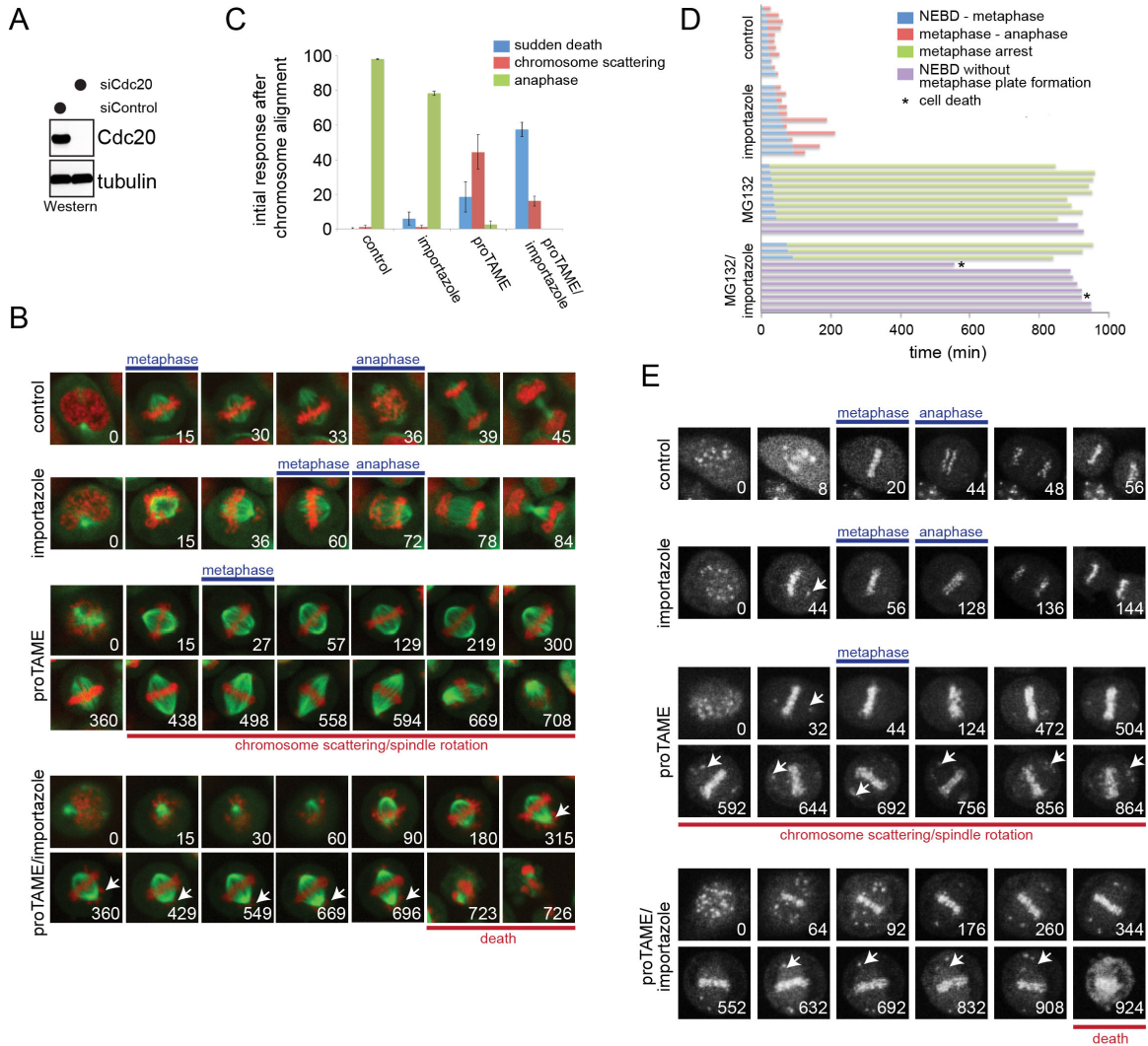


Figure S6 (related to Figure 7): APC/C and importin- β together regulate spindle structure and function. **A.** CDC20-siRNAs efficiently deplete Cdc20 protein in cells. HeLa cells were transfected with characterized Cdc20-siRNAs (Williamson, et al., 2009), and protein levels were measured with Western blotting. **B.** Small-molecule inhibition of the APC/C (with proTAME) and importin- β (with importazole) produces synergistic effects on spindle formation and cell division. HeLa cells expressing $mCherry$ histone H2B and GFP tubulin were treated with proTAME, importazole, or both, and their progression through mitosis was monitored with video microscopy. **C.** Quantification of cell division defects observed upon APC/C and/or importin- β -inhibition. Results represent three independent experiments; $n > 50$ per condition. **D.** Proteasome-inhibition synergizes with loss of importin- β -activity during mitosis. HeLa cells stably expressing $mCherry$ histone H2B and GFP tubulin were treated with proteasome inhibitor MG132, importazole, or both, and their progression through mitosis was monitored with video microscopy. Cells were analyzed for the time taken from nuclear envelope breakdown to completion of chromosome congression (blue); the time between metaphase and anaphase initiation (red); the time for metaphase arrest (green); and the time of pre-anaphase arrest without ever establishing a metaphase plate (purple). The asterisk denotes cells that underwent cell death during the time course of the experiment. **E.** Synergistic effects of APC/C- and importin- β -inhibition during mitosis can also be observed in cells expressing a kinetochore marker. HeLa cells stably expressing GFP CenpA were treated with proTAME, importazole, or both, and their progression through mitosis was monitored by video microscopy.

References

- Aguirre-Portoles, C., Bird, A.W., Hyman, A., Canamero, M., Perez de Castro, I., and Malumbres, M. 2012. Tpx2 controls spindle integrity, genome stability, and tumor development. Cancer Res. **72**: 1518-1528.
- Andrews, P.D., Ovechkina, Y., Morrice, N., Wagenbach, M., Duncan, K., Wordeman, L., and Swedlow, J.R. 2004. Aurora B Regulates MCAK at the Mitotic Centromere. Developmental Cell. **6**: 253-268.
- Ang, X.L. and Harper, J.W. 2005. SCF-mediated protein degradation and cell cycle control. Oncogene. **24**: 2860-2870.
- Ballister, E.R., Riegman, M., and Lampson, M.A. 2014. Recruitment of Mad1 to metaphase kinetochores is sufficient to reactivate the mitotic checkpoint. J. Cell Bio. **204**: 901-908.
- Buschhorn, B.A., Petzold, G., Galova, M., Dube, P., Kraft, C., Herzog, F., Stark, H., and Peters, J.M. 2011. Substrate binding on the APC/C occurs between the coactivator Cdh1 and the processivity factor Doc1. Nature Struc Mol Bio. **18**: 6-13.
- Cai, S. Weaver, L.N., Ems-McClung, S.C., and Walczak, C.E. 2009. Kinesin-14 family proteins HSET2/XCTK2 control spindle length by cross-linking and sliding microtubules. Mol Biol Cell. **20**: 1348-1359.
- Carmena, M., Ruchaud, S., and Earnshaw, W.C. 2009. Making the Auroras glow: regulation of Aurora A and B kinase function by interacting proteins. Curr Opin Cell Biol. **21**: 796-805.
- Carter, S., Bischof, O., Dejean, A., and Vousden, K.H. 2007. C-terminal modifications regulate MDM2 dissociation and nuclear export of p53. Nat. Cell. Biol. **9**: 428-435.
- Chait, R., Craney, A., and Kishony, R. 2007. Antibiotics that select against resistance. Nature. **446**: 668-671.
- Chao, W.C., Kulkarni, K., Zhang, Z., Kong, E.H., and Barford, D. 2012. Structure of the mitotic checkpoint complex. Nature. **484**: 208-213.
- Cheeseman, I.M., Chappie, J.S., Wilson-Kubalek, E.M., and Desai, A. 2006. The conserved KMN network constitutes the core microtubule-binding site of the kinetochore. Cell. **127**: 983-997.
- Cheeseman, I.M. and Desai, A. 2008. Molecular architecture of the kinetochore-microtubule interface. Nat Rev Mol Biol. **9**: 33-46.

Chou, C-P., Huang, N-C., Jhuang, S-J., Pan, H-B., Peng, N-J, Cheng, J-T., Chen, C-F., Chen, Chen, J-J., Chang, T-H. 2014. Ubiquitin-conjugating enzyme Ube2C is highly expressed in breast microcalcification lesions. PLoS ONE. **9**: e93934.

Ciechanover, A., Finley, D., and Varshavsky, A. 1984. Ubiquitin dependence of selective protein degradation demonstrated in the mammalian cell cycle mutant ts85. Cell. **37**: 57-66.

Civelekoglu-Scholey, G., He, B., Shen, M., Wan, X., Roscioli, E., Bowden, B., and Cimini, D. 2013. Dynamic bonds and polar ejection force distribution explain kinetochore oscillations in PtK1 cells. J Cell Biol. **201**: 577-593.

Cleveland, D.W., Hwo, S.Y., and Kirschner, M.W. 1977. Purification of tau, a microtubule-associated protein that induces assembly of microtubules from purified tubulin. J. Mol. Biol. **116**: 207-225.

Clift, D., Bizzari, F., and Marston, A.L. 2009. Shugoshin prevents cohesin cleavage by PP2A^{Cdc55}-dependent inhibition of separase. Genes Dev. **23**: 766-780.

Craney, A. and Rape, M. 2013. Dynamic regulation of ubiquitin-dependent cell cycle control. Curr Opin Cell Biol. **25**: 704-710.

da Fonseca, P.C., Kong, E.H., Zhang, Z., Schreiber, A., Williams, M.A., Morris, E.P., and Barford, D. 2011. Structures of APC/C(Cdh1) with substrates identify Cdh1 and Apc10 as the D-box co-receptor. Nature. **470**: 274-278.

Daum, J.R., Potapova, T.A., Sivakumar, S., Daniel, J.J., Flynn, J.N., Rankin S., and Gorbsky, G.J. 2011. Cohesion fatigue induces chromatid separation in cells delayed at metaphase. Curr Biol. **21**: 1018-1024.

DeLuc, J.G., Gall, W.E., Ciferri, C., Cimini, D., Musacchio, A., and Salmon, E.D. 2006. Kinetochore microtubule dynamics and attachment stability are regulated by Hec1. Cell. **127**: 969-982.

DeLuca, J.G., Dong, Y., Hergert, P., Strauss, J., Hickey, J.M., Salmon, E.D., and McEwen, B.F. 2005. Hec1 and Nuf2 are core components of the kinetochore outer plate essential for organizing microtubule attachment sites. Mol Biol Cell. **16**: 519-531.

Jennifer G. DeLuca. 2010. Kinetochore-Microtubule Dynamics and Attachment Stability. Chapter 4, In L. Cassimeris (Ed.), *Microtubules: in vivo*. Academic Press.

den Elzen, N. and Pines, J. 2001. Cyclin A is destroyed in prometaphase and can delay chromosome alignment and anaphase. J. Cell Biol. **153**: 121-135.

Deshaies, R.J. 2014. Proteotoxic crisis, the ubiquitin-proteasome system, and cancer therapy. BMC Biology. **12**: 94-107.

Deshaies, R.J., and Joazeiro, C.A. 2009. RING domain E3 ubiquitin ligases. Annu Rev Biochem. **78**: 399-434.

Dikic, I., Wakatsuki, S., and Walters, K.J. 2009. Ubiquitin-binding domains from structures to functions. Nat Rev Mol Cell Biol. **10**: 659-671.

Ems-McClung, S.C., Zheng, Y., and Walczak, C.E. 2004. Importin α/β and Ran-GTP Regulate XCTK2 Microtubule Binding through a Bipartite Nuclear Localization Signal. Molecular Biology of the Cell. **15**: 46-57.

Finley, D., Ciechanover, A., and Varshavsky, A. 1984. Thermolability of ubiquitin-activating enzyme from the mammalian cell cycle mutant ts85. Cell. **37**: 43-55.

Foley, E.A., Maldonado, M., and Kapoor, T. 2011. Nat Cell Biol. Formation of stable attachments between kinetochores and microtubules depends on the B56-PP2A phosphatase. **13**: 1265-1272.

Foster, S.A. and Morgan, D. O. 2012. The APC/C subunit Mnd2/Apc15 promotes Cdc20 autoubiquitination and spindle assembly checkpoint inactivation. Mol Cell. **47**: 921-932.

Frost, A., Elgort, M.G., Brandman, O., Ives, C., Collins, S.R., Miller-Vedam, L., Weibezahn, J., Hein, M.Y., Poser, I., Mann, M., Hyman, A.A., and Weissman, J.S. 2012. Functional repurposing revealed by comparing *S. pombe* and *S. cerevisiae* genetic interactions. Cell. **149**: 1339-1352.

Gable, A., Qiu, M., Titus, J., Balchand, S., Ferenz, N.P., Ma, N., Collins, E.S., Fagerstrom, C., Ross, J.L., Yang, G., *et al.* 2012. Dynamic reorganization of Eg5 in the mammalian spindle throughout mitosis requires dynein and TPX2. Mol Biol. Cell. **23**: 1254-1266.

Ganem, N.J., Upton, K., and Compton, D.A. 2005. Efficient mitosis in human cells lacking poleward microtubule flux. Curr Biol. **15**: 1827-1832.

Garcia-Higuera, I., Manchado, E., Dubus, P., Canamero, M., Mendez, J., Moreno, S., and Malumbres, M. 2008. Genomic stability and tumour suppression by the APC/C cofactor Cdh1. Nature Cell Biol. **10**: 802-811.

Garnett, M.J., Mansfeld, J., Godwin, C., Matsusaka, T., Wu, J., Russell, P., Pines, J., and Venkitaraman, A.R. 2009. UBE2S elongates ubiquitin chains on APC/C substrates to promote mitotic exit. Nature Cell Biol. **11**: 1363-1369.

Geley, S, Kramer, E., Gieffers, C., Gannon, J., Peters, J-M., and Hunt, T. 2001. Anaphase-promoting complex/cyclosome-dependent proteolysis of human cyclin A starts at the beginning of mitosis and is not subject to the spindle assembly checkpoint. J. Cell Biol. **153**: 137-147.

Godek, K.M., Kabeche, L., and Compton D.A. 2015. Regulation of kinetochore-microtubule attachments through homeostatic control during mitosis. Nat Rev Mol Cell Biol. **16**: 57-64.

Goron, D.J., Resio, B., and Pellman, D. 2012. Causes and consequences of aneuploidy in cancer. Nature Reviews Genetics. **13**: 189-203.

Görlich, D., Henklein, P., Laskey, R.A., and Hartmann, E. 1996. A 41 amino acid motif in importin-alpha confers binding to importin-beta and hence transit into the nucleus. EMBO J. **15**: 1810-1817.

Goshima, G., Wollman, R., Goodwin, S.S., Zhang, N., Scholey, J.M., Vale, R.D., and Stuurman, N. 2007. Genes required for mitotic spindle assembly in *Drosophila* S2 cells. Science. **316**: 417-421.

Gruss, O.J., Carazo-Salas, R.E., Schatz, C.A., Guarguaglini, G., Kast, J., Wilm, M., Le Bot, N., Vernos, I., Karsenti, E., and Mattaj, I.W. 2001. Ran induces spindle assembly by reversing the inhibitory effect of importin alpha on TPX2 activity. Cell. **104**: 83-93.

Gruss, O.J., Wittmann, M., Yokoyama, H., Pepperkok, R., Kufer, T., Sillje, H., Karsenti, E., Mattaj, I.W., and Vernos, I. 2002. Chromosome-induced microtubule assembly mediated by TPX2 is required for spindle formation in HeLa cells. Nature Cell Biol. **4**: 871-879.

Gulzar, Z.G., McKenney, J.K., and Brooks, J.D. 2013. Increased expression of NuSAP in recurrent prostate cancer is mediated by E2F1. Oncogene. **32**: 70-77.

Hames, R.S., Wattam, S.L., Yamano, H., Bacchieri, R., and Fry, A.M. 2001. APC/C-mediated destruction of the centrosomal kinase Nek2A occurs in early mitosis and depends upon a cyclin A-type D-box. EMBO J. **20**: 7117-7127.

Haas, A.L., Warms, J.V.B., Hershko, A., and Rose, I.A. 1982. Ubiquitin-activating enzyme. Mechanism and role in protein-ubiquitin conjugation. J. Biol. Chem. **257**: 2543-2548.

Hayes, M.J., Kimata, Y., Wattam, S.L., Lindon, C., Mao, G., Yamano, H., and Fry, A.M. 2006. Early mitotic degradation of Nek2A depends on Cdc20-independent interaction with the APC/C. Nat Cell Biol. **8**: 607-614.

Hershko, A., Ciechanover, A., Heller, H., Haas, A.L., and Rose, I.A. 1980. Proposed role of ATP in protein breakdown: conjugation of protein with multiple chains of the polypeptide of ATP-dependent proteolysis. Proc Natl Acad Sci U.S.A. **77**: 1783-1786.

Herzog, F., Primorac, I., Dube, P., Lenart, P., Sander, B., Mechtler, K., Stark, H., and Peters, J.M. 2009. Structure of the anaphase-promoting complex/cyclosome interacting with a mitotic checkpoint complex. Science. **323**: 1477-1481.

Hoege, C., Pfander, B., Moldovan, G.L., Pyrowolakis, G., and Jentsch, S. 2002. RAD6-dependent DNA repair is linked to modification of PCNA by ubiquitin and SUMO. Nature. **419**: 135-41.

Hong, L., Rankin, S., and Yu, H. 2013. Phosphorylation-enabled binding of Sgo1-PP2A to cohesin protects sororin and centromeric cohesion during mitosis. Nat. Cell Biol. **15**: 40-49.

Hu, Y., Wu, G., Rusch, M., Lukes, L., Buetow, K.H., Zhang, J., and Hunter, K.W. (2012). Integrated cross-species transcriptional network analysis of metastatic susceptibility. Proc Natl Acad Sci USA. **109**: 3184-3189.

Huang, Y., Yao, Y., Xu, H-Z., Wang, Z-G., Lu, L., and Dai, W. 2009. Defects in chromosome congression and mitotic progression in KIF18A-deficient cells are partly mediated through impaired functions of CENP-E. Cell Cycle. **8**(16): 2643-2649.

Jaqaman, K., King, E.M., Amaro, A.C., Winter, J.R., Dorn, J.F., Elliott, H.L., Mchedlishvili, N., McClelland, S.E., Porter, I.M., Posch, M., Toso, A., Danuser, G., McAnish, A.D., Meraldi, P., and Swedlow, J.R. 2010. Kinetochore alignment within the metaphase plate is regulated by centromere stiffness and microtubule depolymerases. J. Cell Biol. **188**: 665-679.

Jiang, L., Bao, Y., Luo, C., Hu, G., Huang, C., Ding, X., Sun, K., and Lu, Y. 2010. Knockdown of ubiquitin-conjugating enzyme E2C/Ubch10 expression by RNA interference inhibits glioma cell proliferation and enhances cell apoptosis in vitro. J Cancer Res Clin Oncol. **136**: 211-217.

Jin, L., Williamson, A., Banerjee, S., Philipp, I., and Rape, M. 2008. Mechanism of ubiquitin-chain formation by the human anaphase-promoting complex. Cell. **133**: 653-665.

Jung, C.R., Hwang, K.S., Yoo, J., Cho, W.K., Kim, J.M., Kim, W.H., and Im, D.S. 2006. E2-EPF UCP targets pVHL for degradation and associates with tumor growth and metastasis. Nat Med. **12**: 809-816.

Kabeche, L. and Compton, D. 2013. Cyclin A regulates kinetochore microtubules to promote faithful chromosome segregation. Nature. **502**: 110-113.

Kafri, R., Levy, J., Ginzberg, M.B., Oh, S., Lahav, G. and Kirschner, M.W. 2013. Dynamics extracted from fixed cells reveal feedback linking cell growth to cell cycle. Nature. **494**: 480-494.

Kalab, P., and Heald, R. 2008. The RanGTP gradient - a GPS for the mitotic spindle. J. Cell Sci. **121**: 1577-1586.

Kalab, P., Weis, K., and Heald, R. 2002. Visualization of a Ran-GTP Gradient in Interphase and Mitotic *Xenopus* Egg Extracts. Science. **295**: 2452-2456.

Kalab, P., Weis, Pralle, A., Isacoff, E.Y., Heald, R., and Weis, K. 2006. Analysis of a RanGTP-regulated gradient in mitotic somatic cells. Nature. **440**: 697-701.

Kapoor, T.M., Lampson, M.A., Hergert, P., Cameron, L., Cimini, D., Salmon, E.D., McEwen, B.F., and Khodjakov, A. 2006. Chromosomes can congress to the metaphase plate before biorientation. Science. **311**: 388-391.

Kelly, A., Wickliffe, K.E., Song, L., Fedrigo, I., and Rape, M. 2014. Ubiquitin chain elongation requires E3-dependent tracking of the emerging conjugate. Molecular Cell. **56**: 232-245.

Khodjakov, A. and Kapoor, T. 2005. Microtubule flux: what is it good for? Curr Biol. **23**: R966-R968.

Kim, S., and Yu, H. 2011. Mutual regulation between the spindle checkpoint and APC/C. Semin Cell Dev Biol. **22**: 551-558.

Kim, Y., Holland, A.J., Lan, W., and Cleveland, D.W. 2010. Aurora kinases and protein phosphatase 1 mediate chromosome congression through regulation of CENP-E. Cell. **142**: 444-455.

Kirkpatrick, D.S., Hathaway, N.A., Hanna, J., Elsasser, S., Rush, J., Finley, D., King, R.W., and Gygi, S.P. 2006. Quantitative analysis of in vitro ubiquitinated cyclin B1 reveals complex chain topology. Nat Cell Biol. **8**: 700-710.

Koffa, M.D., Casanova, C.M., Santarella, R., Kocher, T., Wilm, M., and Mattaj, I.W. 2006. HURP is part of a Ran-dependent complex involved in spindle formation. Curr Biol. **16**: 743-754.

Komander, D., Clague, M.J., and Urbé, S. 2009. Breaking the chains: structure and function of the deubiquitinases. Nat Rev Mol Cell Biol. **10**: 550-563.

Komander, D., and Rape, M. 2012. The ubiquitin code. Annu Rev Biochem. **81**: 203-229.

Kraft, C., Herzog, F., Gieffers, C., Mechtler, K., Hagting, A., Pines, J., and Peters, J-M. 2003. Mitotic regulation of the human anaphase-promoting complex by phosphorylation. EMBO. **24**: 6598-6609.

Kufer, T.A., Sillje, H.H., Korner, R., Gruss, O.J., Meraldi, P., and Nigg, E.A. 2002. Human TPX2 is required for targeting Aurora-A kinase to the spindle. The J. Cell Bio. **158**: 617-623.

Kuijt, T.E.F., Omerzu, M., Saurin, A.T., and Kops, G.J.P.L. 2014. Conditional targeting of Mad1 to kinetochores is sufficient to reactivate the spindle assembly checkpoint in metaphase. Chromosoma. **123**: 471-480.

Kumar, J., Choudhary, B.C., Metpally, R., Zheng, O., Nonet, M.L., Ramanathan, S., Klopfenstein, D.R., and Koushika, S.P. 2010. The *Caenorhabditis elegans* Kinesin-3 Motor UNC-104/KIF1A is Degraded upon Loss of Specific Binding to Cargo. PLoS Genetics. **6**: 1-19.

Lee, K., Kenny, A.E., and Rider, C.L. 2010. P38 Mitogen-activated protein kinase activity is required during mitosis for timely satisfaction of the mitotic checkpoint but not for the fidelity of chromosome segregation. Mol Biol Cell. **21**: 2150-2160.

Liu, D., Vleugel, M., Backer, C.B., Hori, T., Fukagawa, T., Cheeseman, I.M., and Lampson, M.A. 2010. Regulated targeting of protein phosphatase 1 to the outer kinetochore by KNL1 opposes Aurora B kinase. J. Cell Bio. **188**: 809-820.

Luo, Ju., Emanuele, M.J., Li, Danan., Creighton, C.J., Schlabach, M.R., Westbrook, T.F., Wong, K., and Elledge, S.J. 2009. A genome-wide RNAi screen identifies multiple synthetic lethal interactions. Cell. **137**: 835-848.

Maldonado, M., and Kapoor, T.M. 2011. Constitutive Mad1 targeting to kinetochores uncouples checkpoint signaling from chromosome biorientation. Nat. Cell Biol. **13**: 475-482.

Manchado, E., Guillamot, M., de Carcer, G., Eguren, M., Trickey, M., Garcia-Higuera, I., Moreno, S., Yamano, H., Canamero, M., and Malumbres, M. 2010. Targeting mitotic exit leads to tumor regression in vivo: Modulation by Cdk1, Mastl, and the PP2A/B55alpha,delta phosphatase. Cancer Cell. **18**: 641-654.

Matsumoto, M.L.*, Wickliffe, K.E.*, Dong, K.C., Yu, C., Bosanac, I., Bustos, D., Phu, L., Kirkpatrick, D.S., Hymoqitz, S.G., Rape, M., Kelley, R.F., and Dixit, V.M.

2010. K11-linked polyubiquitination in cell cycle control revealed by a K11 linkage-specific antibody. Mol. Cell. **39**: 477-484.

Mattiuzzo, M., Vargiu, G., Totta, P., Fiore, M., Ciferri, C., Musacchio, A., and Degrossi, F. 2011. Abnormal kinetochore-generated pulling forces from expressing a N-terminally modified Hec1. PLoS ONE. **6**: e16307.

Meadows, J.C., Shepperd, L.A., Vanoosthuysen, V., Lancaster, T. C., Sochaj, A.M., Buttrick, G.J., Hardwick, K.G., and Millar, J.B.A. 2011. Spindle checkpoint silencing requires association of PP1 to both Spc7 and kinesin-8 motors. Dev. Cell. **20**: 739-750.

Measday, V., Baetz, K., Guzzo, J., Yuen, K., Kwok, T., Sheikh, B., Ding, H., Ueta, R., Hoac, T., Cheng, B., Pot, I., Tong, A., Yamaguchi-Iwai, Y., Boone, C., Hieter, P., and Andrews, B. 2005. Systematic yeast synthetic lethal and synthetic dosage lethal screens identify genes required for chromosome segregation. Proc Natl Acad Sci USA. **102**: 13956-13961.

Meyer, H-J. and Rape, M. 2011. Processive ubiquitin chain formation by the anaphase-promoting complex. Seminars in Cell & Developmental Biology. **22**: 544-550.

Meyer, H-J. and Rape, M. 2014. Enhanced Protein Degradation by Branched Ubiquitin Chains. Cell. **157**: 910-921.

Mitchison, T.J. 1989. J. Cell Biol. Polewards microtubule flux in the mitotic spindle: evidence from photoactivation of fluorescence. **109**: 637-652.

Musacchio, A., and Salmon, E.D. 2007. The spindle-assembly checkpoint in space and time. Nat Rev Mol Cell Biol. **8**: 379-393.

Nachury, M.V., Maresca, T.J., Salmon, W.C., Waterman-Storer, C.M., Heald, R., Weis, K. 2001. Importin β is a Mitotic Target of the Small GTPase Ran in Spindle Assembly. Cell. **104**: 95-106.

Ogo, N., Oishi, S., Matsuno, K., Sawada, J., Fujii, N., and Asai, A. 2007. Synthesis and biological evaluation of L-cysteine derivatives as mitotic kinesin Eg5 inhibitors. Bioorganic & Medicinal Letters. **17**: 3921-3924.

Perez de Castro, I., and Malumbres, M. 2012. Mitotic Stress and Chromosomal Instability in Cancer: The Case for TPX2. Genes Cancer. **3**: 721-730.

Peters, J.M. 2006. The anaphase promoting complex/cyclosome: a machine designed to destroy. Nat Rev Mol Cell Biol. **7**: 644-656.

Pickart, C.M. 2004. Back to the Future with Ubiquitin. **116**: 181-190.

Pierce, N.W., Kleiger, G., Shan, S., and Deshaies, R.J. 2009. Detection of sequential polyubiquitylation on a millisecond timescale. Nature. **462**: 615-619.

Rago, F., Gascoigne, K.E., and Cheeseman, I.M. 2015. Distinct organization and regulation of the outer kinetochore KMN network downstream of CENP-C and CENP-T. Curr Biol. **25**: 671-677.

Rape, M., and Kirschner, M.W. 2004. Autonomous regulation of the anaphase-promoting complex couples mitosis to S-phase entry. Nature. **432**: 588-595.

Rape, M., Reddy, S.K., and Kirschner, M.W. 2006. The processivity of multiubiquitination by the APC determines the order of substrate degradation. Cell. **124**: 89-103.

Ribbeck, K., Groen, A.C., Santarella, R., Bohnsack, M.T., Raemaekers, T., Kocher, T., Gentzel, M., Gorlich, D., Wilm, M., Carmeliet, G., *et al.* 2006. NuSAP, a mitotic RanGTP target that stabilizes and cross-links microtubules. Mol Biol Cell. **17**: 2646-2660.

Reddy, S.K., Rape, M., Margansky, W.A., and Kirschner, M.W. 2007. Ubiquitination by the anaphase-promoting complex drives spindle checkpoint inactivation. Nature. **446**: 921-925.

Roguev, A., Bandyopadhyay, S., Zofall, K., Fischer, T., Collins, S.R., Qu, H., Shales, M., Park, H.O., Hayles, J., Hoe, K.L., Kim, D.U., Ideker, T., Grewal, S.I., Weissman, J.S., and Krogan, N.J. 2008. Conservation and rewiring of functional modules revealed by an epistasis map in fission yeast. Science. **322**: 405-410.

Rosenberg, J.S., Cross, F.R., and Funabiki, H. 2011. KNL1/Spc105 recruits PP1 to silence the spindle assembly checkpoint. Curr. Biol. **21**: 942-947.

Santaguida, S., Tighe, A., D'Alise, A.M., Taylor, S.S., and Musacchio, A. 2010. Dissecting the role of MPS1 in chromosome biorientation and the spindle checkpoint through the small molecule inhibitor reversine. J. Cell Biol. **190**: 73-87.

Santaguida, S., Vernieri, C., Villa, F., Ciliberto, A., and Musacchio, A. 2011. Evidence that Aurora B is implicated in spindle checkpoint signaling independently of error correction. EMBO J. **30**: 1508-1519.

Saurin, A.T., van der Waal, M.S., Medema, R.H., Lens, S.M., and Kops, G.J. 2011. Aurora B potentiates Mps1 activation to ensure rapid checkpoint establishment at the onset of mitosis. Nat. Commun. **2**: article 316.

Schlesinger, M.J. 1990. The Ubiquitin System and the Heat Shock Response. In Stress Proteins. G.M. Santoro and E. Garaci (Eds). Springer Berlin Heidelberg. pp. 81-88.

Schulman, B.A. and Harper, J.W. 2009. Ubiquitin-like protein activation by E1 enzymes: the apex for downstream signaling pathways. Nat Rev Mol Cell Biol. **10**: 319-331.

Schreiber, A., Stengel, F., Zhang, Z., Enchev, R.I., Kong, E.H., Morris, E.P., Robinson, C.V., da Fonseca, P.C., and Barford, D. 2011. Structural basis for the subunit assembly of the anaphase-promoting complex. Nature. **470**: 227-232.

Sedgwick, G.G., Hayward, D.G., Di Fiore, B., Pardo, M., Yu, L., Pines, J., and Nilsson, J. 2013. Mechanisms controlling the temporal degradation of Nek2A and Kif18A by the APC/C-Cdc20 complex. Embo J. **32**: 303-314.

Sillje, H.H., Nagel, S., Korner, R., and Nigg, E.A. 2006. HURP is a Ran-importin beta-regulated protein that stabilizes kinetochore microtubules in the vicinity of chromosomes. Curr Biol. **16**: 731-742.

Sivakumar, S. and Gorbsky, G.J. 2015. Spatiotemporal regulation of the anaphase-promoting complex in mitosis. Nat Rev Mol Cell Biol. **16**: 82-94.

Skibbens, R.V., Skeen, V.P., and Salmon, E.D. 1993. Directional instability of kinetochore motility during chromosome congression and segregation in mitotic newt lung cells: a push-pull mechanism.

Soderholm, J.F., Bird, S.L., Kalab, P., Sampathkumar, Y., Hasegawa, K., Uehara-Bingen, M., Weis, K., and Heald, R. 2011. Importazole, a small molecule inhibitor of the transport receptor importin-beta. ACS Chem Biol. **6**: 700-708.

Song, L., and Rape, M. 2010. Regulated degradation of spindle assembly factors by the anaphase-promoting complex. Mol Cell. **38**: 369-382.

Song, L., Craney, A., and Rape, M. 2014. Microtubule-dependent regulation of mitotic protein degradation. Mol Cell. **53**: 179-192.

Sowa, M.E., Bennett, E.J., Gygi, S.P., and Harper, J.W. 2009. Defining the human deubiquitinating enzyme interaction landscape. Cell. **138**: 389-403.

Stevens, D., Gassmann, R., Oegema, K., and Desai, A. 2011. Uncoordinated loss of chromatid cohesion is a common outcome of extended metaphase arrest. PLoS One. **6**: e22969.

Stewart, S., and Fang, G. 2005. Anaphase-promoting complex/cyclosome controls the stability of TPX2 during mitotic exit. Mol Cell Biol. **25**: 10516-10527.

Stumpff, J., von Dassow, G., Wagenback, M., Ashbury, C., and Wordeman, L. 2008. The kinesin-8 motor KIF18A suppresses kinetochore movements to control mitotic chromosome alignment. Dev Cell. **14**: 252-262.

Stumpff, J., Wagenback, M., Franck, A., Asbury, C.L., and Wordeman, L. 2012. Kif18A and chromokinesins confine centromere movements via microtubule growth suppression and spatial control of kinetochore tension. Dev. Cell. **22**: 1017-1029.

Suijkerbuijk, S.J.E., Vleugel, M., Teixeira, A., and Kops, G.J.P.L. 2012. Integration of kinase and phosphatase activities by BUBR1 ensures formation of stable kinetochore-microtubule attachment. Dev Cell. **23**: 745-755.

Teixeira, L.K. and Reed, S.I. 2013. Ubiquitin Ligases and Cell Cycle Control. Annu. Rev. Biochem. **18**: 14.1-14.28.

Thrower, J.S., Hoffman, L., Rechsteiner, M., and Pickart, C.M. 2000. Recognition of the polyubiquitin proteolytic signal. EMBO. **19**: 94-102.

Tian, W., Li, B., Warrington, R., Tomchick, D.R., Yu, H., and Luo, X. 2012. Structural analysis of human Cdc20 supports multisite degron recognition by APC/C. Proc Natl Acad Sci USA. **109**: 18419-18424.

Tokunaga, F., Sakata, S., Saeki, Y., Satomi, Y., Kirisako, T., Kamei, K., Nakagawa, T., Kato, M., Murata, S., Yamaoka, S., Yamamoto, M., Akira, S., Takao, T., Tanaka, K., and Iwai, K. 2009. Involvement of linear polyubiquitylation of NEMO in NF- κ B activation. Nat Cell Bio. **11**: 123-132.

Torres, E.M., Dephoure, N., Paneerselvam, A., Tucker, C.M., Whittaker, C.A., Gygi, S.P., Dunham, M.J., and Amon, A. 2010. Identification of aneuploidy-tolerating mutations. Cell. **143**: 71-83.

Torres, E.M., Williams, B.R., and Amon, A. 2008. Aneuploidy: cells losing their balance. Genetics. **179**: 737-746.

Tsai, C.Y., Chou, C.K., Yang, C.W., Lai, Y.C., Liang, C.C., Chen, C.M., and Tsai, T.F. 2008. HURP deficiency in mice leads to female infertility caused by an implantation defect. J. Biol Chem. **283**: 26302-26306.

Tsou, A.P., Yang, C.W., Huang, C.Y., Yu, R.C., Lee, Y.C., Chang, C.W., Chen, B.R., Chung, Y.F., Fann, M.J., Chi, C.W., *et al.* 2003. Identification of a novel cell cycle regulated gene, HURP, overexpressed in human hepatocellular carcinoma. Oncogene. **22**: 298-307.

Uehara, R., and Goshima, G. 2010. Functional central spindle assembly requires de novo microtubule generation in the interchromosomal region during anaphase. J. Cell Biol. **191**: 259-267.

Uzunova, K., Dye, B.T., Schutz, H., Ladurner, R., Petzold, G., Toyoda, Y., Jarvis, M.A., Brown, N.G., Poser, I., Novatchkova, M., Mechtler, K., Hyman, A.A., Stark, H., Schulman, B.A., and Peters, J.M. 2012. APC15 mediates CDC20 autoubiquitylation by APC/C(MCC) and disassembly of the mitotic checkpoint complex. Nat Struct Mol Biol. **19**: 1116-1123.

van Ree, J.H., Jeganathan, K.B., Malureanu, L., and van Deursen, J.M. 2010. Overexpression of the E2 ubiquitin-conjugating enzyme UbcH10 causes chromosome missegregation and tumor formation. J. Cell Biol. **188**: 83-100.

Varetti, G., Guida, C., Santaguida, S., Chirotti, E., and Musacchio, A. 2011. Homeostatic control of mitotic arrest. Mol Cell. **44**: 710-720.

Visintin, R., Prinz, S., and Amon, A. 1997. CDC20 and CDH1: a family of substrate-specific activators of APC-dependent proteolysis. Science. **278**: 460-463.

Wagner, K.W., Sapinoso, L.M., El-Rifai, W., Frierson, H.F., Butz, N., Mestan, J., Hofmann, F., Deveraux, Q.L., and Hampton, G.M. 2004. Overexpression, genomic amplification and therapeutic potential of inhibiting the UbcH10 ubiquitin conjugase in human carcinomas of diverse anatomic origin. Oncogene. **23**: 6621-6629.

Walczak, C, Verma, S., and Mitchinson, T.J. 1997. XCTK2: A Kinesin-related Protein That Promotes Mitotic Spindle Assembly in *Xenopus laevis* Egg Extracts. **136**: 859-870.

Waters, J.C., Mitchinson, T.J., Rieder, C.L., and Salmon, E.D. 1996. The kinetochore microtubule minus-end disassembly associated with poleward flux produces a force that can do work. Mol Biol. Cell. **7**: 1547-1558.

Weaver, L.N., Ems-McClung, S.E., Stout, J.R., LeBlanc, C. Shaw, S.L., Gardner, L.K., and Walczak, C.E. 2011. Kif18A uses a microtubule binding site in the tail for plus-end localization and spindle length regulation. Curr Biol. **21**: 1500-1506.

Weis, K., Ryder, U., and Lamond, A.I. 1996. The conserved amino-terminal domain of hSRP1 α is essential for nuclear protein import. EMBO J. **15**: 1818-1825.

Welburn, J.P.I. and Cheeseman, I.M. 2008. Toward a molecular structure of the eukaryotic kinetochore. Dev Cell. **15**: 645-655.

Welburn, J.P.I., Vleugel, M., Liu, D., Yates, J.R.III., Lampson, M.A., Fukagawa, T., and Cheeseman, I.M. 2010. Aurora B phosphorylates spatially distinct targets to differentially regulate the kinetochore-microtubule interface. Mol Cell. **38**: 383-392.

Wickliffe, K.E., Lorenz, S., Wemmer, D.E., Kuriyan, J., and Rape, M. 2011. The mechanism of linkage-specific ubiquitin chain elongation by a single-subunit E2. Cell. **144**: 769-781.

Williamson, A., Banerjee, S., Zhu, X., Philipp, I., Iavarone, A.T., and Rape, M. 2011. Regulation of ubiquitin chain initiation to control the timing of substrate degradation. Mol Cell. **42**: 744-757.

Williamson, A., Wickliffe, K.E., Mellone, B.G., Song, L., Karpen, G.H., and Rape, M. 2009. Identification of a physiological E2 module for the human anaphase-promoting complex. Proc Natl Acad Sci U S A. **106**:18213-18218.

Wittmann, T., Wilm, M., Karsenti, E., and Vernos, I. 2000. TPX2, A novel xenopus MAP involved in spindle pole organization. J. Cell Biol.**149**: 1405-1418.

Wolthuis, R., Clay-Farrace, L., van Zon, W., Yekezare, M., Koop, L., Ogink, J., Medema, R., and Pines, J. 2008. Cdc20 and Cks direct the spindle checkpoint-independent destruction of cyclin A. Mol Cell. **30**: 290-302.

Wong, J., and Fang, G. 2006. HURP controls spindle dynamics to promote proper interkinetochore tension and efficient kinetochore capture. J. Cell Biol. **173**: 879-891.

Wong, J., Lerrigo, R., Jang, C.Y., and Fang, G. 2008. Aurora A regulates the activity of HURP by controlling the accessibility of its microtubule-binding domain. Mol Biol. Cell. **19**: 2083-2091.

Wu, T., Merbl, Y., Huo, Y., Gallop, J.L., Tzur, A., and Kirschner, M.W. 2010. UBE2S drives elongation of K11-linked ubiquitin chains by the anaphase-promoting complex. Proc Natl Acad Sci U S A. **107**(4): 1355-1360.

Xia, G., Luo, X., Habu, T., Rizo, J., Matsumoto, T., and Yu, H. 2004. Conformation-specific binding of p31^{comet} antagonizes the function of Mad2 in the spindle checkpoint. EMBO. **23**: 3133-3143.

Xu, Z., Cetin, B., Anger, M., Cho, U.S., Helmhart, W., Nasmyth, K., and Xu, W. 2009. Structure and function of the PP2A-shugoshin interaction. Mol Cell. **35**: 426-441.

Ye, Y. and Rape, M. 2009. Building ubiquitin chains: E2 enzymes at work. Nat Rev Mol Cell Biol. **10**: 755-764.

Yu, H., King, R.W., Peters, J.M., and Kirschner, M.W. 1996. Identification of a novel ubiquitin-conjugating enzyme involved in mitotic cyclin degradation. Curr Biol. **6**: 455-466.

Yvon, A-M.C., Wadsworth, P., and Jordan, M.A. 1999. Taxol suppresses dynamics of individual microtubules in living human tumor cells. Mol Biol.Cell. **10**: 947-959.

Zeng, X., Sigoillot, F., Gaur, S., Choi, S., Pfaff, K.L., Oh, D.C., Hathaway, N., Dimova, N., Cuny, G.D., and King, R.W. (2010). Pharmacologic inhibition of the anaphase-promoting complex induces a spindle checkpoint-dependent mitotic arrest in the absence of spindle damage. Cancer Cell. **18**: 382-395.

Zhao, W-m., Coppinger, J.A., Seki, A., Cheng, X-l., Yates, J.R., and Fang, G. 2008. RSC1, a substrate of the APC/C, controls the metaphase to anaphase transition. Proc Natl Acad Sci. **105**: 13415-13420.

Zhu, C., Zhao, J., Bibikova, M., Levenson, J.D., Bossy-Wetzel, E., Fan, J-B., Abraham, R.T., and Jiang, W. 2005. Functional Analysis of Human Microtubule-based Motor Proteins, the Kinesins and Dyneins, in Mitosis/Cytokinesis Using RNA Interference. 2005. Molecular Biology of the Cell. **16**: 3187-3199.

Appendix A

Co-depletion of Ube2S and Kif18A results in a synergistic mitotic arrest that is dependent upon Aurora A kinase signaling

Craney, A. and Rape, M. Unpublished data 2011-2013.

Introductory Summary:

Early in my dissertation career, I became interested in whether early mitotic processes were regulated by the APC/C. To me, this represented a prime opportunity for identifying regulatory mechanisms that could be exploited to target cancer cells exhibiting both proteotoxic stress and spindle challenges. Chapter 1 of my thesis describes a screen that identifies regulators of spindle microtubule plus ends and microtubule-kinetochore attachments as genetic interactors of the APC/C.

During the validation of the screen, we identified suppressor proteins that were required for maintaining the mitotic arrest caused by depletion of Ube2S and a genetic interactor, such as Kif18A. In Chapter 1, the suppression of the mitotic arrest when a spindle assembly checkpoint protein (Mad2, Mps1, BubR1) is depleted is characterized. However, our search for suppressive genetic interactions also revealed a role for Aurora A kinase signaling in maintaining the mitotic arrest caused by Ube2S and Kif18A co-depletion.

Aurora A kinase signaling is noted for its importance in regulating mitotic entry and spindle assembly (Carmena, et al., 2009; Kim, et al., 2010). Additionally, Aurora A localizes to the spindle poles and targets many of its substrates at this location. We were surprised to observe that its kinase activity might affect the Kif18A and Ube2S phenotype, which we believe targets the plus-ends of spindle microtubules, unless loss of Aurora A improved the overall balance of spindle forces.

This story will not be encompassed in the manuscript detailing our genetic interaction screen and its implications for early mitotic events. However, I believe it has the potential to define novel insight into the function and regulation of Kif18A, and potentially defines a genetic interaction between Ube2S and Aurora A. This Appendix will describe the work that I was able to do during my doctorate, while I primarily focused on the work in Chapters 1-2. I also propose important experiments I believe should be completed in order to follow up on these findings.

Results:

To elucidate the mechanism through which Kif18A and Ube2S genetically interact, we searched for genetic suppressors of the synergistic arrest. Interestingly, in our flexiplate screens (Chapter 1), we identified that Aurora A is required for maintaining the mitotic arrest. We were able to validate this result through individual oligos targeting Aurora A. However, we also noted that loss of Aurora A significantly dampened the mitotic arrest caused by depletion of Kif18A alone (Figure 1).

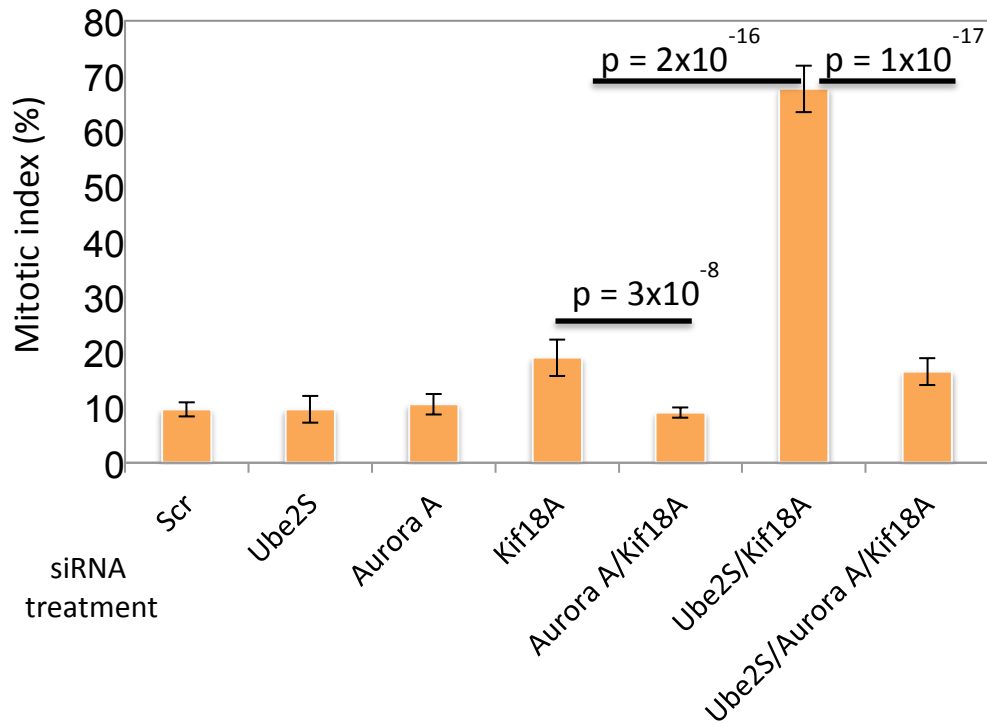


Figure 1. Aurora A is required for the synergistic mitotic arrest caused by co-depletion of Kif18A and Ube2S/Kif18A. The single, double, and triple depletions of Ube2S, Aurora A, and Kif18A were performed in HeLa cells. 48hrs after depletion, cells were fixed, stained for DNA (Hoescht) and imaged. The mitotic index was quantified by an unbiased training set. Depletion of Aurora A does not affect the mitotic index in a Ube2S-depleted background, but it significantly decreases the mitotic index of both Kif18A-depleted cells and Ube2S/Kif18A-depleted cells.

We further validated the genetic suppression by quantifying the mitotic index resulting from Ube2S/Kif18A/Aurora A triple depletion with two separate oligos targeting Aurora A. Notably, oligo #2 was experimentally verified by Qiagen and produced a stronger rescue (Figure 2). However, depletion of Aurora A by both independent oligos resulted in a significant decrease in the mitotic index (Figure 2).

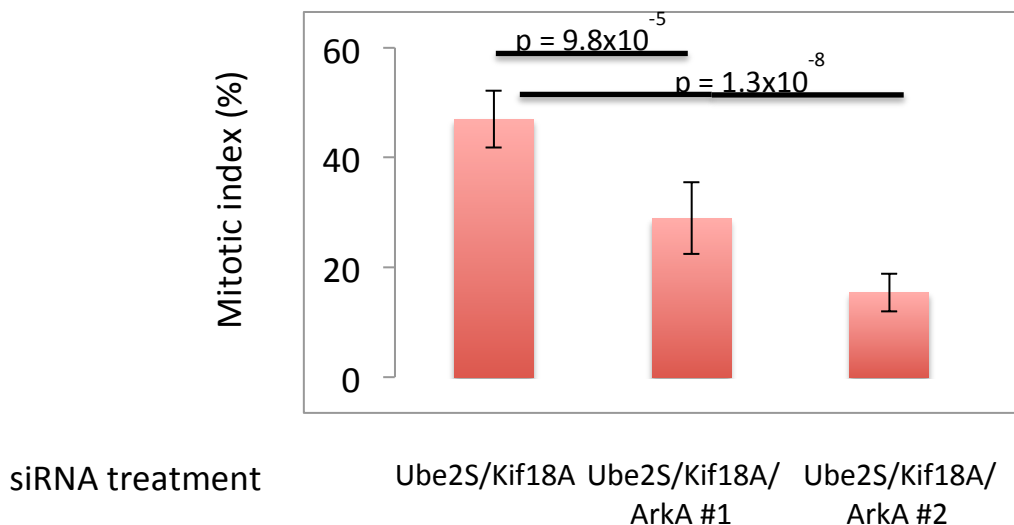


Figure 2. Verification that Aurora A is required for the synergistic mitotic arrest caused by co-depletion of Ube2S and Kif18A. Ube2S/Kif18A co-depletion was performed in combination with either scrambled, or Aurora A (ArkA) siRNA. Two individual siRNAs targeting Aurora A were used. Oligo #2 was verified by the manufacturer (Qiagen) to cause >80% knockdown of the gene product. Cells were treated with siRNA for 48hr, fixed, and imaged for DNA (Hoescht). Mitotic index was calculated by Cell Profiler/Analyst using an unbiased training set. Analysis was performed using Python and Excel (Microsoft). Both oligos targeting Aurora A significantly decreased the Ube2S/Kif18A mitotic index.

We were initially perplexed by this result, as to our knowledge, Aurora A has not been directly linked to SAC signaling, and other phenotypic suppressor proteins were important SAC activators. One possibility for this rescue is that Aurora A is important for maintaining the mitotic arrest under these conditions. However, it is also possible that the rescue occurs due to a specific genetic interaction with either Kif18A or Ube2S. We decided to examine whether Aurora B depletion also rescued the mitotic arrest. Interestingly, while depletion of Aurora B, which has been linked to maintenance of the SAC signal (Santaguida, et al., 2011; Saurin, et al., 2011) rescued the mitotic index caused by co-depletion of Ube2S/Sgo1 and Ube2S/Hec1 (personal observations), it did not rescue the Ube2S/Kif18A co-depletion. In fact, loss of Aurora B kinase resulted in a synergistic increase in mitotic arrest when combined with Kif18A depletion (Figure 3).

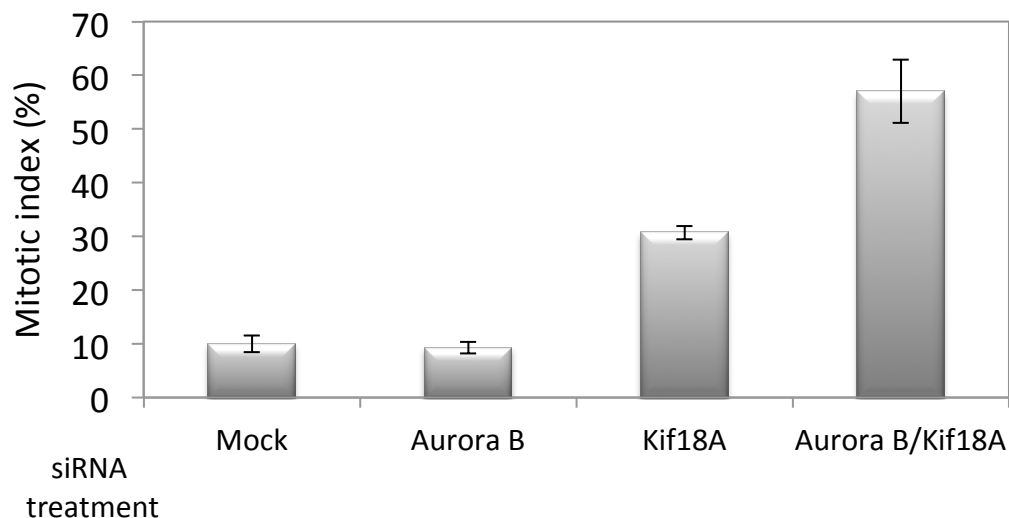


Figure 3. Aurora B, despite its role in promoting SAC signaling, is not essential for maintaining the mitotic arrested caused by co-depletion of Kif18A. Cells depleted of Aurora B, Kif18A, or the combination were imaged and analyzed for overall mitotic index.

These results prompted us to think about a more specific role for Aurora A in the regulation of Kif18A. We first wanted to determine whether Aurora A itself was required, or whether its kinase activity was required to maintain the arrest. As shown in Figure 4, addition of an inhibitor to Aurora A kinase activity (MLN8237) resulted in significant decreases in the mitotic index caused by Ube2S and Kif18A co-depletion.

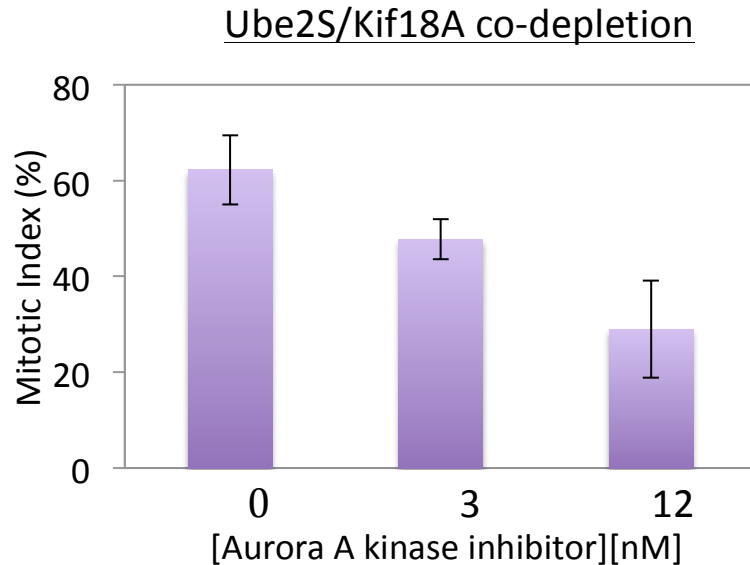
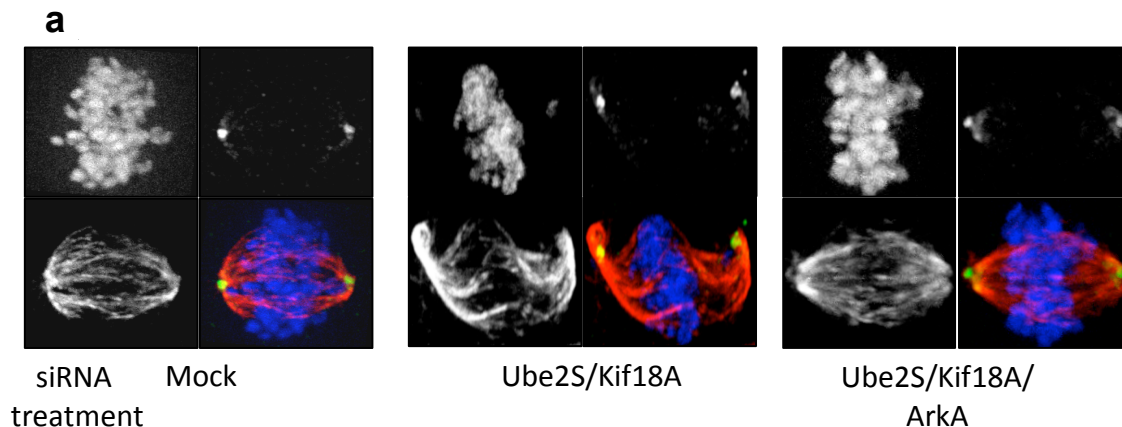


Figure 4. Aurora A kinase signaling is required for the synergistic mitotic arrest caused by co-depletion of Ube2S and Kif18A. Ube2S/Kif18A co-depletion was performed, and after 24hrs, the Aurora A inhibitor MLN8237 was added for an additional 24hr. Cells were fixed and imaged for DNA (Hoescht). Mitotic index was calculated by Cell Profiler/Analyst using an unbiased training set. Analysis was performed using Python and Excel (Microsoft).

Importantly, Aurora A depletion not only rescued the mitotic index phenotype, but also rescued spindle defects that result from co-depletion of Ube2S and Kif18A. One notable phenotype of the co-depletion is elongation of spindle microtubules. Aurora A depletion in the background of Kif18A/Ube2S depletion rescues the pole-to-pole distance to that of control treatment (Figure 5). Also, while we did not quantify this particular phenotype, one observation we noted is that cells depleted of Ube2S and Kif18A often exhibited acentric spindle poles (Figure 5A, middle). This could suggest increased microtubule growth emanating from the spindle poles, resulting from unchecked forces at the minus end. Loss of Aurora A appeared to also rescue the acentric centrosome phenotype (Figure 5A, top right).



b

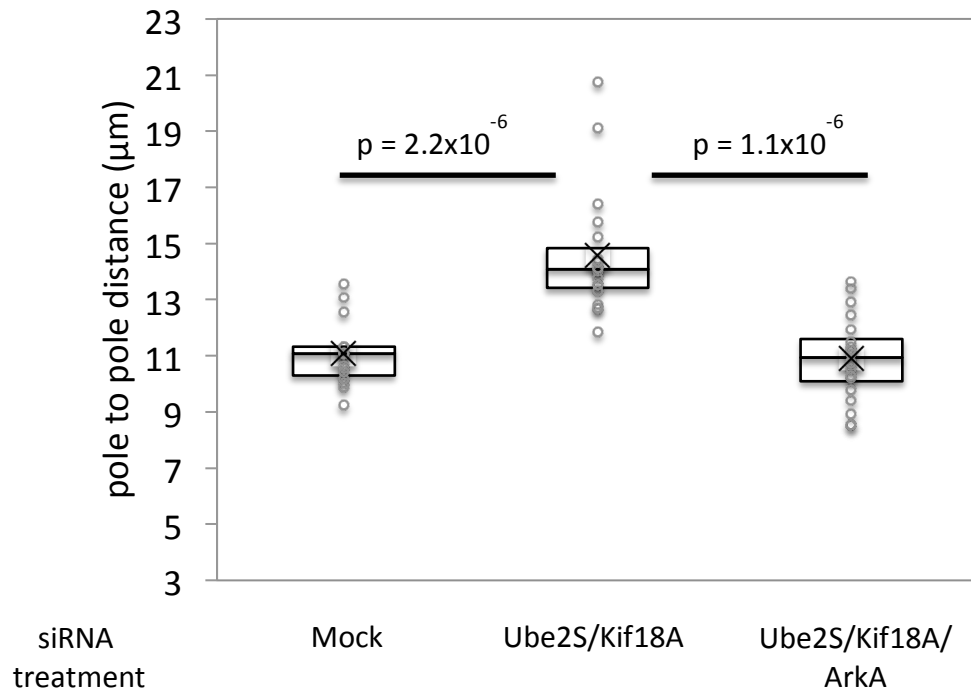


Figure 5. Aurora A is required for the synergistic mitotic arrest caused by co-depletion of Ube2S and Kif18A. Ube2S/Kif18A co-depletion was performed in combination with either scrambled, or Aurora A (ArkA) siRNA. (A) HeLa cells were treated with siRNA, fixed after 48hrs, and stained for spindle poles (γ -tubulin; green; top right), microtubules (tubulin; red; bottom left), and DNA (blue; top left). Cells co-depleted of Ube2S and Kif18A have elongated spindle microtubules, and often present with acentric spindle poles. (B) Quantification of spindle length. Images were taken at 100X on an epifluorescence microscope (Olympus), and the distance between spindle poles was quantified using Metamorph, and analyzed using Excel (Microsoft). Loss of Aurora A in a Ube2S/Kif18A co-depletion background results in a significant decrease in spindle length, with an overall pole-to-pole distance not significantly different from mock siRNA treatment.

The inclusion of Aurora A into our analysis made us think about some of the earliest phenotypes we noted when characterizing the Ube2S/Kif18A depletion phenotype. For example, we had previously noted that loss of Kif18A resulted in a decrease of the plus-end directed kinesin CENP-E from the spindle microtubules (Figure 6; see also Huang, et al., 2009). We had originally explored whether the mitotic phenotype was caused by loss of CENP-E, but had been unable to specifically attribute it to the double depletion. Interestingly, however, other groups have linked Aurora A to the proper localization of CENP-E (Kim, et al., 2010). We therefore decided to analyze the localization of CENP-E under varying conditions.

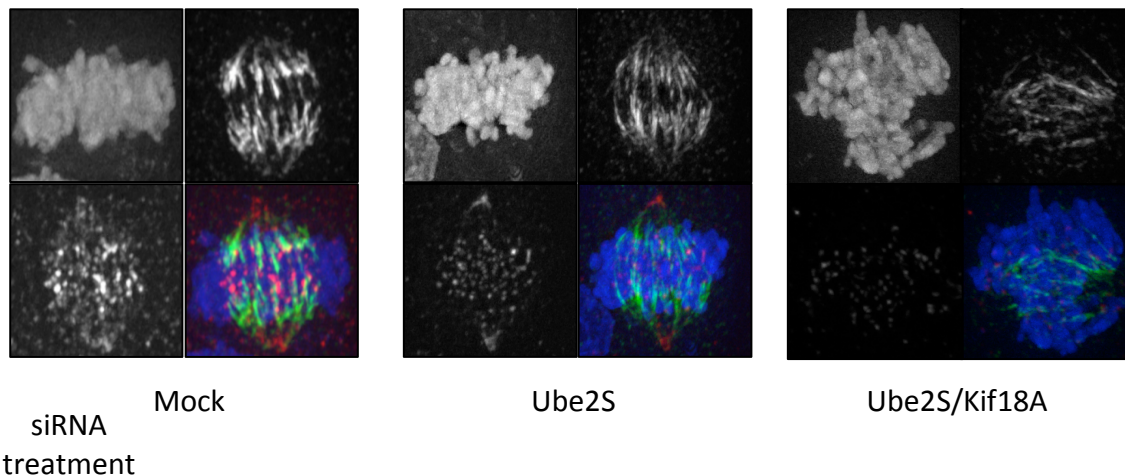
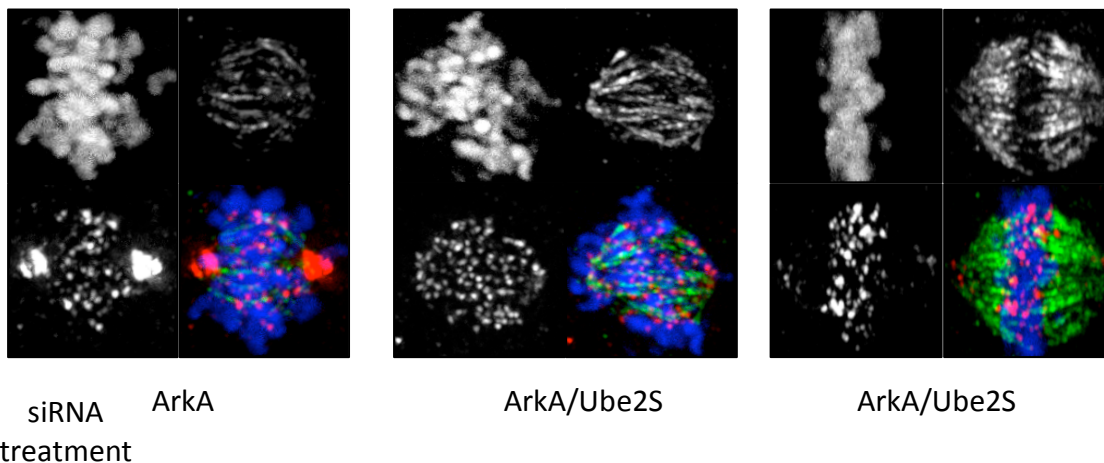


Figure 6. Ube2S and Kif18A are required for proper CENP-E localization. HeLa cells were treated with siRNA, fixed after 48hrs, and stained for CENP-E (red; bottom left), kinetochore fibers (HURP; green; top right), and DNA (blue; top left). Cells co-depleted of Ube2S and Kif18A have a noticeable decrease in CENP-E staining at spindle microtubule plus ends. Images were taken at 100X on an epifluorescence microscope (Olympus) using consistent exposures across treatments. Loss of spindle-bound CENP-E after Kif18A depletion has been previously reported (Huang, et al., 2009).

Work by Kim, et al. had previously shown that Aurora A is required for CENP-E movement from the spindle poles (Kim, et al., 2010; Figure 7). Excitingly, we noted that Ube2S also participates in this process. Upon examination of CENP-E localization under varying siRNA-depletion conditions, we observed that if Ube2S was co-depleted with Aurora A, the proper localization of CENP-E was largely restored (Figure 7). While the full implications of this finding have not been explored, our data demonstrate a previously unobserved connection between the APC/C and Aurora A kinase.

a



b

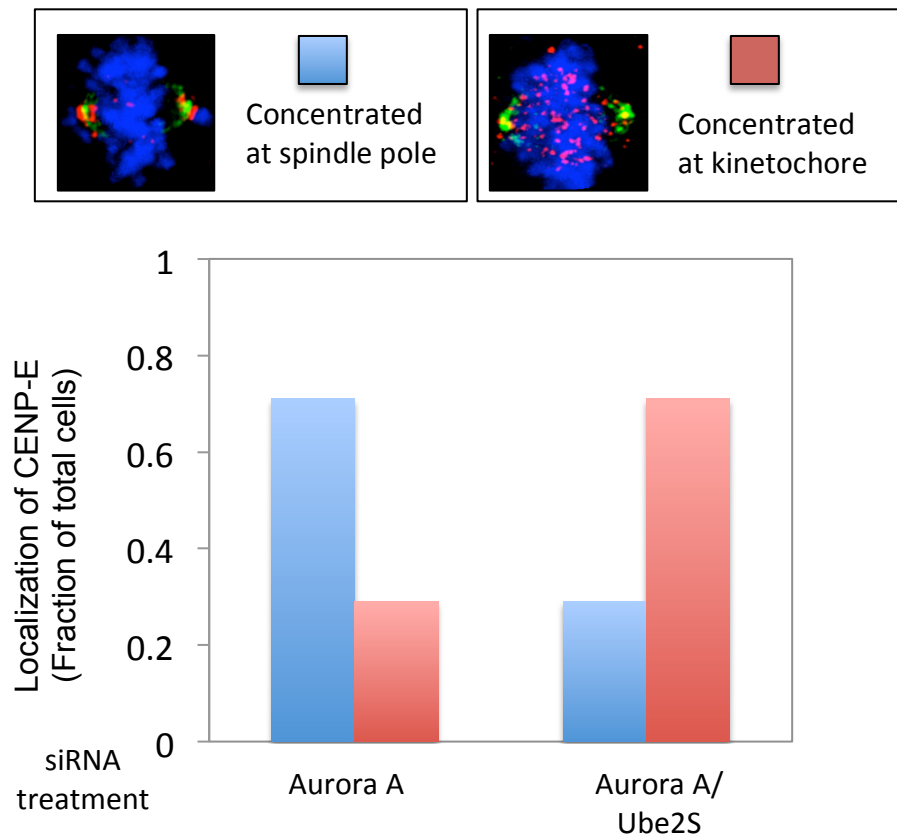


Figure 7. Ube2S is important for maintaining CENP-E at the spindle poles when Aurora A activity has been lost. (A) Cells were treated with siRNA targeting Aurora A or Aurora A/Ube2S for 48hrs, fixed, and stained for endogenous CENP-E (red; bottom left), kinetochore-fibers (HURP; green; top right), and DNA (blue; top left). CENP-E normally travels from the spindle poles to the kinetochores during prometaphase, in a manner dependent upon Aurora kinase and phosphatase signaling (Figure 3; Kim, et al., 2010). When Aurora A activity is lost, CENP-E is unable to efficiently travel to the kinetochore, and becomes heavily concentrated at the spindle poles (Kim, et al., 2010). Further loss of Ube2S in an Aurora A-siRNA background largely restores CENP-E to kinetochores. (B) Quantification of the fraction of total cells possessing CENP-E concentrated at the spindle poles (top left; blue) or at kinetochores (top right; red). Images above the plot are representative cells for each category (green: spindle poles; red: CENP-E; blue: DNA). The average of two independent experiments is shown here.

Discussion:

The identification of suppressive genetic interactions can reveal a great deal about the nature of the underlying biochemistry. For example, in Chapter 1, we detail how the SAC is required for maintaining a persistent mitotic arrest when Ube2S and a genetic interactor are co-depleted. However, with all discoveries, especially those depicting genetic interactions, fleshing out the underlying biochemistry can be difficult.

In this case, we were initially struck by the suppression of mitotic arrest when Aurora A was depleted by siRNA or chemical inhibition (Figures 1-2, 4). While the Aurora kinases (A and B in particular) have been well documented as important mitotic regulators, the link between Aurora A and either the kinetochore or the SAC is much less clear when one examines the body of literature on Aurora B. Aurora B activity is important for SAC signaling, especially in situations in which the outer kinetochore has sustained a challenge (Saurin, et al., 2011). Its activity is likely required downstream of SAC establishment, either in the propagation or in the maintenance of the response (Maldonado and Kapoor, 2011; Santaguida, et al., 2011; Saurin, et al., 2011). Aurora A, alternatively, plays a critical role at the spindle poles, regulating mitotic entry and supporting spindle assembly through various activities (Carmena, et al., 2009; Kim, et al., 2010).

In many cases regarding a challenged mitosis, Aurora B activity is required for maintaining the mitotic arrest, through its promotion or propagation of the SAC (Maldonado and Kapoor, 2011; Santaguida, et al., 2011). Here, however, we discovered that while SAC signaling is critical for maintaining an arrest caused by either Kif18A or Ube2S/Kif18A depletion (see Chapter 1), Aurora B is not essential. Instead, further loss of Aurora B antagonizes the mitotic arrest (Figure 3; also, see Chapter 1). On the other hand, when we examined Aurora B in the context of Ube2S depletion with other genetic interactors, Sgo1 and Hec1, further loss of Aurora B did result in rescue of the mitotic arrest (personal observation). Thus, Aurora B and Kif18A appear to genetically interact in order to help promote progression through mitosis.

The rescue of the Ube2S/Kif18A phenotype by Aurora A depletion, however, was puzzling. We validated this suppression by use of two separate siRNAs targeting Aurora A, as well as chemical inhibition of Aurora A signaling (Figures 1-2, 4). Not only was the mitotic arrest phenotype suppressed, but the spindle elongation phenotype was also rescued (Figure 5), and the spindles in the triple-depleted cells appeared much more similar to the mock treated cells than the double-depleted cells (Figure 5).

Our first thought was that perhaps the Ube2S/Kif18A depletion phenotype was due to stabilization of an APC/C substrate that was activated by Aurora A phosphorylation. We designed a genetic interaction screen, using Ube2S/Kif18A siRNA a query, and co-depleted dozens of Aurora A substrates to see if any suppressed the mitotic arrest (data not shown). We did not find one substrate that was mimicked the Aurora A suppression. Therefore, we concluded that

either multiple substrates of Aurora A contributed to the mitotic arrest, or that Aurora A's role in promoting spindle assembly and spindle pole forces may be necessary for the mitotic arrest.

Additionally, we noticed that Aurora A did not specifically rescue the Ube2S/Kif18A depletion phenotype; it also rescued the mitotic index caused by depletion of Kif18A alone (Figure 1). Therefore, the suppression of the double depletion may simply be through relief of the Kif18A single phenotype, thus relieving the system of a synergistic hit. To our knowledge, Kif18A had not been previously predicted as an Aurora A substrate, although this is a potential explanation. Experiments such as Kif18A localization and *in vitro* movement along microtubules with and without Aurora A signaling, as well as direct phosphorylation assays, would be very interesting in addressing this hypothesis.

From our initial study of Kif18A, both through our own work, and through literature research, we had found interesting links between Kif18A and another plus-end directed kinesin, CENP-E. CENP-E is important for chromosome congression and for timely completion of mitosis (Kapoor, et al., 2006; Kim, et al., 2010). It also is a well-documented substrate of Aurora A (Kim, et al., 2010). Early in our research upon Kif18A, we had noted that depletion of Kif18A, or Ube2S/Kif18A, resulted in loss of CENP-E localization to the spindle (Figure 6). This finding had also been previously reported (Huang, et al., 2009).

While the loss of CENP-E from the spindle when Kif18A is depleted is not fully elucidated, the link between CENP-E localization and Aurora A signaling is much more clear. Aurora A phosphorylates CENP-E at the spindle pole, which allows the protein to travel toward the plus ends of the spindle (Kim, et al., 2010). When Aurora A signaling is depleted, CENP-E becomes concentrated at the spindle pole (Figure 7; Kim, et al., 2010). However, we were excited to also note a role for Ube2S in this pathway. When Aurora A and Ube2S were co-depleted, the localization of CENP-E to the spindle microtubules and kinetochores was largely rescued (Figure 7).

The implications of these results are not yet clear, and more research is needed in order to flesh out the underlying interactions between Ube2S, Kif18A, CENP-E, and Aurora A. However, it is clear to us that a novel link between Aurora A and Kif18A has been identified in this work. Additionally, a role for Ube2S in the CENP-E pathway has also been identified. These results represent interesting and fruitful paths into learning more about the function of Kif18A and potentially defining another function for the APC/C in early mitosis.

Material and Methods:

Antibodies and siRNA oligos

Antibodies

The antibodies used in this Appendix are as follows: α -tubulin (mouse monoclonal, Calbiochem, DM1A), α -CENP-E [1H12] (mouse monoclonal, Abcam, ab5093), α - γ tubulin (rabbit polyclonal, Sigma, T6657), and α -HURP (rabbit polyclonal; Bethyl Laboratories, A300-853A).

siRNA

The following sequences were used: Ube2S (3'UTR: GGCACUGGGACCUGGAUUUUU, Dharmacon; ORF: CCCGATGGCATCAAGGTCTTT, Qiagen flexitube #5), Kif18A (ORF: Qiagen flexitubes #1,3,5; ON-TARGETplus siRNA-SMARTpool; 3'UTR: two distinct oligos designed using Dharmacon tools), All Stars negative control (CAGGGTATCGACGATTACAAA, Qiagen), and Aurora A (ORF, Qiagen flexitube AurkA#1 and Stk6#5).

Cell culture and synchronizations

Cells were maintained at 37°C and 5% CO₂ in DMEM media containing 10% FBS. Cells were passaged every two to three days after reaching 80-90% confluence. MLN8237 (Selleck Chemicals Co., Ltd.) was used as indicated.

siRNA transfection and immunofluorescence

See Chapter 1 for complete description of siRNA transfection, immunofluorescence procedures, and analysis. Pole-to-pole distances were calculated by identifying each pole, and drawing a line-scan between the edge of one pole to the edge of the opposite pole. Monopolar or tripolar cells (rare) were excluded from the analysis. The distance was then calculated using Metamorph, and the calculations were performed and further analyzed using Excel (Metamorph).

Analysis of Microscopy Screening data

Data from siRNA screens were performed as described (see Chapter 1). The following is a sample script used to parse screening data in order to determine the number of cells for each condition, filter sites that possessed 40% or greater unfocused cells, and determine the percentage of interphase versus mitotic and dead cells. In addition, this script combines data from all sites imaged of a given condition (up to nine sites). For all screens, modifications of this Python script were performed, along with random routine consistency checks by calculations performed by hand. Conditions of particular interest were additionally examined by eye after blind scoring and analysis. This script was provided to other members of the Rape Lab in order to improve the efficiency of data analysis.

```
#import module with built-in stats functions
import sys, numpy

#define a function to determine the maximum value in a list
def max(li):
    i = 0
    m = 0
    while i <=len(li)-1:
        x=li[i]
        if x > m:
            m=x
        i= i + 1
    print "biggest:", m,
```

```

#def a function to determine the minimum value in a list
def min(li):
    i = 0
    m = ""
    while i <=len(li)-1:
        x = li[i]
        if x < m:
            m=x
        i=i+1
    print "littlest:", m,
    print

#Open and read in file.
fn = open('Screen14_DATA_trainingupdated130221.csv', 'rU')
lines = fn.readlines()
fn2 = open('Screen14_MAP_E2Sandcontrols.csv', 'rU')
lines2 = fn2.readlines()
for line2 in lines2:
    columns2 = line2.split(',')
    well = columns2[0]

#In yellow below are initialized variables. You don't need to initialize variables here if you don't
want, but it looks a bit cleaner.
plate_number = ""
well_number = ""
plate_well_identifier = ""
unfocused_cells = ""
mitoticordead_cells = ""
interphase_cells = ""
total_cells = ""
total_focused_cells = ""
percent_unfocused_cells = ""
plate_well_dict = {}
mitotic_index_perwell = ""
sum_of_mitotic_indices = ""
number_of_sites_counted = ""
average_mitotic_index = ""
dict_of_mitoticcells = {}
dict_of_interphasecells = {}

#Next loop reads in data file line by line. Because it's a .csv file, split by comma to get individual
columns.
for line in lines:
    columns = line.split(',')

#Excludes the header line which begins with 'TableNumber'
if columns[0] == 'TableNumber':
    pass
else:
    plate_number = columns[2]
    #print plate_number
    well_number = columns[3]
    if plate_number == '100':
        for line2 in lines2:
            columns2 = line2.split(',')

```

```

well_number2 = columns2[0]
gene_name = columns2[1]
stripped_gene_name = gene_name.strip()
if well_number == well_number2:
    well_number_complete = well_number + '_' + stripped_gene_name
#print well_number

#This next line creates a plate_well_identifier by concatenating the plate_number and
well_number
    plate_well_identifier = plate_number + '_' + well_number_complete
#print plate_well_identifier

#The next several lines create and assign important variables described below.
unfocused_cells = int(columns[6]) #number of unfocused cells
#print plate_well_identifier, '\t', 'unfocused', unfocused_cells
mitoticordead_cells = int(columns[7]) #number of mitotic(or dead) cells
#print well_number_complete, mitoticordead_cells
interphase_cells = int(columns[5]) #number of interphase cells
total_cells = int(columns[4]) #includes unfocused, mitoticordead, interphase
total_focused_cells = int(mitoticordead_cells + interphase_cells) #includes
interphase and mitoticordead

#Check that cells were actually in site photos- if not, print the identifier and the number of total
cells
    #if total_cells == 0:
        #print 'no cells in pic %s' % plate_well_identifier

#Filter out sites that have more than 40% unfocused cells. First, calculate percentage of
unfocused cells, then print the identifiers of any that have more than 40% unfocused. Proceed
and calculates mitotic index with those that have < 40% unfocused.
    if interphase_cells > 0:
        percent_unfocused_cells = (float(unfocused_cells)/float(total_cells)) * 100
        if percent_unfocused_cells >= 40:
            mitotic_index_perwell = 'x'
            #print 'this site %s' % plate_well_identifier, 'has %f percent unfocused cells' %
percent_unfocused_cells
        else:
            mitotic_index_perwell = float(mitoticordead_cells)/float(total_focused_cells) *
100

    #total_unfocused_and_interphase_cells = float
    identifier_nooligonumber = plate_well_identifier.split('_')
    identifier_wellonly = identifier_nooligonumber[1]
#print identifier_wellonly
#print plate_well_identifier, mitotic_index_perwell
    if dict_of_mitoticcells.has_key(identifier_wellonly):
        dict_of_mitoticcells[identifier_wellonly].append(mitoticordead_cells)
    else:
        dict_of_mitoticcells[identifier_wellonly] = []
        dict_of_mitoticcells[identifier_wellonly].append(mitoticordead_cells)
    if dict_of_interphasecells.has_key(identifier_wellonly):
        dict_of_interphasecells[identifier_wellonly].append(interphase_cells)
    else:
        total_interphaseandunfocused_cells = float(interphase_cells +
unfocused_cells)
        dict_of_interphasecells[identifier_wellonly] = []

```

```

#could append interphase alone or interphase plus unfocused here. for
aileen, only inter.
    dict_of_interphasecells[identifier_wellonly].append(interphase_cells)

#Sets up a loop that will save the mitotic indices for each site. May have up to eight.
    if mitotic_index_perwell != 'x':
        if plate_well_dict.has_key(plate_well_identifier):
            plate_well_dict[plate_well_identifier].append(mitotic_index_perwell)
        else:
            plate_well_dict[plate_well_identifier] = []
            plate_well_dict[plate_well_identifier].append(mitotic_index_perwell)
#print plate_well_dict

for value in dict_of_mitoticcells.values():
    sum_of_all_mitoticcells = sum(value)
    std_dev_ofmitoticcells = numpy.std(value)
    value.insert(0, sum_of_all_mitoticcells)
    value.insert(1, std_dev_ofmitoticcells)

for value in dict_of_interphasecells.values():
    sum_of_all_interphasecells = sum(value)
    #print value
    #print sum_of_all_interphasecells
    std_dev_ofinterphasecells = numpy.std(value)
    value.insert(0, sum_of_all_interphasecells)
    value.insert(1, std_dev_ofinterphasecells)

#for value in dict_of_unfocusedcells.value():
for key, value in dict_of_mitoticcells.items():
    if dict_of_interphasecells.has_key(key):
        new_average_mitoticindex = float(float(value[0])/(float(value[0] +
dict_of_interphasecells[key][0]))) * 100
        #print key, value[0], dict_of_interphasecells[key][0], new_average_mitoticindex
        #print key, '\t', new_average_mitoticindex
        for line3 in lines2:
            columns3 = line3.split(',')
            well_number_3 = columns3[0]
            gene_number_3 = columns3[1].strip()
            if key == well_number_3:
                new_key_3 = key + '_' + gene_number_3
                print new

```


Appendix B

The mitotic motor KIFC1 is protected from APC/C-dependent degradation by importin- α

Craney, A., Song, L., and Rape, M. Unpublished data 2010-2012.

Contributions and Acknowledgements

The project elucidating the role of importin β and the Ran system to jointly regulate APC/C dependent degradation of HURP was completed by Ling and Michael prior to my joining the lab in 2010. Ling also performed initial experiments to suggest that KIFC1 was an APC/C substrate. When I joined the lab in 2010, Ling provided training and support, and helped me write the protocols and perform the experiments in this appendix. I performed the experiments shown in this Appendix. The purified importin proteins were generated by Ling, with materials and protocol help from members of the Weis and Heald labs at UC Berkeley.

Introductory Summary:

Coordination of spindle assembly factor (SAF) activity is necessary in early mitosis for formation of a stable, bipolar spindle. The small protein Ran plays an important role in this regulation. Ran cycles between a GTP-bound state, promoted by the guanine exchange factor RCC1, and a GDP-bound state, dependent upon the activity of RanGAP and its co-factor RanBP2 (Kalab, et al., 2002). The compartmentalization of RCC1 and RanGAP in the nucleus and cytoplasm respectively provides directionality of nuclear-cytoplasmic transport. The nuclear transport factor importin β , either independently or with importin α , binds its cargo in the cytoplasm and facilitates nuclear transfer. In the nucleus, Ran-GTP binds directly to importin β , releasing it from cargo.

Importin β forms an inhibitory complex with SAFs blocking their function (Nachury, et al., 2001). A mitotic Ran gradient exists *in vivo* (Kalab, et al., 2002; Kalab, et al., 2006) with the highest concentration of Ran-GTP existing near chromatin. This localization ensures that the activation of SAFs like NuSAP, NUMA, and HURP will occur in a localized manner. However, the discovery that the APC/C also regulates the activities of some SAFs (Song and Rape, 2010) added a new level of complexity.

In order to determine how general the dual recognition of SAFs by APC/C and importins is, we identified importin β interacting partners in mitosis (Song and Rape, 2010). Along with expected interactors such as other nuclear transport factors and nuclear pore proteins, we also identified a mitotic kinesin, KIFC1, that had previously been shown to interact with importin α/β (Ems-McClung, et al., 2004). KIFC1 is a minus-end directed kinesin that crosslinks microtubules and is important for bipolar spindle formation (Cai, et al, 2009; Walczak, et al., 1997; Zhu, et al., 2005). KIFC1 possesses a conserved bipartite NLS in its tail/cargo domain that directly interacts with importin α/β ; association with importins blocks

microtubule binding of the KIFC1 tail domain to microtubules (Ems-Clung, et al., 2004; Cai, et al., 2009), likely preventing its crosslinking activity.

Here, we show that KIFC1 is also an APC/C substrate. Similar to HURP, KIFC1 is jointly regulated by microtubules and the APC/C. In contrast to HURP, which binds importin β in order to mediate the regulation between microtubules and APC/C, KIFC1 is bound by importin α directly, and may represent a different mechanism of spindle regulation than previous substrates (Song, et al., 2014; Song and Rape, 2010).

Results:

KIFC1 is targeted by the APC/C for proteasomal degradation *in vitro*. We cloned KIFC1 into a pCS2- or pCS2-HA-vector background, and expressed it in a rabbit reticulocyte transcription/translation system in the presence of ^{35}S -Met/Cys. We then incubated the translated ^{35}S -KIFC1 with HeLa extract prepared from G1 synchronized cells, and stimulated APC/C activity by the addition of ubiquitin, ATP, and Ube2C. KIFC1 is degraded within two hours of incubation with active APC/C; however, when we added the APC/C inhibitor, Emi1, to the cell extract, KIFC1 was stabilized, suggesting that its degradation is dependent upon APC/C E3 ligase activity (Figure 1A).

APC/C substrates often have canonical recognition motifs that are required for their interaction with APC/C, referred to as KEN-boxes (residues: lysine-glutamic acid-asparagine) and/or Destruction boxes (D-boxes) (residues: arginine/lysine-X-X-asparagine) (Peters, 2006; Teixeira and Reed, 2013). D-boxes are usually followed by a ubiquitin initiation motif, characterized by a high percentage of positively charged residues downstream of the D-box (Williamson, et al., 2011). Therefore, we wished to identify whether KIFC1 possessed canonical APC/C recognition sites.

KIFC1 does not possess a KEN-box (see Appendix C), but sequence analysis suggests that it has several D-boxes followed by putative initiation sites. In order to determine if these putative recognition motifs were truly APC/C interaction sites, we performed truncational analyses on the protein, and determined that the important recognition sites exist with the first 100 amino acids of the protein (data not shown). From there, we performed site-directed mutagenesis to determine the exact sites, and found that mutation of the 'R' and 'L' residues of an N-terminal D-box (aa 5-8), resulted in stabilization of the protein in our *in vitro* degradation system (Figure 1B).

While APC/C-specific degradation strongly suggests that KIFC1 is first ubiquitylated by the ligase, we wished to examine the presence of ubiquitin chains upon KIFC1. Therefore, we generated radioactively translated KIFC1 protein, and incubated it with APC/C purified from HeLa G1 cell extract that had been charged with APC/C E2s, ubiquitin, ubiquitin E1, and ATP. Wild-type KIFC1 was robustly ubiquitylated by purified APC/C, as shown by KIFC1 turnover and the presence of upper-molecular weight bands (Figure 1C). However, either mutation of KIFC1's D-box (Figure 1D), addition of the inhibitor Emi1 (Figures 1C-1D), or addition of a substrate competitor, his-securin (Figures 1C-1D) largely blocked the presence of ubiquitin chains detected upon KIFC1 and turnover of

the full-length protein. Thus, we conclude that KIFC1 is an *in vitro* APC/C substrate dependent upon an N-terminal D-box for recognition and efficient ubiquitylation.

Our next goal was to determine if KIFC1 was also degraded by the APC/C *in vivo*. First, we analyzed the protein stability of KIFC1 over time. We synchronized HeLa cells in early mitosis with nocodazole, washed the drug out of the cells, and released into fresh media for 12hrs, frequently assessing for the presence of KIFC1 protein. KIFC1 was readily detectable in early mitosis (0hr timepoint) and the signal disappeared with kinetics similar to the degradation of canonical APC/C substrates geminin and securin (Figure 2).

We confirmed that the loss of KIFC1 protein product occurs soon after mitotic entry. Again, we synchronized HeLa cells in mitosis, and generated extract from arrested cells. We stimulated APC/C activity by the addition of ubiquitin, Ube2C, and the Mad2 competitor protein p31^{comet} (Xia, et al. 2004; Reddy et al., 2007), and analyzed KIFC1 stability. As observed in Figure 2, the KIFC1 protein product rapidly disappears upon APC/C activation (Figure 3).

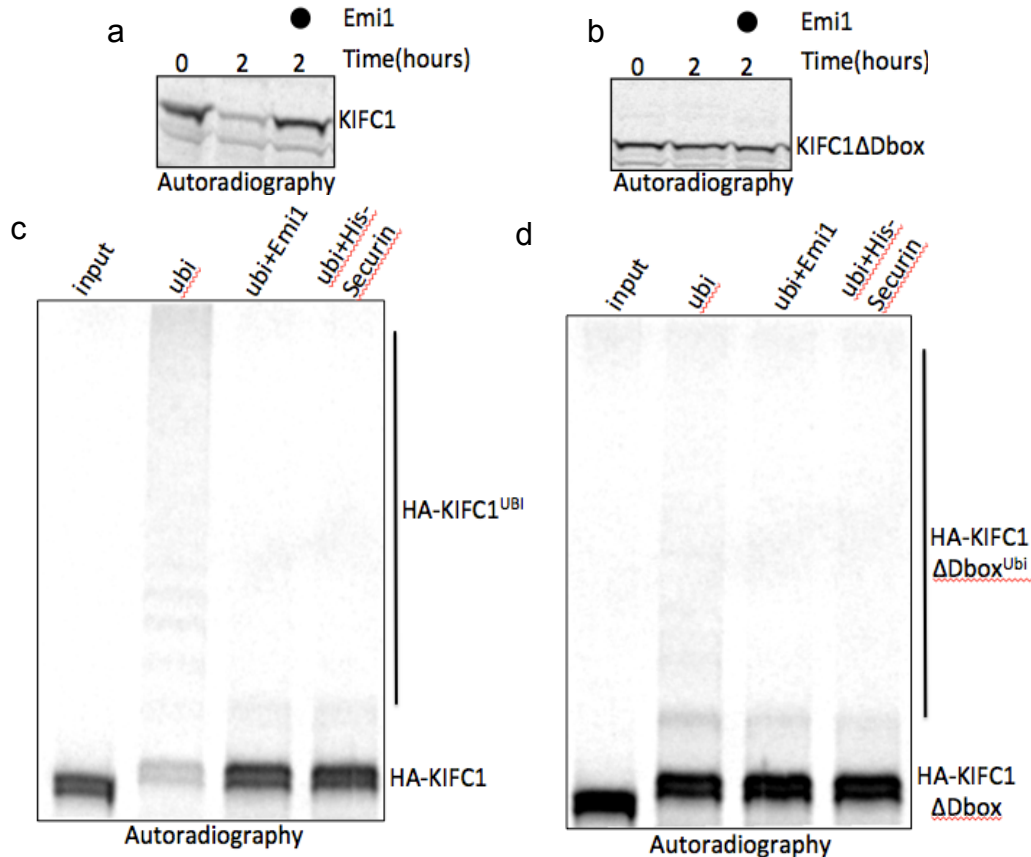


Figure 1. KIFC1 is a substrate of the APC/C *in vitro*. (a,b) KIFC1, but not KIFC1 ΔDbox, is degraded by the APC/C. ³⁵S-KIFC1 (a) or ³⁵S-KIFC1 ΔDbox (b) was generated by IVT/T and incubated with HeLa G1 extract, Ube2C and ubiquitin for the indicated time at 30°C. The APC/C inhibitor Emi1 was added to determine APC/C specificity. (c,d) KIFC1 is ubiquitylated by the APC/C. ³⁵S-KIFC1 (c) or ³⁵S-KIFC1 ΔDbox (d) was generated by IVT/T and incubated with APC/C^{Cdh1}, Ube2C, Ube2S, E1 and ubiquitin, and incubated at 25°C for 30min. Emi1 or a substrate competitor, securin, was added to determine specificity. Reaction products were analyzed by autoradiography.

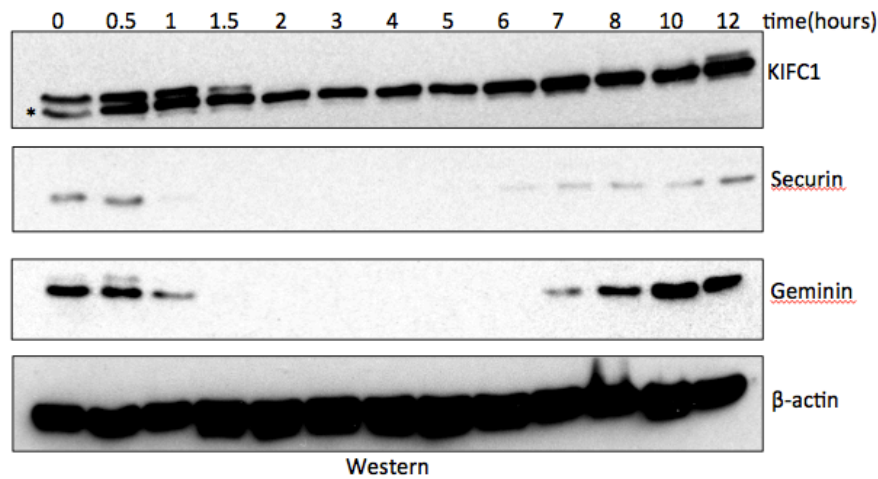


Figure 2. Endogenous KIFC1 is degraded within 2hr of release from nocodazole-induced mitotic arrest in HeLa cells. Cells were synchronized by thymidine and nocodazole treatments. Mitotic cells were harvested by shake-off and released in fresh media. Asterisk marks unspecific binding by KIFC1 antibody. Protein stability was analyzed by Western blotting.

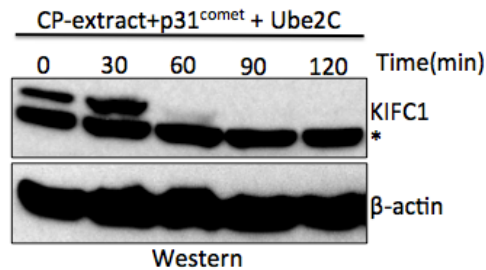


Figure 3. Endogenous KIFC1 is degraded in mitotic extract in which APC/C is activated by addition of p31^{comet} and Ube2C. Asterisk represents unspecific cross-reactive band recognized by the antibody. Protein stability was analyzed by Western blotting.

We initially became interested in KIFC1 after detecting its interaction with importin β and other APC/C substrates from an interactome analysis (Song and Rape, 2010). We therefore asked whether the importin interaction affected the ability of APC/C to regulate KIFC1. We had previously shown that the APC/C-substrate HURP binds directly to importin β , and that this interaction blocked APC/C-dependent degradation (Song and Rape, 2010). Is this regulatory pattern also seen for KIFC1?

We detected a putative bipartite NLS that was located downstream to the D-box, and intriguingly realized that the positive residues characteristic of a NLS resemble ubiquitin initiation sites, as well. Our putative NLS sequence had been previously confirmed as an NLS by the work of others (Ems-McClung, et al., 2004). We first decided to examine how mutation of either segment of the bipartite NLS (denoted as NLS 'a' and NLS 'b') affected the localization of HA-

KIFC1. Using site-directed mutagenesis, we mutated either NLS 'a' or NLS 'b' or both (not shown in this figure) to alanine residues (Figure 4D). While exogenously expressed HA-KIFC1 is predominantly nuclear in its localization (Figure 4A, green), mutation of either NLSa or NLSb results in cytoplasmic localization (Figure 4B and 4C). Additionally, loss of NLSa results in a prominent microtubule bundling phenotype (Figure 4B). Therefore, we confirm that KIFC1 possesses a bipartite NLS as previously published (Ems-McClung, et al., 2004) and that the NLS is proximally located to a major APC/C recognition site.

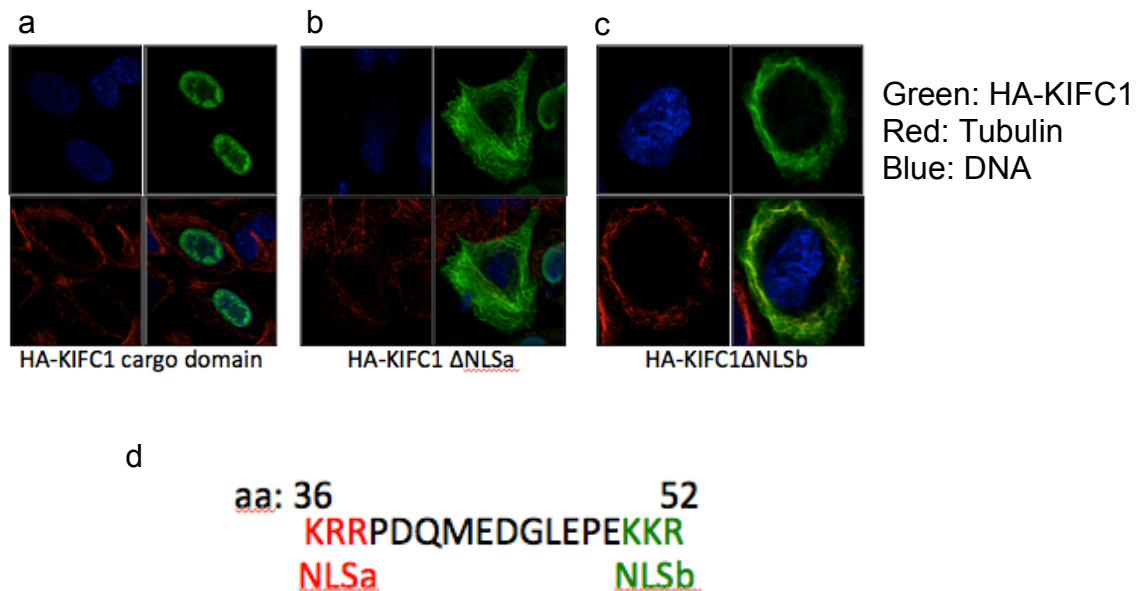


Figure 4. KIFC1 has a bipartite NLS in its N-terminus. (a) HA-tagged KIFC1 cargo domain is nuclear in localization during interphase. Results (not shown) phenocopy endogenous KIFC1. (b-c) ΔNLSa (KRR36-38AAA) (b) ΔNLSb (KKR50-52AAA) (c) results in cytoplasmic localization in interphase. Loss NLSa (b) also results in microtubule bundling. (d) Amino acid sequence of KIFC1 bipartite NLS. IF staining shows DNA (blue), HA-KIFC1 (green), and tubulin (red).

The presence of an NLS downstream of a D-box does not necessarily indicate that these sequences affect APC/C regulation. To analyze this potential circumstance, we first wished to confirm the interaction between importins and KIFC1. We performed an *in vitro* binding reaction in which we generated ³⁵S-KIFC1 using the rabbit reticulocyte system, and incubated it with MBP-importinβ or MBP-importinα, along with other related proteins. We then performed a MBP pulldown, and analyzed whether or not HA-KIFC1 had co-precipitated by autoradiography. As controls, HA-KIFC1 is not detected with beads (amylose resin) or after an MBP-only pulldown (Figure 5, Lanes 2 and 3). Interestingly, HA-KIFC1 did not interact with MBP-importinβ by itself (Figure 5, Lane 4).

Instead, HA-KIFC1 directly interacted with MBP-importinα (Figure 5, Lane 5). Addition of constitutively GTP-charged Ran (RanQ69L) had no effect on the binding of HA-KIFC1 to importinα, which is unsurprising as Ran directly interacts

with importin β to trigger cargo release (Kalab and Heald, 2008) (Figure 5, Lane 6). However, when MBP-importin α was preincubated with his-importin β , allowing for the formation of importin α/β heterodimers, HA-KIFC1 bound with better efficiency (Figure 5, Lane 7). These data suggest that KIFC1 efficiently binds importin α/β heterodimers through an interaction with importin α . If this hypothesis was true, addition of RanGTP should have no effect on the binding of KIFC1 to importin α , but should disrupt or weaken the interaction between KIFC1 and the importin α/β heterodimer, as cargo would be released. In fact, this is what we observed when we performed the experiment (Figure 5, lane 8).

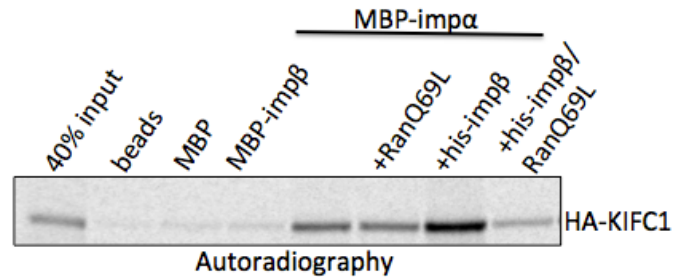


Figure 5. A direct interaction between KIFC1 and importin α is strengthened by the addition of importin β but competed off by the addition of RanQ69L. MBP alone or MBP-importin α or β was immobilized to amylose-coated beads and incubated in the presence of ³⁵S HA-KIFC1 with or without additional proteins to allow for KIFC1/importin binding. Beads were washed extensively and the presence of KIFC1 bound was assayed by autoradiography.

In our previous work, we were struck when we noticed that binding of importin β interfered with the APC/C-dependent regulation of HURP, but not other substrates that do not bind importins, such as cyclin B (Song and Rape, 2010). Therefore, we asked whether KIFC1, an interactor of both importin α and importin α/β heterodimers, would also be subject to this dual regulation. We performed an APC/C-ubiquitylation experiment using the same protocol as shown in Figure 1C, but additionally added either the C-terminus of importin α (which lacks the importin β binding domain, and therefore cannot be released from KIFC1 by any charged Ran present in the reticulocyte or remaining cell extract; See Figure 5; Görlich, et al., 1996; Weis, et al., 1996), or a truncated importin β protein that also cannot be competed off by binding of RanGTP.

While ³⁵S-HA-KIFC1 was efficiently turned over to its ubiquitylated form (Figure 6A, Lane 2), addition of importin α (Figure 6A, Lane 3), but not importin β (Figure 6A, Lane 4), blocked this turnover in a manner compared to APC/C inhibitors Emi1, or a purified APC/C substrate competitor, securin (Figure 6A, Lanes 5-6). Strikingly, this suggests that SAFs that bind importin α/β heterodimers through importin α directly are still jointly regulated by importins and the APC/C. This finding was also confirmed through *in vitro* degradation reactions, as introduction of purified importin α , but not importin β , largely blocked KIFC1 degradation (Figure 6B), while the addition of RanGTP had no effect on this blockage.

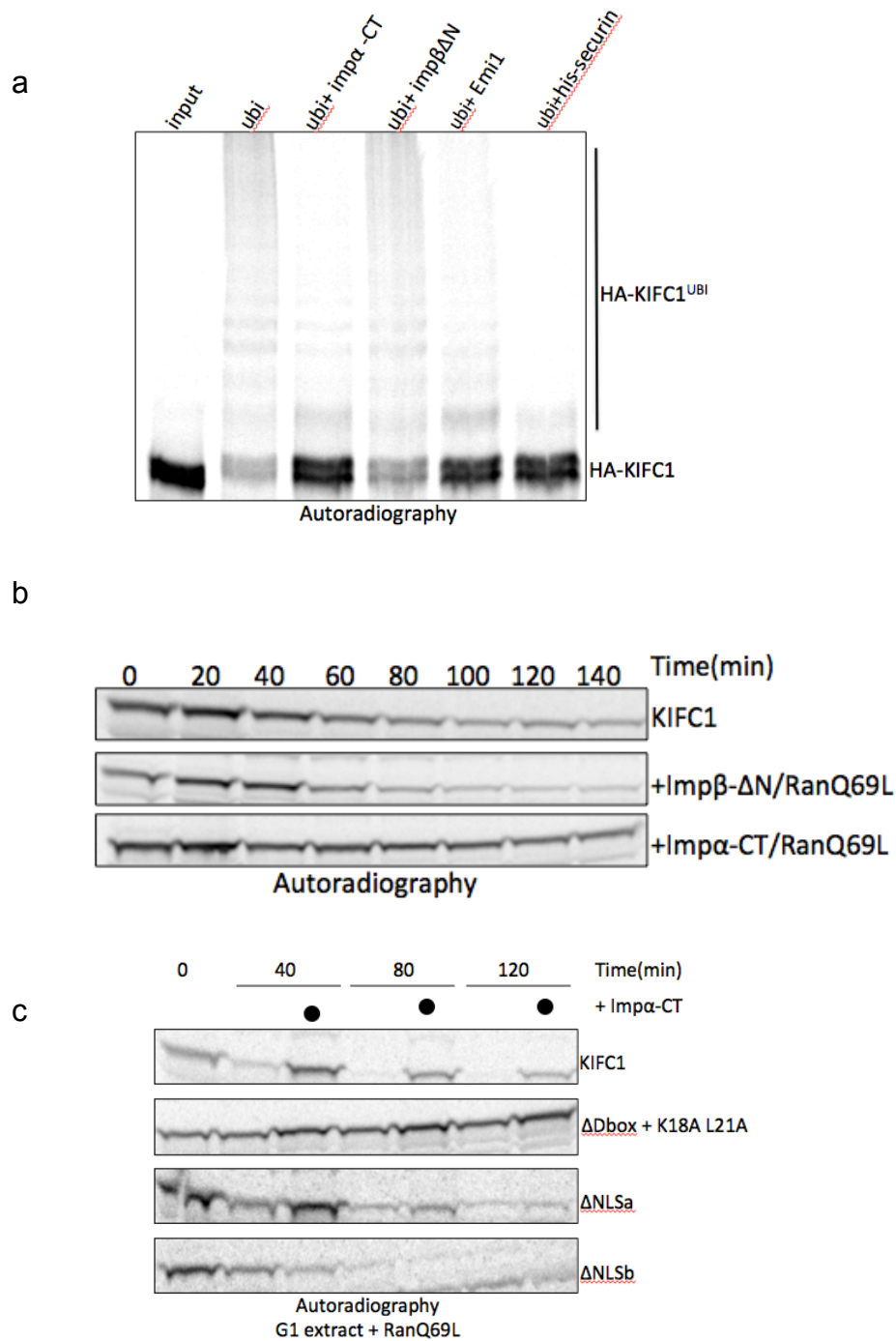


Figure 6. Importin α binding to a bipartite NLS in KIFC1 blocks ubiquitylation and degradation by the APC/C. Importin α , but not β , blocks APC/C recognition *in vitro*. (a) ^{35}S HA-KIFC1 was synthesized by IVT/T and incubated with immunopurified APC/C^{Cdh1} in addition to Ube2C, Ube2S, E1, and ubiquitin and the indicated proteins. (b) ^{35}S HA-KIFC1 was synthesized by IVT/T and incubated with HeLa G1 extract in addition to Ube2C, ubiquitin, and RanQ69L, in addition to indicated proteins. (c) Mutation of NLSa or NLSb abolishes the block to APC recognition, allowing for rapid degradation.

If importin α truly does bind KIFC1 and block APC/C recognition and ubiquitylation, we would expect that a KIFC1 importin α -binding mutant (mutation of either NLSa or NLSb) would still be degraded by the APC/C in the presence of importin α . To test this hypothesis, we performed an *in vitro* degradation assay of KIFC1 identical to that of Figure 1A, except that we performed degradation reactions with and with exogenous addition of importin α -C-terminus (which cannot bind importin β) (Figure 6C). KIFC1 is degraded by the APC/C only in the absence of exogenous importin α -CT, while the D-box mutant is stabilized in extract, with importin α addition making little difference to protein stability (Figure 6C). Conversely, neither NLS mutant was significantly stabilized in the presence of importin α -CT, although the NLSb mutation conferred less binding of importin α -CT than the NLSa mutant (Figure 6C). Therefore, we conclude that KIFC1 is a novel substrate of the APC/C, and that importin α binding blocks ubiquitylation and degradation.

In subsequent work, we have further determined the mechanism of how importin β , microtubules, and the APC/C regulate HURP. While importin β binds HURP, complete binding of the protein to microtubules is blocked. Importin β is released from HURP when it encounters RanGTP near chromatin, and can therefore bind microtubules. Strikingly, when HURP binds microtubules, it is also protected from APC/C-dependent ubiquitylation (Chapter 3; Song, et al., 2014). In an analogous study, we have also examined KIFC1's dependence on microtubules. As shown in Figure 7, microtubules confer slight, but incomplete protection from

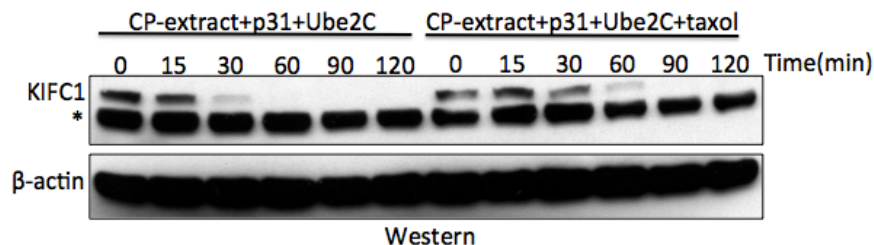


Figure 7. Microtubules delay KIFC1 degradation. (a) KIFC1 is degraded in mitotic extract in which APC/C is activated by addition of p31^{comet} and Ube2C. (b) Taxol treatment has stabilization effect.

degradation. At this time, it is unclear how microtubules fit into the APC/C, importin α dual regulation mechanism, but we are eager to determine the full picture of this regulation.

Conclusion:

The experiments demonstrated in this appendix have elucidated the regulation of KIFC1 by the APC/C, and in part, by importin α . We have discovered that human KIFC1 is an APC/C substrate that is degraded both *in vitro* and *in vivo*. Additionally, we performed sequence analysis in order to determine the major APC/C recognition site, an N-terminal D-box. Interestingly, approximately 30 residues downstream of the D-box, in a site where ubiquitin initiation often occurs (Williamson, et al., 2011), a bipartite NLS is found.

Work by the Walczak lab and others had previously studied the interaction between KIFC1 and importins (Ems-McClung, et al., 2004). Here, we confirmed the presence of a bipartite NLS. By mutating either portion of the NLS sequence, we were able to disrupt the nuclear localization of exogenously expressed KIFC1 in interphase. Additionally, the different KIFC1 NLS mutants showed varying effects upon interphase microtubules. The KIFC1 NLSa mutant, that still contains a wildtype NLSb sequence, results in interphase microtubule bundling, while the corresponding NLSb mutant results in a less severe phenotype (Figure 4).

Wildtype KIFC1 binds importins through its NLS sequence (Ems-McClung, et al., 2004; Figure 6). However, we determined that KIFC1 binds importin α / β heterodimers through importin α directly. Addition of the C-terminus of importin α (which lacks the importin β binding domain) to a reaction containing KIFC1 and active APC/C results in protection of KIFC1 from APC/C-dependent degradation (Figure 6). This result is both similar and unique to our other studies, in which substrates such as HURP are protected from degradation through direct binding to importin β (Song, et al., 2014; Song and Rape, 2010). Thus, our work suggests that joint regulation of APC/C substrates by importins and microtubules (Figure 7, Chapter 2; Song, et al., 2014) may be a prominent mechanism through which to regulate spindle dynamics in mitosis.

Material and Methods

Materials and methods were mostly adapted from our previous work on these topics (Song, et al., 2014; Song and Rape, 2010).

In Vitro Degradation Reactions

HeLa S3 cells were synchronized in mitosis by 2mM thymidine and 100ng/ml nocodazole, and, when indicated, released into drug-free media for 3hr to generate a mainly G1 population. Extract was prepared as described (Jin, et al., 2008). 35 S-KIFC1 was generated by an *in vitro* rabbit reticulocyte lysate premix (Promega) in the presence of 35 S-Met/Cys (Translabel; ICN). Extracts were supplemented with ubiquitin, Ube2C, and energy mix, and 35 S-KIFC1 was added with additional proteins as indicated. Reactions were incubated for up to 2hr at 30°C. Reactions were stopped by addition of gel loading buffer and analyzed by autoradiography.

In Vitro Ubiquitylation Reactions

Human APC/C was purified from concentrated HeLa S3 extracts by immunoprecipitation using Cdc27 antibodies and Protein G agarose (Roche). Washed beads were incubated with human E1, purified Ube2C/Ube2S, ubiquitin and energy mix (15mM creatine phosphate, 2mM ATP, 2mM MgCl₂ and 0.2mM EGTA (pH7.5)), along with 1mM DTT and 35 S-labeled KIFC1 synthesized by IVT/T (Promega system) at room temperature for 30min. Reactions were analyzed by autoradiography.

MBP Pull-Down Assays

Amylose resin was charged with MBP protein fusions in MBP buffer (20mM HEPES (pH7.5), 150mM NaCl, 5mM KCl, 1.5mM MgCl₂, 0.1mg/ml BSA, and 0.1% Tween-20) and incubated with *in vitro* synthesized, radioactively labeled HA-KIFC1 for 3hr at 4°C. Amylose resin was carefully washed of non-interacting proteins and other cell materials in wash buffer (20mM HEPES (pH7.5), 5mM KCl, 1.5mM MgCl₂, and 0.1% Tween-20). Resin-bound proteins were eluted in gel loading buffer and analyzed by autoradiography.

Immunofluorescence

Cells were transfected with pcs2-HA-KIFC1 (and corresponding mutants) with Lipofectamine 2000 (Invitrogen) using standard procedures. Immunofluorescence was performed as described (Song and Rape, 2010; Chapters 1-2). Pictures were taken at 100X using an IX81 epifluorescence microscope (Olympus) with Metamorph software. Images were processed using Metamorph and ImageJ.

Plasmids, siRNAs, antibodies and proteins

KifC1 cDNA was cloned into pCS2 or pCS2-HA for IVT/T or HeLa cell transfection. Site-directed mutagenesis was performed by alanine scanning. For recombinant proteins, cDNAs were cloned into pMAL and pET28 for expression in *E.coli*, and the purification procedures for MBP-tagged and 6xHis-tagged proteins were as described (Song and Rape, 2010). The following antibodies were used: α KifC1 (rabbit polyclonal; Bethyl Laboratories;A300-952A), β -actin (mouse monoclonal, MP Biomedicals LLC, 08691001), α -tubulin (mouse monoclonal, Calbiochem, DM1A), α -Cdc27 (for IP: mouse monoclonal, Santa Cruz, AF3.1), α -HA (rabbit polyclonal, Santa Cruz; and rabbit monoclonal, Cell Signaling:C29F4).

Appendix C:

Kif18A is a novel substrate of the APC/C and is protected from degradation by microtubules

Craney, A.*, Saxton, R.*, Fedrigo, I., and Rape, M. Unpublished data 2011-2013.

* indicates equal contribution

Contributions and Acknowledgements

I performed the bioinformatics and initial substrate discovery for this project. In 2012, I began mentoring an undergraduate researcher, Robert Saxton (currently a graduate student in the Biology department at the Massachusetts Institute of Technology), who performed his thesis on the characterization of Kif18A as an APC/C substrate dually regulated by the APC/C and microtubules. I mentored Robert and trained him in laboratory safety and techniques, and made the initial clones for the project. Robert performed the autoradiography experiments and the sequence analysis of Kif18A. This work was the focus of his undergraduate thesis, for which he won the 2013 best undergraduate thesis prize for the Cell and Developmental Biology division. The microtubule pelleting assays were performed jointly between Robert and myself, and we received training and protocols from Dr. Ling Song (currently of Novartis) and Dr. Kara Helmke (Rebecca Heald's lab).

Dr. Mike Springer (Department of Systems Biology, Harvard University) provided the human proteome dataset in FASTA format (not shown due to space considerations). Dr. Elaine Angelino (currently of the Department of Statistics, University of California, Berkeley) collaborated with me to design a script to interrogate the NCBI database to systematically determine which proteins were designated as human kinesins and what residues were within the motor domains. I developed the criteria and constraints, and Elaine wrote the JSON script (supporting script for Tables 1 and 2).

I would like to especially thank Dr. Terry Lang (currently of the KIPP Foundation, San Francisco, California), Dr. Matt Davis (currently of IBM, Cambridge, MA), the Berkeley Python Summer course (2010), and Code Academy (www.codeacademy.com) for Python support; as well as Dr. Roy Kishony and members of his laboratory: J.B., Noam, Pam, and others, for inspiring me to build my bioinformatics skills; and Dr. Rachel Brem's and Dr. Mike Eisen's genome projects course (2010) for an introduction to coding through Perl.

Note: the data contained in Figures 1-2 and 4, were discovered in our lab, but the substrate recognition elements were subsequently published by another group (Sedgwick, et al., 2013). Our work is unpublished.

Introductory Summary:

The successful partitioning of genomic material and subsequent cell division is essential to the viability of an organism. Errors in mitotic processes can lead to cell death and aneuploidy. A key regulator of mitosis in eukaryotes is the Anaphase Promoting Complex (APC/C), a conserved ubiquitin E3 ligase that is necessary for proper spindle dynamics and for initiation of anaphase and progression through cell division (Peters, 2006; Song, et al., 2014; Song and Rape, 2010). While many substrates of APC/C have been identified (Meyer and Rape, 2011), the overall logic of how APC/C directs proper progression through mitosis is not clear. One critical missing link is to systematically predict novel APC/C substrates, which would allow for important functional studies to dissect the full importance of APC/C activity in mitosis.

In this project, we designed and employed a bioinformatics algorithm aimed at predicting novel APC/C substrates in a systematic process. We took advantage of known APC/C degrons (Peters, 2006) and work from our lab on APC/C ubiquitin initiation sites (Williamson, et al., 2011). This work occurred concurrently with the projects described in Chapter 2 (Song, et al., 2014) and work on KIFC1 (Appendix B). Cumulative knowledge of these projects and others (Song and Rape, 2010) suggested that spindle assembly factors (SAFs) are a growing class of APC/C substrates which illustrate new mechanisms of APC/C control in early mitosis and metaphase.

Results:

Expanding the list of known APC/C mitotic substrates would help illuminate the processes in which APC/C is necessary, and potentially, novel means of ubiquitin-dependent regulation. Here, I designed and wrote a bioinformatics algorithm that would systematically identify substrates of the APC/C. I used known APC/C degron information to specify constraints for this algorithm. Protein sequences were scanned for the presence of canonical APC/C degrons: 'KEN' box and a 'Destruction-box' (D-box; amino acid residues 'RXXL' or 'KXXL') (Peters, 2006; Rape, et al, 2004). Further, meticulous sequence analysis in our lab had previously suggested that the presence of a 'patch' of positively charged residues downstream from the D-box (arginine and lysine; histidine was not included) could represent important ubiquitin chain initiation sites for the APC/C E2 enzyme Ube2C (Williamson, et al., 2011). I scanned the sequences 52 amino acids downstream from each D-box in patches of 6 amino acids at a time, and counted the patch as 'positive' if it possessed lysine or arginine for three or more amino acid residues out of the six.

Using these constraints, I scanned over 20,000 human protein sequences for the presence of APC/C degrons and recognition motifs. Many well-characterized APC/C substrates were identified by this method, as well as many putative APC/C substrates. One caveat to this algorithm is that not all APC/C substrates possess a KEN-box. Therefore, I missed some known APC/C substrates, as well as some novel APC/C substrates (see KIFC1, Appendix B).

The raw data from this algorithm is not shown, because a more fruitful analysis of the data was to examine novel substrates by protein class.

Interestingly, the human kinesin family was overwhelmingly represented in this list. At first, I was concerned that the kinesins were over-represented because they possess large, highly conserved motor domains and microtubule binding sequences that are enriched in positively charged amino acids (Ems-McClung, et al., 2004; Weaver, et al., 2011). These characteristics may have resulted in false positive hits for APC/C recognition motifs. Therefore, I wrote a simple script that would analyze the percentage of positive residues in each protein sequence coded for by the genome. I reasoned that if kinesin proteins were among the most positively charged proteins in the proteome, we may need additional constraints to be included in the substrate prediction algorithm.

This analysis looked at over 20,000 human protein sequences. The average percentage of positive residues in this dataset is 13.8% positive, with a standard deviation of 3.6%. The kinesin family had an average positive residue composition of 15.8%, with a standard deviation of 1.6%. Therefore, the kinesins are not above one standard deviation 'more positive' than the average protein in the human proteome. A family that did fall out of this analysis, though, was the family of ribosomal proteins, which have close to 30% or more positive residues in their sequences.

Table 1 lists the human kinesin genes and whether or not the protein products are predicted to have all three APC/C sequence recognition elements: a KEN-box, D-box, and a positive patch. Of the 43 kinesins, 18 (41.9%) have these APC/C recognition elements. Another, KIFC1, had been predicted by Ling Song to be a novel substrate and was subsequently characterized by myself (see Appendix B), but does not possess a KEN box.

Table 1. Human kinesin genes (identified by 'kinesin' in FASTA sequence identifier)

KINESIN GENES IN HUMAN GENOME (IDENTIFIED BY 'KINESIN' in FASTA SEQUENCE NAME, excluding light and heavy chains and trafficking proteins)	
Gene Name	 KEN + D-box + Pos Patch
1. KIF1A	
2. KIF1B	
3. KIF1C	Y
4. KIFC1	<i>possesses D-box + Pos Patch but no KEN-box</i>
5. KIFC2	
6. KIFC3	
7. KIF2A	
8. KIF2B	
9. KIF2C	
10. KIF3A	
11. KIF3B	
12. KIF3C	Y
13. KIFAP3	
14. KIF4A	Y

15. KIF4B	Y
16. KIF5A	
17. KIF5B	Y
18. KIF5C	Y
19. KIF6	
20. KIF7	
21. KIF9	Y
22. KIF11	Y
23. KIF12	
24. KIF13A	Y
25. KIF13B	
26. KIF14	
27. KIF15	Y
28. KIF16B	
29. KIF17	
30. KIF18A	Y
31. KIF18B	
32. KIF19	
33. KIF20A	
34. KIF20B	Y
35. KIF21A	Y
36. KIF21B	Y
37. KIF22	Y
38. KIF23	Y
39. KIF24	
40. KIF25	
41. KIF26A	
42. KIF26B	Y
43. KIF27	Y

I was primarily interested in identifying mitotic APC/C substrates by this analysis, and was intrigued by the kinesin family given the results in Table1 and our KIFC1 research. Therefore, I examined the mitotic kinesin proteins in more detail. A mitotic kinesin was defined by a kinesin that had been previously published to have a role in mitosis, and/or was characterized by gene ontology to be a mitotic kinesin. 18 of the 43 kinesin proteins were characterized as 'mitotic' by these criteria. 8 of these 18 kinesins (44%) possess putative APC/C degrons.

Table 2. Mitotic kinesin proteins that possess APC/C recognition sites. Proteins were chosen using gene ontology (GO) terms (<http://geneontology.org/page/go-enrichment-analysis>) of “M Phase”, “Cell Division”, and/or “Mitotic Cell Cycle Process.”

**genes that have experimental evidence linking them to cell division even if GO terms are not specified.*

#protein products are identified in this work as novel human APC/C substrates

^publication by another group subsequent to this discovery (Sedgwick, et al., 2013).

Gene Name	 KEN + D-box + Pos Patch
1. KIFC1 [#]	<i>possesses D-box + Pos Patch but no KEN-box</i>
2. KIF2A	
3. KIF2B	
4. KIF2C	
5. KIF3B	
6. KIFC3 ^{*#} (data not shown)	
7. KIF4A [*]	Y
8. KIF11	Y
9. KIF13A	Y
10. KIF14 [*]	
11. KIF15	Y
12. KIF18A ^{#^}	Y
13. KIF18B	
14. KIF20A	
15. KIF20B	Y
16. KIF22	Y
17. KIF23	Y
18. KIF25	

Taken together, work from Ling Song (Song and Rape, 2010), this bioinformatics algorithm, Appendix B, and my main thesis work (see Chapters 1-2), made me particularly interested in exploring mitotic kinesins as a category of SAFs that were regulated by the APC/C. Thus, APC/C may play a role in spindle assembly, disassembly, and/or spindle dynamics.

As my research in Chapter 1 dictates, I had orthogonally become interested in Kif18A and its genetic interaction with the APC/C. Therefore, I decided to use Kif18A as a model candidate to explore the prediction potential of the algorithm. I first examined the stability of Kif18A over time when incubated with active APC/C. HeLa cell mitotic extract was prepared from 1L of cells treated with thymidine and nocodazole. APC/C activity was stimulated in this extract by addition of Ube2C, p31, ubiquitin, and ATP and incubated at 30°C for the indicated time periods. Kif18A protein levels begin to decrease and disappear with similar dynamics to known APC/C substrates, securin and geminin. Importantly, addition of MG132, which blocks proteasomal degradation, largely rescued the depletion phenotype of Kif18A, securin, and geminin, suggesting that their degradation was proteasome dependent.

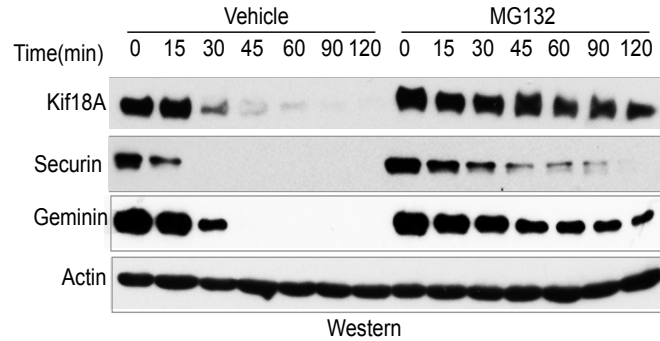


Figure 1. Kif18A is degraded by the mitotic ubiquitin-proteasome system (UPS). HeLa mitotic cell extract was generated from cells arrested by nocodazole. APC/C activity, and potentially other ligases, were stimulated by addition of Ube2C, p31^{comet}, ubiquitin and ATP. Reactions were incubated at 30°C or 37°C for the indicated time periods with or without MG132. Protein stability was assayed by Western blot.

However, it is possible that other E3 ubiquitin ligases were also active in the HeLa mitotic extract. Therefore, I performed two APC/C sufficiency experiments in a similar fashion as Figure 1, only in one condition, I added an excess of dominant negative Ube2C instead of wild-type (data not shown), and in the second condition, I depleted the APC/C co-activator CDC20 from the extract before beginning the degradation assay (Figure 2). In both cases, blocking APC/C activity stabilized Kif18A and known substrates in the extract, suggesting that Kif18A is indeed a novel mitotic APC/C substrate.

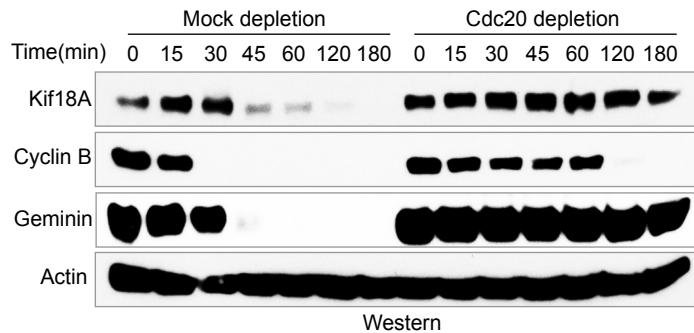


Figure 2. Kif18A is degraded by APC/C in mitosis. HeLa mitotic cell extract was generated from cells arrested in mitosis by nocodazole. The amount of the APC/C co-activator CDC20 was greatly diminished by two rounds of depletion by a CDC20 antibody; a mock depletion targeting IgG was also performed as a control. APC/C activity was then stimulated by addition of Ube2C, p31^{comet}, ubiquitin and ATP. Reactions were incubated at 30°C or 37°C for the indicated time periods. Protein stability was assayed by Western blot.

I therefore had validated the predictive power of my substrate algorithm by characterizing a novel APC/C substrate. I had preliminary data to suggest that the APC/C degron sequences existed in the cargo domain of the protein. This was interesting as the non-cargo domain of the protein, the motor domain, is conserved among kinesins (see also Figure 4). If the degron had existed in the motor domain, it could be that multiple kinesins also possessed the same degron(s). Instead, the evidence suggested that certain kinesins evolved APC/C

recognition motifs over time, perhaps to accommodate mitosis with an increasingly complex genome and spindle to coordinate. Interestingly, I was able to identify the primary APC/C recognition site for KIFC1 by site-directed mutagenesis (Appendix B). The important degron is an N-terminal D-box. Intriguingly, while the KIFC1 N-terminal D-box is conserved also in rat and mouse species, in zebrafish, the D-box is incomplete, but is replaced by a KEN box (ncbi.nlm.nih.gov).

Other mechanisms of SAF regulation were being studied in the lab (see Appendix B). I first looked at whether addition of importin β or importin α stabilized Kif18A, as it does HURP (see Chapter 3) or KIFC1 (Appendix B), respectively. The presence of importins did not affect Kif18A stability (not shown). However, the presence of microtubules did stabilize Kif18A (Figure 3), as it does HURP and KIFC1. This was very interesting as it suggested that the dual recognition of APC/C and microtubules of Kif18A might be distinct from that of KIFC1 and HURP, which regulate their microtubule binding through importins (Ems-McClung, et al., 2004; Song, et al., 2014; Song and Rape, 2010; Wong, et al., 2008). Degradation of soluble substrates, geminin and securin, were unaffected by the presence of microtubules in the extract (Figure 3, Song, et al., 2014).

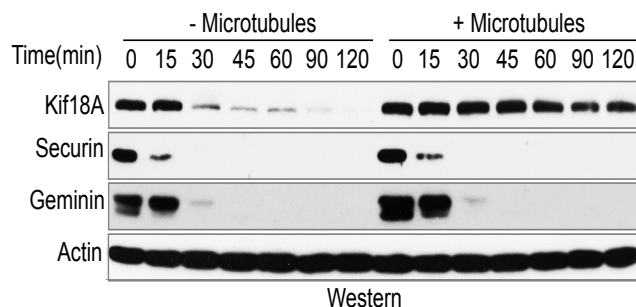


Figure 3. The presence of microtubules retards Kif18A degradation in HeLa cell mitotic extract, but not the degradation of soluble APC/C substrates securin and geminin. HeLa mitotic cell extract was generated from cells arrested in mitosis by nocodazole. Extract was warmed to 30°C and incubated with taxol to generate microtubules, or DMSO as a vehicle control. APC/C activity was then stimulated by addition of Ube2C, p31^{comet}, ubiquitin and ATP. Reactions were incubated at 30°C for the indicated time periods. Protein stability was assayed by Western blot.

We delved more deeply into the sequence elements that APC/C recognizes in Kif18A. First, we determined that HA-Kif18A could be *in vitro* transcribed and translated in a rabbit reticulocyte system and that ³⁵S-HA-Kif18A could be degraded by the APC/C. We also confirmed, as suspected earlier and as predicted bioinformatically, that the minimal APC/C substrate is the Kif18A cargo domain (Figure 4).

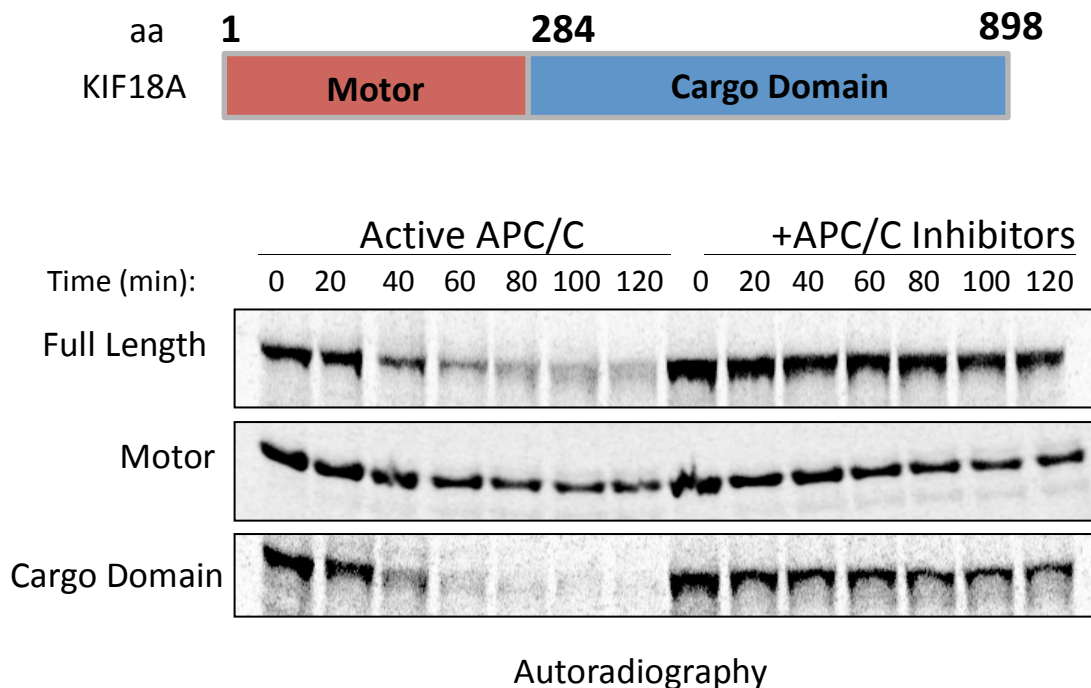


Figure 4. HA-Kif18A cargo domain is a minimal APC/C substrate. (top schematic) Kif18A was cloned into a pcs2-HA backbone as a full-length clone, a motor domain truncation (aa 285-989) or a cargo domain truncation (aa 1-284). (bottom) Clones were *in vitro* transcribed/translated in a rabbit reticulocyte system in the presence of ³⁵S. The radiolabeled HA-Kif18 constructs were incubated with HeLa mitotic extract generated from cells arrested by nocodazole. APC/C activity was stimulated by addition of Ube2C, p31^{comet}, ubiquitin and ATP. Reactions were incubated at 30°C for the indicated time periods with and without APC/C inhibitors (consisting of a substrate competitor and dominant negative Ube2C). Protein stability was assayed by autoradiography.

However, exhaustive mutagenesis of the D-boxes and the KEN-box in various combinations had little to no effect on Kif18A stability. We were able to detect some dependence on a region between aa603-678 (data not shown), but truncation of this region still allowed for retarded degradation of Kif18A, and we were not sure whether or not truncating the clone resulted in mis-folding of the protein. Sequence analysis, however, showed us that the C-terminal residues of Kif18A are 'LR' (leucine-arginine). An APC/C substrate invisible to the SAC, Nek2A, possesses the amino acids 'MR' (methionine-arginine) at its C-terminus. These residues are required for degradation of Nek2A through targeting of the protein to the APC/C in prometaphase (Hayes, et al., 2006). We decided to investigate whether or not the chemically similar C-terminus of Kif18A was required for its degradation by the APC/C.

Indeed, as demonstrated in Figure 5, and by others (Sedgwick, et al., 2013), Kif18A degradation is dependent upon an LR motif at its C-terminus.

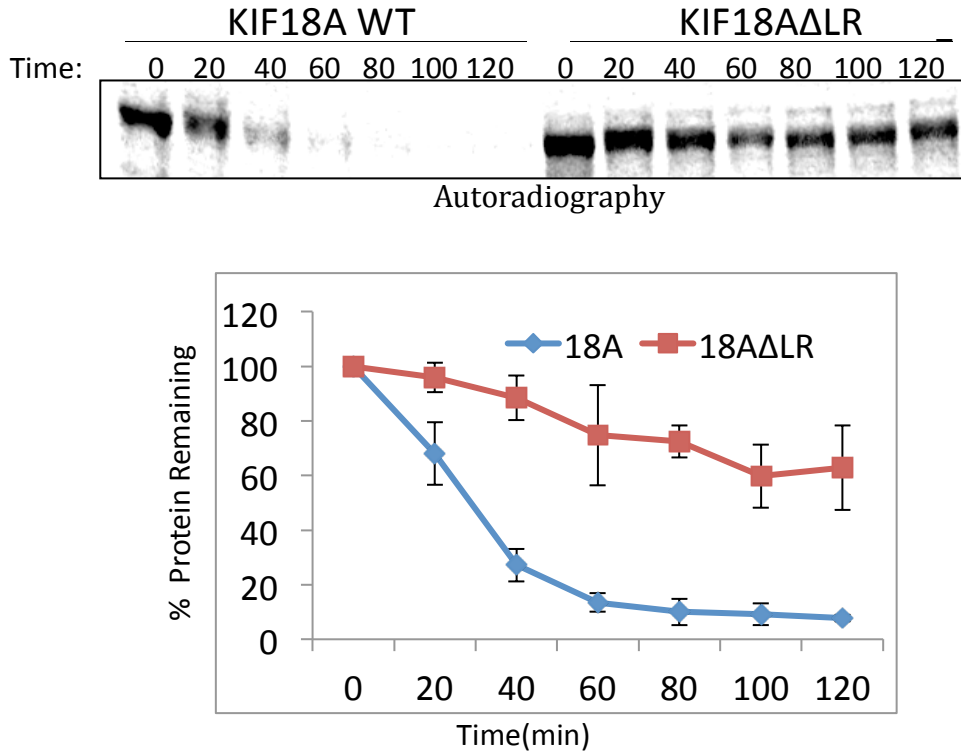


Figure 5. Degradation of Kif18A requires a leucine followed by an arginine at its C-terminus. (top) pCS2-FL Kif18A or pCS2 Kif18A with its LR truncated were *in vitro* transcribed/translated in a rabbit reticulocyte system in the presence of ^{35}S . The radiolabeled HA-Kif18A constructs were incubated with HeLa mitotic extract generated from cells arrested by nocodazole. APC/C activity was stimulated by addition of Ube2C, p31^{comet}, ubiquitin and ATP. Reactions were incubated at 30°C for the indicated time periods and the protein stability was assayed by autoradiography. (bottom) Three independent replicates of the degradation experiments were performed and quantified by Image J. The average percentage protein remaining and the standard deviation were calculated and graphed using Excel (Microsoft).

As the MR motif of Nek2A mediates association with APC/C (Hayes, et al., 2006), we wished to determine if Kif18A associates stably with the APC/C. Many substrates are unable to be detected with the APC/C in immunoprecipitations, likely because of the rapid pace of ubiquitylation (Pierce, et al., 2009; Rape, et al., 2004). However, substrates like Nek2A and cyclin A can be detected when APC/C activity is lowered, either by Ube2S siRNA (Figure 6), addition of dominant negative Ube2C, or addition of MG132 (see Chapter 1).

We performed Ube2S or Mock siRNA in HeLa cells, arrested with either nocodazole, which depolymerizes microtubules, or S-T-L-C, which stabilizes microtubules, before generating extract from the cells. We then immunoprecipitated the APC/C and analyzed co-precipitating proteins. Whereas Nek2A only interacted stably with the APC/C when Ube2S was depleted, Kif18A interacted in a detectable manner regardless of microtubule status before extract preparation and the presence of Ube2S (Figure 6). Kif18A has also been detected on the APC/C in prometaphase via mass spectrometry (Sedgwick, et al., 2013, HJM unpublished data). Therefore, despite some chemical similarities of the C-terminal two residues with Nek2A, Kif18A likely does not interact with

APC/C via the same mechanism. It likely interacts with the APC/C in a manner distinct from its ubiquitylation.

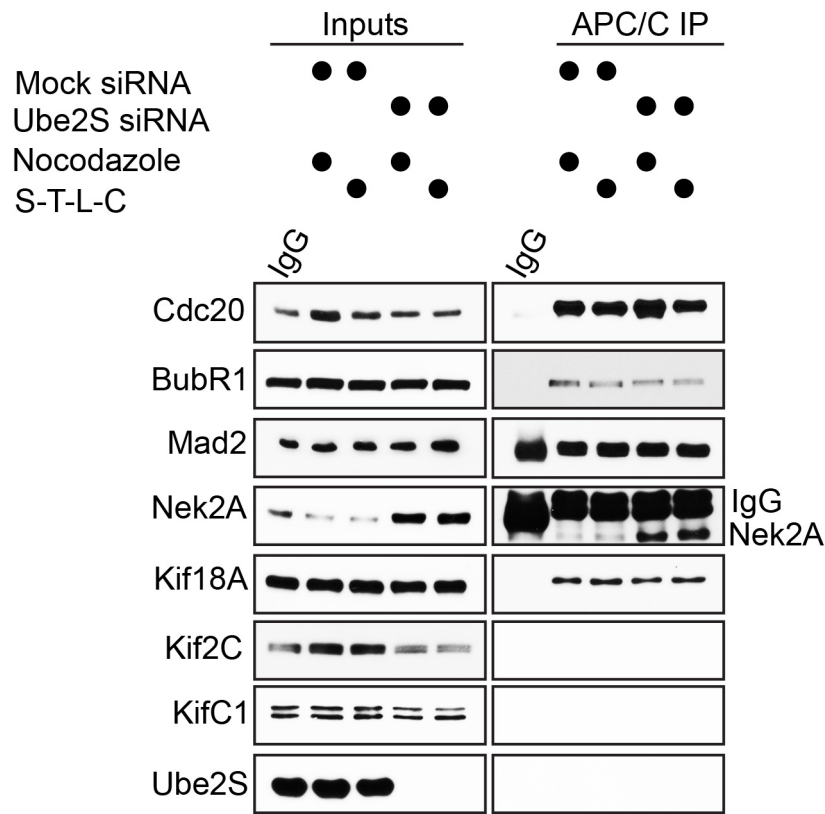


Figure 6. Kif18A associates with the APC/C in HeLa cell extract arrested in prometaphase. HeLa cells were transfected with 4-5nM Ube2S or Mock siRNA. At least four hours after transfection, cells were arrested with thymidine followed by either nocodazole (which depolymerizes microtubules) or S-T-L-C (which stabilizes microtubules). Extract was prepared from all conditions, normalized to total protein content, and APC/C was immunoprecipitated based on standard methods (Wickliffe, et al., 2011). Co-precipitating proteins were analyzed by Western blot. While Nek2A requires loss of Ube2S to stably associate with the APC/C (see also Meyer and Rape, 2014), Kif18A associates with the APC/C independent of Ube2S presence and of the presence of microtubules prior to extract preparation.

We also wished to characterize Kif18A's interactions with microtubules. First, radiolabeled Kif18A was stabilized by microtubules. As we were performing substrate characterization experiments, another lab published the detection of a microtubule binding domain (MTB) within Kif18A's cargo domain (Weaver, et al., 2011). We decided to examine whether or not this MTB domain was required for

the taxol-dependent substrate stabilization (Figure 7-8). Indeed, the cargo domain is stabilized by the presence of microtubules (Figure 7).

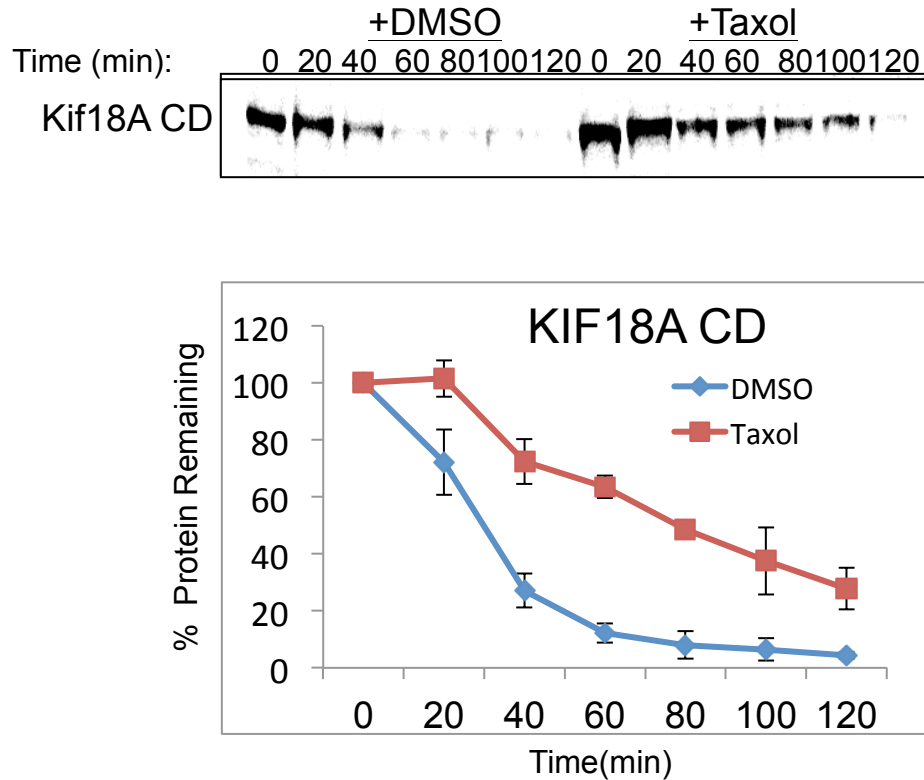


Figure 7. Kif18A possesses a microtubule binding domain (MTD) in its cargo domain that allows for protection from degradation when bound to microtubules. (top) Kif18A's cargo domain is degraded in the absence of microtubules, but stabilized when microtubules are present. The soluble substrate, geminin, is degraded in the presence or absence of microtubules. The radiolabeled HA-Kif18A cargo domain and HA-Geminin constructs were incubated with HeLa mitotic extract generated from cells arrested by nocodazole. Taxol or DMSO was added to pre-warmed extract before beginning the degradation assay. APC/C activity was stimulated by addition of Ube2C, p31^{comet}, ubiquitin and ATP. Reactions were incubated at 30°C for the indicated time periods and the protein stability was assayed by autoradiography. (bottom) At least three independent replicates of the degradation experiments were performed and quantified by Image J. The average percentage protein remaining and the standard deviation were calculated and graphed using Excel (Microsoft).

After alanine scanning throughout the region identified in Weaver, et al., we made nine mutations of positively charged residues to alanine, referred to as

the Δ MTB. The Δ MTB clone failed to stabilize in the presence of microtubules, but its degradation was APC/C dependent (Figure 8). While this result does not rule out the possibility of the motor domain's binding to microtubules also conferring stability, it does suggest that the microtubule binding of the cargo domain is important for stabilizing the protein. According to Weaver, et al., the microtubule-binding region in the cargo domain is important for the plus-end localization of Kif18A. Thus, this could support our hypothesis that Kif18A may be degraded in pools that fall off of the spindle during microtubule flux.

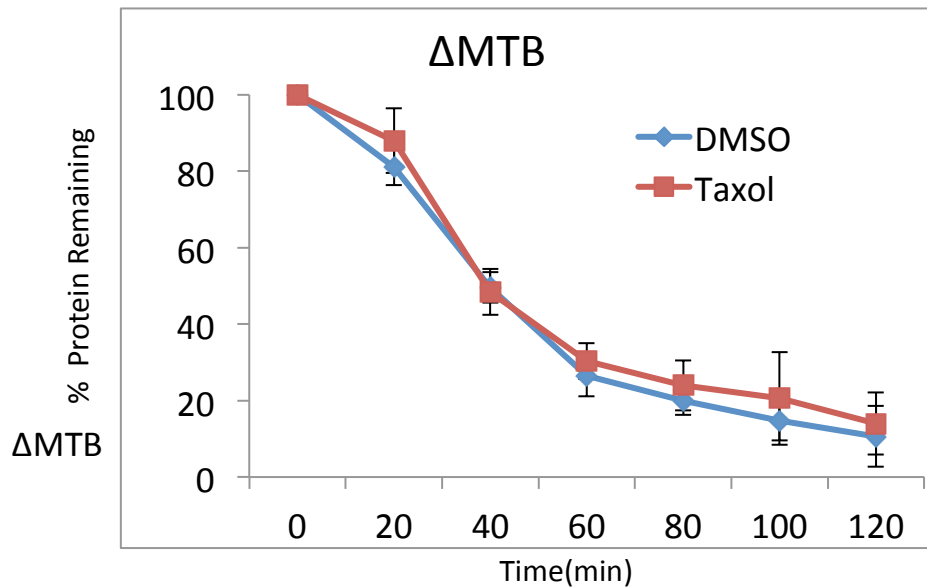
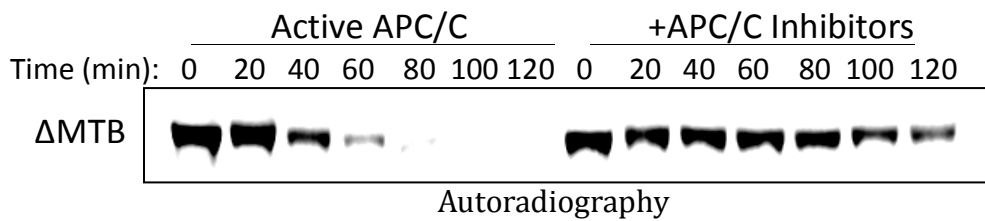
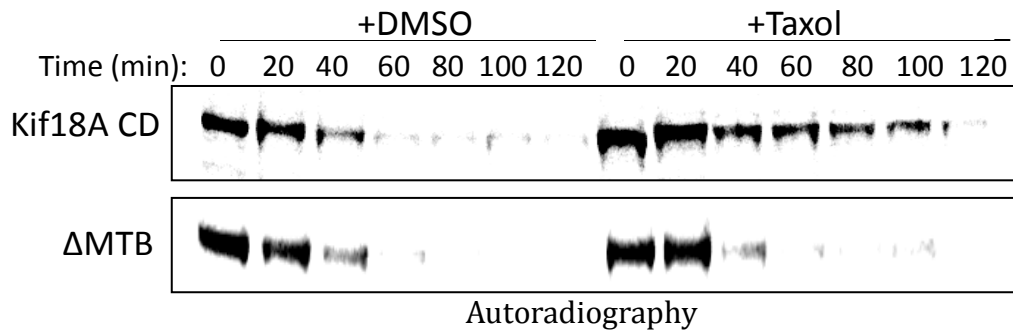


Figure 8. Identification of Kif18A's microtubule binding domain (MTB) in its cargo domain. (top) Kif18A's cargo domain is degraded in the absence of microtubules, but stabilized when microtubules are present. When nine positively charged amino acids are mutated in the cargo domain (referred to as the MTB region), Kif18A is degraded in the presence or absence of microtubules. This is dependent upon the APC/C as addition of APC/C inhibitors stabilizes the mutant. The radiolabeled HA-Kif18A constructs were incubated with HeLa mitotic extract generated from cells arrested by nocodazole. Taxol or DMSO was added to pre-warmed extract before beginning the degradation assay. APC/C activity was stimulated by addition of Ube2C, p31^{comet}, ubiquitin and ATP. Reactions were incubated at 30°C for the indicated time periods and the protein stability was assayed by autoradiography. (bottom) At least three independent replicates of the degradation experiments were performed and quantified by Image J. The average percentage protein remaining and the standard deviation were calculated and graphed using Excel (Microsoft).

Discussion

Bioinformatics algorithm predicts at least two novel APC/C substrates

In this project, we developed a successful bioinformatics algorithm that predicted many putative APC/C substrates based upon known degron and recognition sequences. We have exhaustively characterized one of these substrates, Kif18A, in terms of its degrons and other regulatory sequences. Somewhat ironically, Kif18A possesses a non-canonical APC/C recognition site at its extreme C-terminus that is required for robust Kif18A degradation and was not predicted by our algorithm (Figure 5; Sedgwick, et al., 2014). Other APC/C interacting proteins and substrates, including CDC20 and Nek2A, possess chemically similar C-termini that are required for their association with the APC/C (Nek2A) and its degradation by the APC/C (Nek2A and CDC20) (Hayes, et al., 2006; personal communication with A. Kelly, Rape Lab).

Kif18A depends upon a non-canonical APC/C recognition motif for its degradation

Kif18A, like Nek2A and CDC20, interacts with the APC/C in prometaphase extract (Figure 6, Sedgwick, et al., 2013), although its degradation does not follow the same kinetics as Nek2A. For example, Nek2a is thought to use its 'MR' motif in order to access the MCC-bound APC/C to be degraded despite an active SAC (Hayes, et al., 2006; Sedgwick, et al., 2013). Kif18A appears to be degraded later in mitosis as published by another group (Sedgwick, et al., 2013), immunofluorescence data (not shown), and Figures 1-3, which show the presence of Kif18A persisting past that of securin and geminin, which are degraded at metaphase.

One possibility is that pools of Kif18A are degraded via their LR motif. Intriguingly, microtubules stabilize Kif18A (Figure 3, Figures 7-8), leading to an attractive hypothesis that perhaps non-microtubule bound Kif18A pools independently bind the APC/C to be degraded once they have fallen off of microtubules, or once microtubules are destabilized. This would be an attractive hypothesis, especially considering the broad implications that loss of a kinesin cargo may trigger its degradation by ubiquitylation. Indeed, this regulatory pattern

has previously been identified in at least one eukaryotic kinesin (Kumar, et al., 2010). If small pools of Kif18A are degraded in prometaphase, and the bulk pool is degraded in anaphase, it may be difficult to detect with techniques of immunofluorescence and western blot analysis. Unfortunately, overexpression of Kif18A through various techniques and varying transfection levels, inducibility, and tags has largely failed, leading to difficulty in performing *in vivo* analysis of Kif18A mutants. However, this failure also supports the hypothesis that Kif18A levels must be very finely tuned, and that APC/C-mediated degradation is critical to the viability and health of human tissue culture cells.

Evolution of APC/C recognition motifs

One interesting note regards the evolution of APC/C recognition domains in human kinesins. This is a topic in which I have long been interested, but have not performed more than a cursory analysis. The human kinesins, KIFC1 and Kif18A, which we have characterized as APC/C substrates, possess APC/C recognition elements in their cargo domains, despite being jointly regulated by microtubules and APC/C. KIFC1 degradation is dependent upon an N-terminal D-box conserved in mammals, but the zebrafish KIFC1 possesses a KEN box at the identical location. Similarly, hsKif18A degradation is largely dependent upon its C-terminal LR motif, while the mouse Kif18A sequence possesses a KEN-box at its C-terminus. It would be very interesting to systematically identify the evolution of APC/C recognition elements and cross correlate that information with knowledge of how the APC/C's activity and structure is changed in order to glean a novel look at APC/C structure and function.

In summary, in this project, we have designed, performed, and validated a means through which to predict APC/C substrates. We performed in depth analysis of one novel substrate, Kif18A, and determined that like HURP, it is jointly regulated by microtubules, but unaffected by importins. Also, we discovered that Kif18A interacts with APC/C in prometaphase and that its degradation is largely due to a non-canonical APC/C recognition motif that mediates interaction between other proteins and APC/C. A key next step for this work is to integrate Kif18A's role as a genetic interactor of the APC/C (see Chapter 1) with its physical interactor and substrate status.

Materials and Methods

Determination of putative APC/C substrates possessing a D-box, KEN box, and 'positive patch' of amino acids near the sites

The following Python script interrogates the human proteome to analyze which proteins possess APC/C recognition sites.

```
#Import SeqIO to read fasta file
from Bio import SeqIO

#Open Fasta file and read in lines
fn = open('copy_uniprot-homo+sapiens+reviewed%3Ayes-1.fasta', 'rU')
lines = fn.readlines()
```



```

#Initialize dictionaries and lists to be used
protein_dict = {}
protein_name = ""
protein_dict[protein_name] = []
Dbox_dict = {}
Dbox_name = ""
Dbox_dict[Dbox_name] = ""

#This for loop reads in the sequence in FASTA format and creates a dictionary where the 'term' is
the protein name and the 'definition' is the sequence. All Fasta file names begin with the '>'
character, so by asking the program to identify these lines, the script can easily distinguish
between names and sequences and can 'count' the number of proteins by counting the number of
'>' signs. If the line does not start with '>,' then it is a sequence line and will be continuously
added to the sequence until the next line beginning with a '>' comes along.
for line in lines:
    if line.startswith('>'):
        protein_name = line[1:]
        protein_dict[protein_name] = []
    else: protein_dict[protein_name] += line

#Loop through all protein names and all sequences one-by-one
for name, aa in protein_dict.items():

#Reset variables to '0' to restart the count for each new sequences
    KEN_count = 0
    pos_residue_count = 0
    percent_posresidue = float(0)

#Loop through sequence, excluding the last three amino acids, searching for KEN boxes (lysine-
glutamine-asparagine). Each time it finds a KEN box, it will add 1 to the KEN count so that we will
have the sum of the number of KEN boxes in the protein sequence. We exclude the last three
amino acids because the rest of the script looks at the downstream sequence from the KEN. If
the protein ends in a KEN box, there is no downstream sequence, so we don't need to keep
sequences that end in this.
    for x in range(len(aa)-3):
        if (aa[x]=='K') and (aa[x+1]=='E') and (aa[x+2]=='N'):
            KEN_count = KEN_count+1
    for x in range(len(aa)):
        if (aa[x] == 'R') or (aa[x] == 'H') or (aa[x] == 'K'):
            pos_residue_count = pos_residue_count + 1
            percent_posresidue = float(float(pos_residue_count/float(len(aa)))*100)
    if KEN_count > 0: #and (percent_posresidue > 9.829) and (percent_posresidue < 22.00):
        print name, len(aa), 'aa.', ';', '#pos residues:', pos_residue_count, ';', 'percent pos:',
percent_posresidue, ';', 'Ken count = ', KEN_count
        for x in range(len(aa)-3-56):
            if (aa[x] == 'R') and (aa[x+3] == 'L') and (aa[x+1] != '\n' and aa[x+1] != "") and (aa[x+2] !=
'\n' and aa[x+2] != "") :
                Dbox_name = aa[x]+ aa[x+1]+ aa[x+2]+ aa[x+3]
                Dbox_dict[Dbox_name] = ""
                print Dbox_name
                count = 0
            #Instead of repeating these things, make an outside loop that add a variable that at
each incrementation adds 6 at the end of the loop.
            for y in range(6):
                if (aa[y+x+4] == 'R' or aa[y+x+4] == 'K'):
                    count = count + 1

```

```

if (count > 2) and (count < 6):
    for z in range(6):
        Dbox_dict[Dbox_name]+=(aa[z+x+4])
count = 0
for y in range(6):
    if (aa[y+x+10] == 'R' or aa[y+x+10] == 'K'):
        count = count + 1
if (count > 2) and (count < 6):
    for z in range(6):
        Dbox_dict[Dbox_name]+=(aa[z+x+10])
count = 0
for y in range(6):
    if (aa[y+x+16] == 'R' or aa[y+x+16] == 'K'):
        count = count + 1
if (count > 2) and (count < 6):
    for z in range(6):
        Dbox_dict[Dbox_name]+=(aa[z+x+16])
count = 0
for y in range(6):
    if (aa[y+x+22] == 'R' or aa[y+x+22] == 'K'):
        count = count + 1
if (count > 2) and (count < 6):
    for z in range(6):
        Dbox_dict[Dbox_name]+=(aa[z+x+22])
count = 0
for y in range(6):
    if (aa[y+x+28] == 'R' or aa[y+x+28] == 'K'):
        count = count + 1
if (count > 2) and (count < 6):
    for z in range(6):
        Dbox_dict[Dbox_name]+=(aa[z+x+28])
count = 0
for y in range(6):
    if (aa[y+x+34] == 'R' or aa[y+x+34] == 'K'):
        count = count + 1
if (count > 2) and (count < 6):
    for z in range(6):
        Dbox_dict[Dbox_name]+=(aa[z+x+34])
count = 0
for y in range(6):
    if (aa[y+x+40] == 'R' or aa[y+x+40] == 'K'):
        count = count + 1
if (count > 2) and (count < 6):
    for z in range(6):
        Dbox_dict[Dbox_name]+=(aa[z+x+40])
count = 0
for y in range(6):
    if (aa[y+x+46] == 'R' or aa[y+x+46] == 'K'):
        count = count + 1
if (count > 2) and (count < 6):
    for z in range(6):
        Dbox_dict[Dbox_name]+=(aa[z+x+46])
count = 0
for y in range(6):
    if (aa[y+x+52] == 'R' or aa[y+x+52] == 'K'):
        count = count + 1

```

```

if (count > 2) and (count < 6):
    for z in range(6):
        Dbox_dict[Dbox_name]+= (aa[z+x+52])
    count = 0
if Dbox_dict != "":
    print 'This Dbox(es) have at least one positive patch within50aa:', Dbox_name
Ken_count = 0

```

***In Vivo* Degradation Assays**

In vivo degradation assays were performed as described (Song, et al., 2014; Song and Rape, 2010). To test microtubule-dependent stabilization of substrates, 20mM paclitaxel/taxol (Sigma) was added to HeLa S3 extracts (pre-warmed to 30 °C) to promote microtubule polymerization. To deplete Cdc20, 400ml mitotic extract was depleted twice at 4°C for 1h with 2 mg monoclonal α Cdc20 antibody. For proteasome dependence, 20-200 μ M MG132 (Boston Biochem or UBPBio) was added to extract.

Plasmids, siRNAs, antibodies and proteins

Kif18A and geminin cDNA was cloned into pCS2-HA for IVT/T. A N-terminal Flag-tag was introduced into pcDNA5/FRT/TO by PCR. For the cargo domain generation, Kif18A amino acids 1-284 were expressed as a truncation and a methionine was added at its N-terminus. For recombinant proteins, cDNAs were cloned into pMAL and pET28 for expression in *E.coli*, and the purification procedures for MBP-tagged and 6xHis-tagged proteins were as described (Song and Rape, 2010). Site-directed mutagenesis was used to identify residues within the MTB (also see Weaver, et al., 2011).

The following antibodies were used: α Cdc20/p55CDC [E-7], (monoclonal; Santa Cruz Biotechnology); α cyclin B1, α geminin, α securin (polyclonal; Santa Cruz Biotechnology); α Kif18A, α KifC1 (rabbit polyclonal; Bethyl Laboratories; A301-080A, A300-952A), β -actin (mouse monoclonal, MP Biomedicals LLC, 08691001), and normal mouse IgG (Santa Cruz, 2025), α Kif2C (mouse monoclonal, Santa Cruz, 81305), α Mad2 (mouse monoclonal, BD Biosciences, 610679), α Ube2S (rabbit polyclonal, Novus Biologicals, 22570002), α BubR1 (mouse monoclonal, Abcam, 54894), α Nek2A (mouse monoclonal, BD Biosciences).

***In Vitro* degradation and ubiquitylation Reactions**

APC/C- degradation and ubiquitylation of ³⁵S-labeled substrates were performed as described (Appendix B; Song and Rape, 2010; Wickliffe *et al.*, 2011). To test microtubule-dependent stabilization of substrates, 20mM paclitaxel/taxol (Sigma) was added to HeLa S3 extracts (pre-warmed to 30 °C) to promote microtubule polymerization.

Appendix D:

This section possesses the Python scripts used to parse and analyze data from Chapter 1.

The following is a Python script named AllisonMS01.py that reads through a raw CompPASS file and discards non-unique identifiers while saving protein isoforms. The script was modified from an original form (not shown, written by myself) by Eugene Oh, and was annotated and edited to fit specific criteria by myself.

```
- Created on Jan 6, 2014
Finished on Jan 6, 2014
@author: eugeneoh
@editor: allisoncraney
Custom script for ACC to analyze MS data
Notes added by ACC Jan 7, 2014
Before I used the script, I removed the header line from the text file and had to convert some
windows specific text to a newline character through the following:
tr '\r' '\n' < inputfile > outputfile

Input files:
1:/Users/allisoncraney/screening_club/MassSpec/140106-results-CDC20_unix.txt
2:/Users/allisoncraney/screening_club/MassSpec/140106-results-C114S_unix.txt
3:/Users/allisoncraney/screening_club/MassSpec/140106-results-MG132_unix.txt

'''

#Note: set up a function called MSdata that will be performed as 'main'
def MSdata(inputfile, outputfile):

#open the defined input and output files
    f=open(inputfile,'r')
    o=open(outputfile,'w')

#initial a dictionary called 'd'
    d={}

#Loop through each line in the input file and split so that columns can be called individually
    for line in f:
        field=line.split('\t')

#Set up an 'if' loop that will ask if the unique column 8 (the name of the putative protein interactor)
already exists in the dictionary.
#If the name already exists, that means we have an entry for the putative interactor and will NOT
re-add this protein.
#Drawback is that we lose the unique GI that linked to the protein that was named twice or more in
the input file.
        if field[8] in d:
            pass
            #print 'ok'
#If the protein does not already exist in the dictionary, this line will write all of the columns to the
defined output file.
        else:
#Filter for only putative interactors that have a z-score greater than or equal to 1
            if field[7] >= '1':
```

```
o.write(field[0]+'\\t'+field[1]+'\\t'+field[2]+'\\t'+\
        field[3]+'\\t'+field[4]+'\\t'+field[5]+'\\t'+\
        field[6]+'\\t'+field[7]+'\\t'+field[8])
```

#This command is within the loop but outside of the 'if and else' loops, so it will be performed for each line in the input file.

#This will set field 8 (the name) as the key of a dictionary (with no value), so that the dictionary will be populated for each

#column 8 and so that the 'if else' loop will occur properly.

```
d[field[8]]=""
```

##'Main' is built-into python. When 'main' is called in this script, the function MSdata will be run.

```
if __name__=='__main__':
```

```
    inputfile='/Users/allisoncraney/screening_club/MassSpec/140106-results-MG132_unix.txt'
```

```
    outputfile='/Users/allisoncraney/screening_club/MassSpec/FILTERED-results-MG132.txt'
```

```
    MSdata(inputfile,outputfile)
```

The following is a Python script named AllisonMS02.py and is intended to process the output of AllisonMS01.py shown above. As mass spectrometry databases cannot necessarily distinguish between protein isoforms, and as the database will interrogate a subsequent database in which human proteins have multiple names, the raw CompPASS reads possess a great deal of redundancy, leading to inaccuracy in the analysis. This script uses properties of the raw CompPASS file to remove non-unique proteins and protein isoforms from the analysis. While performing bench top verification, the knowledge that isoforms of a given protein were not considered in the data parsing was kept forefront. The script was written by myself, but possesses a few lines of code from AllisonMS01.py, most of which was written by Eugene Oh.

```
"""
This is to be used after Allison MS01. MS01 generates a parsed CompPASS text file where there
are only unique protein interactor names.
```

```
That knowledge is important to understand some of the assumptions made in the code below.
```

```
The purpose of this script is to compare spectral counts between two CompPASS files.
```

```
I will be making two comparisons:
```

```
-FLAG-CDC20 versus FLAG-CDC20 co-expressed with pcs2 Ube2C C114S
```

```
-FLAG-CDC20 versus FLAG-CDC20 + MG132
```

```
Created on Jan 7, 2014
```

```
Written by: Allison
```

```
Some code comes from Allison MS01 (Eugene and Allison are authors)
```

```
Input files:
```

```
1:/Users/allisoncraney/screening_club/MassSpec/FILTERED-results-C114S.txt
```

```
2:/Users/allisoncraney/screening_club/MassSpec/FILTERED-results-CDC20.txt
```

```
3:/Users/allisoncraney/screening_club/MassSpec/FILTERED-results-MG132.txt
```

```
"""
```

```
#Note: set up a function called CompareMSdata that will be performed as 'main'
```

```
def CompareMSdata(inputfile, inputfile2, outputfile):
```

```

#open the defined input and output files
    #inputfile1 will be FLAG-CDC20 alone
    f=open(inputfile,'r')
    #inputfile2 will be comparison file: either MG132 or C114S CompPASS files
    f2=open(inputfile2, 'r')
    o=open(outputfile,'w')

#initial a dictionary
    CDC20interactors={}

#Loop through each line in the input file and split so that columns can be called individually
    for line in f:
        field=line.split('\t')
        Bait = field[1].strip()
        #Field 3 is the spectral count after running CompPASS. I believe this is the sum of the spectral
        counts for each individual bait for each 'Run' done in the analysis
        Spectralcount = field[3]
        Interactingprotein = field[8].strip()
        #print Interactingprotein
        #These next sets of commands set up a dictionary where the key is the name of the interacting
        protein
        #After setting up the key, I generate a list of values, where the [0] value is the spectral count
        for CDC20
        #The [1] value is the name of the comparison bait (CDC20 or MG132)
        #The [2] value is set as zero, and will be replaced with the spectral count of comparison bait if
        it exists in the mass spec
        CDC20interactors[Interactingprotein] = []
        CDC20interactors[Interactingprotein].append(Bait)
        CDC20interactors[Interactingprotein].append(Spectralcount)
        CDC20interactors[Interactingprotein].append('MG132')
        CDC20interactors[Interactingprotein].append('0')
        #for keys, values in CDC20interactors.items():
        #    print keys, '\t', values

    for line2 in f2:
        field2 = line2.split('\t')
        Bait2 = field2[1].strip()
        Spectralcount2 = field2[3]
        Interactingprotein2 = field2[8].strip()
        #If the comparison bait interacting protein exists in the CDC20 interactome, it will replace
        the '0' with the spectral count
        if Interactingprotein2 in CDC20interactors.keys():
            CDC20interactors[Interactingprotein2][3] = Spectralcount2
        #If interactingprotein2 is not in the CDC20 interactors dictionary already, add it as a key
        #Add the first value as 'CDC20,' the second value as '0,' the third value as 'C114S,' or
        'MG132' and the last value as the C114S or Mg132 spectral count
        else:
            CDC20interactors[Interactingprotein2] = []
            CDC20interactors[Interactingprotein2].append('CDC20')
            CDC20interactors[Interactingprotein2].append('0')
            CDC20interactors[Interactingprotein2].append('MG132')
            CDC20interactors[Interactingprotein2].append(Spectralcount2)

    for key, value in CDC20interactors.items():
        print key, '\t', value[0], '\t', value[1], '\t', value[2], '\t', value[3]

```

```

                #o.write(CDC20interactors(Interactingprotein2), '\t', CDC20interactor.value(), '\t',
Spectralcount2)
#If the protein does not already exist in the dictionary, this line will write all of the columns to the
defined output file.
# else:
#   if field[7] >= '1':
#       o.write(field[0]+'\\t'+field[1]+'\\t'+field[2]+'\\t'+\\
#           field[3]+'\\t'+field[4]+'\\t'+field[5]+'\\t'+\\
#           field[6]+'\\t'+field[7]+'\\t'+field[8])

#Main is built-into python. When 'main' is called in this script, the function MSdata will be run.
if __name__ == '__main__':
    inputfile='/Users/allisoncraney/screening_club/MassSpec/FILTERED-results-CDC20.txt'
    inputfile2 = '/Users/allisoncraney/screening_club/MassSpec/FILTERED-results-MG132.txt'
    outputfile='/Users/allisoncraney/screening_club/MassSpec/Comparison.txt'
    CompareMSdata(inputfile, inputfile2, outputfile)

```

The following Python script was used to parse raw data from Metamorph in order to calculate the total percentage of microtubules remaining for a given cell area after cold treatment.

```

#Python script to parse Metamorph log files for cold stability assays
#Open and read in file
fn = open('130501-ube2s-tubulin-log.LOG', 'rU')
lines = fn.readlines()
for line in lines:
    columns = line.split(',')
    name = columns[0]
    area = columns[1]
    fluorescence = columns[4]
    print name, '\t', area, '\t', fluorescence, '\n'

```